

Using Landscape Genomics to Conserve Adaptive Capacity:

A Case Study with a Southern Appalachian Salamander

by

Brenna Renee Forester

University Program in Ecology
Duke University

Date: _____

Approved:

Dean L. Urban, Supervisor

Robert R. Dunn

Thomas F. Schultz

Jennifer J. Wernegreen

Dissertation submitted in partial fulfillment of
the requirements for the degree of
Doctor of Philosophy in the University Program in Ecology
in the Graduate School of Duke University

2017

ABSTRACT

Using Landscape Genomics to Conserve Adaptive Capacity:

A Case Study with a Southern Appalachian Salamander

by

Brenna Renee Forester

University Program in Ecology
Duke University

Date: _____

Approved:

Dean L. Urban, Supervisor

Robert R. Dunn

Thomas F. Schultz

Jennifer J. Wernegreen

An abstract of a dissertation submitted in partial fulfillment of
the requirements for the degree of
Doctor of Philosophy in the University Program in Ecology
in the Graduate School of Duke University

2017

Copyright by
Brenna Renee Forester
2017

Abstract

Landscape genomics is an emerging field that investigates how environmental features drive patterns of neutral and adaptive genetic variation across landscapes. Importantly, landscape genomics can provide insight into the adaptive potential of wild populations of non-model species, since these analyses do not require prior genomic information or the use of manipulative experiments such as reciprocal transplants. However, a fundamental challenge in landscape genomics is detecting genetic markers under selection from large genomic data sets. This analytical step is particularly important since partitioning these data into neutral and adaptive components of genetic diversity provides the information upon which management decisions are based.

Difficulties with the partitioning step include distinguishing neutral demographic signals from signals of selection, detecting selection across heterogeneous landscapes, and detecting signals of selection that are derived from multilocus adaptive processes. To address these issues, I used two different sets of landscape genetic simulations to test a suite of genotype-environment association (GEA) analyses across a range of landscape heterogeneities, selection strengths, dispersal abilities, demographic histories, sample sizes, sampling designs, and genetic architectures. I found that multivariate GEA methods showed a superior combination of low false positive and high true positive rates across simulation scenarios, providing a powerful tool for investigating the genetic basis of local adaptation and improving management actions.

I then applied a multivariate GEA approach to a reduced representation genomic data set for Weller's salamander (*Plethodon welleri*). This endemic, fully terrestrial, forest-dwelling salamander is a species of conservation concern across its small range in the Southern Appalachian Mountains. Its restriction to mountaintop habitats makes it particularly vulnerable to ongoing habitat fragmentation and climate change. I developed and illustrated the use of an “adaptive dissimilarity” index to characterize the scope of adaptive variation across the Weller’s salamander range. In combination with other metrics including neutral genetic variation, population differentiation, and effective population size, I addressed a series of conservation scenarios that were improved by the explicit consideration of differences in adaptive genetic variation among populations. These scenarios included: (1) site prioritization to ensure evolutionary resiliency across the species range; (2) genetic rescue to increase genetic diversity and population fitness while minimizing the risk of outbreeding depression; and (3) assisted gene flow to maximize adaptive potential in response to rapid climate change. These analyses are helping us better understand the capacity of species to adapt to changing conditions and what management actions will be most effective to conserve biodiversity under global change. These efforts must be part of the broader effort to stem the biodiversity crisis by conserving not just genetic diversity, but also the ecological and evolutionary processes that sustain it.

Dedication

I dedicate this dissertation to my mentors, Dean and Andy; to my mom, Nancy; to the memory of FitzRoy; and to my wonderful husband, David. And last but not least, to the salamanders.

Contents

Abstract	iv
List of Tables.....	xi
List of Figures	xii
Acknowledgements	xv
1. Landscape genomics and the importance of conserving genetic diversity under global change.....	1
2. Detecting spatial genetic signatures of local adaptation in heterogeneous landscapes .	7
2.1 Introduction.....	7
2.2 Methods	13
2.2.1 Simulation framework.....	13
2.2.2 Simulation scenarios	13
2.2.3 Isolation by distance and local adaptation	16
2.2.4 Genotype-environment association methods.....	18
2.3 Results	23
2.3.1 Isolation by distance and local adaptation	23
2.3.2 Effects of landscape, selection, and dispersal on detection probability	27
2.3.3 Method comparison	27
2.3.4 Effect of mutation rate	28
2.4 Discussion.....	32
2.4.1 Evaluation of detection methods.....	35
2.4.2 Future directions.....	41
3. Using genotype-environment associations to identify multilocus local adaptation	42

3.1 Introduction.....	42
3.2 Methods	45
3.2.1 Statistical approaches to GEA.....	45
3.2.1.1 Constrained ordinations	47
3.2.1.2 Redundancy analysis of components.....	48
3.2.1.3 Random Forest	49
3.2.1.4 Latent factor mixed models	51
3.2.2 Correction for population structure.....	52
3.2.3 Simulations.....	53
3.2.4 Evaluation statistics.....	55
3.2.5 Weak selection	57
3.3 Results	57
3.3.1 Population corrections.....	57
3.3.2 Ranked results.....	58
3.3.3 Cutoff results.....	59
3.3.4 Weak selection	63
3.3.5 Combining detections.....	63
3.4 Discussion.....	67
3.4.1 Constrained ordinations.....	68
3.4.2 Random Forest.....	73
3.4.3 Latent factor mixed models	74
3.4.4 Should results from different tests be combined?	75

3.4.5 Conclusions and recommendations.....	77
4. Conserving adaptive capacity in a Southern Appalachian salamander threatened by climate change	79
4.1 Introduction.....	79
4.2 Methods	85
4.2.1 Overview	85
4.2.2 Data collection.....	86
4.2.3 RADseq library construction and sequencing.....	88
4.2.4 Bioinformatics	89
4.2.5 Filtering.....	90
4.2.6 Data analysis	92
4.2.7 Conservation scenarios.....	94
4.3 Results	96
4.3.1 Scenario 1: Site prioritization for conservation	103
4.3.2 Scenario 2: Genetic rescue	106
4.3.3 Scenario 3: Assisted gene flow.....	107
4.4 Discussion.....	108
4.4.1 Scenario 1: Site prioritization for conservation	110
4.4.2 Scenario 2: Genetic rescue	112
4.4.3 Scenario 3: Assisted gene flow.....	114
4.4.4 Conclusions	116
5. Concluding remarks	118
5.1 Synopsis	119

5.2 Prospectus for future research.....	121
Appendix A: Supporting information for Chapter 2 - Detecting spatial genetic signatures of local adaptation in heterogeneous landscapes.....	124
Appendix B: Supporting information for Chapter 3 - Using genotype-environment associations to identify multilocus local adaptation.....	132
Appendix C: Supporting information for Chapter 4 -Conserving adaptive capacity in a Southern Appalachian salamander threatened by climate change	150
References	156
Biography	175

List of Tables

Table 1. Average elevation and environmental conditions (March-November) of Weller's salamander populations sampled across the range.	87
Table 2. Observed heterozygosity (H_o), expected heterozygosity (H_e), and nucleotide diversity (π) of adaptive and neutral markers within each population. Effective population size (N_e) was estimated from neutral markers filtered to maximize retained individuals while minimizing missing data. Salamander sample sizes are provided for diversity statistics and N_e estimation.	101
Table 3. Pairwise F_{ST} of Weller's salamander populations, shaded from low values (light gray) to high values (dark gray).	101
Table 4. Adaptive dissimilarity of Weller's salamander populations, shaded from low values (light gray) to high values (dark gray). Average adaptive dissimilarity for each population is provided in the bottom row.	103
Table 5. Weller's salamander population rankings based on different input criteria (columns). Sites are sorted from highest to lowest ranked.	105

List of Figures

- Figure 1. Landscape selection configurations used for simulations. (a) Continuous selection gradient representing selection for AA genotypes in the North (dark) and aa genotypes in the South (light). Examples of discrete selection landscapes, from least to most aggregated: (b) H1, (c) H5, and (d) H9. Dark areas represent AA habitat and light areas represent aa habitat. Points represent the 500 sampled individuals. 9
- Figure 2. Isolation by distance, assessed by spatial eigenfunction and redundancy analysis, averaged across ten replicates of each simulation scenario (a). The strength of local adaptation, assessed by correlation between the selected locus and environment, averaged across ten replicates of each simulation scenario (b). 25
- Figure 3. Strength of local adaptation across dispersal levels and landscape selection configurations, with one plot per selection strength. Local adaptation is assessed by correlation between the selected locus and environment, averaged across ten replicates of each simulation scenario. 26
- Figure 4. Average true positive rate (TPR) across ten replicates of each simulation scenario. TPR scales from 0 (worst performance, 0% TPR, light shades) to 1 (best performance, 100% TPR, dark shades). Results for (a) principal components analysis, (b) principal coordinates analysis, (c) redundancy analysis, (d) distance-based redundancy analysis, and (e) latent factor mixed models. 29
- Figure 5. Average genotype-environment association (GEA) index across ten replicates of each simulation scenario. Correct detection (3) has dark shading, with no detection (0) in light shading. Results for (a) principal components analysis, (b) principal coordinates analysis, (c) redundancy analysis, (d) distance-based redundancy analysis, and (e) latent factor mixed models. 30
- Figure 6. Average false positive rate (FPR) across ten replicates of each simulation scenario. FPR scales from 0 (best performance, 0% FPR, light shades) to 1 (worst performance, 100% FPR, dark shades). Results for (a) principal components analysis, (b) principal coordinates analysis, (c) redundancy analysis, (d) distance-based redundancy analysis, and (e) latent factor mixed models. 31
- Figure 7. Examples of ordination plots for PCA (top row) and RDA (bottom row). Simulation plotted is replicate 10 from the H1 landscape configuration, strong (50%) selection, and 5% dispersal. Plots show the distribution of loci (red circles) and individual genotypes (gray pluses) in the ordination space. The correlation of the predictor variables with the axes is shown with the blue vectors. In this case, PCA did

not detect the selected locus on the first three axes (a-b), while RDA did detect the selected locus (circled in green) on axis 3, correctly correlated with habitat (d). Note how x and y load strongly on the first two RDA axes (c), while habitat loads strongly on RDA axis 3 (d). This is in contrast to PCA, where habitat fails to load strongly on any of the first three axes (a-b)..... 40

Figure 8. Average true positive (blue) and false positive (red) rates for all loci under selection from five methods (columns) using locus rankings (i.e. number of positive detections out of number of loci under selection). Each method shows results for different sampling strategies (R = random, P = pairs, T = transects), demographies (1R and 2R = refugial expansion, IBD = equilibrium isolation by distance, IM = equilibrium island model), and sample sizes (rows)..... 60

Figure 9. Average true positive rates for different levels of selection (rows) from five methods (columns) using locus rankings and a sample size of 20 individuals per deme. Each method shows results for different sampling strategies (R = random, P = pairs, T = transects) and demographies (1R and 2R = refugial expansion, IBD = equilibrium isolation by distance, IM = equilibrium island model). Only the IBD demography included very weak selection ($s=0.001$)..... 61

Figure 10. Average true positive (blue) and false positive (red) rates from five methods (columns) using the best cutoff for each method. Each method shows results for different sampling strategies (R = random, P = pairs, T = transects), demographies (1R and 2R = refugial expansion, IBD = equilibrium isolation by distance, IM = equilibrium island model), and sample sizes (rows)..... 62

Figure 11. Average true positive (blue) and false positive (red) rates for RDA and cRDA (columns) on simulations with weak selection only. The first two columns show results for locus rankings, while the third and fourth columns show results for the best cutoff for each method. Results are presented for different sampling strategies (R = random, P = pairs, T = transects), demographies (1R and 2R = refugial expansion, IBD = equilibrium isolation by distance, IM = equilibrium island model), and sample sizes (rows)..... 65

Figure 12. Average counts of true positive (blue) and false positive (red) detections for two methods, RDA and LFMM. The first column shows the average number of loci detected by both methods. The second and third columns show the average number of detections that are unique to RDA and LFMM, respectively. Results are presented for different sampling strategies (R = random, P = pairs, T = transects), demographies (1R and 2R = refugial expansion, IBD = equilibrium isolation by distance, IM = equilibrium island model), and sample sizes (rows)..... 66

Figure 13. Redundancy analysis plots showing loci with point size scaled by their correlation with the driving environmental variable (“Habitat”), and correlation of predictor variables with the constrained RDA axes (arrows). Plots are shown for an equilibrium island model (IM), equilibrium isolation by distance model (IBD), and non-equilibrium one- and two- refugial expansion models (1R and 2R) for paired sampling (6 individuals/deme) on environmental surface “453” 72

Figure 14. Location of sampled Weller’s salamander populations in the Southern Appalachian Mountains. Inset photo of Weller’s salamander by Katherine Cain. 82

Figure 15. Three climatic parameters relevant to terrestrial salamander biology and ecology across the Weller’s salamander range, with sampled populations for this study shown as white circles. Climate normals (1981-2010) at left and ensemble projections (CMIP5) for 2080 under the RCP 8.5 (high emissions) scenario at right. Climate data from (AdaptWest Project 2015; Wang *et al.* 2016)..... 84

Figure 16. Flowchart of methods. Gray ovals are field data collection; white ovals are data analysis; hexagons are intermediate data products; gray rectangles are final outputs, showing data used for the three conservation scenarios..... 85

Figure 17. Discriminant analysis of principal components of 6004 neutral SNPs (a) and 66 potentially adaptive SNPs (b, c) from nine Weller’s salamander populations. Adaptive DAPC shows axes 1 and 2 (b), and axes 2 and 3 (c). Colors match populations in range map (Figure 14)..... 99

Acknowledgements

Primary thanks go to my dissertation committee: Tom Schultz, Jennifer Wernegreen, Rob Dunn, and especially my advisor and mentor, Dean Urban. A special thank you to Andy Bunn and Erin Landguth for their efforts to support my research and career, and for their friendship. This work was greatly improved by my collaborators: Matt Jones, Stéphane Joost, Erin Landguth, Jesse Lasky, and Helene Wagner. Thanks to Saira Haider for her contributions to temperature and humidity modeling in Chapter 4.

This work was made possible by funding from the American Museum of Natural History, the American Society of Naturalists, the Duke University Graduate School, the Foundation for the Conservation of Salamanders, the National Science Foundation, PEO International, Sigma Xi, and the Society for the Study of Amphibians and Reptiles. Thank you to these organizations for supporting conservation science!

I am indebted to Lori Williams, my salamandering guru, mentor, and friend. Others whose help and good cheer in the field were invaluable: Charles Lawson, Rick Carpenter, Steve Spear, Kevin Hamed, Danica Schaffer-Smith, Kayleigh Somers, Irene Liu, Arianne Messerman, Nicki Cagle, Nicole Heller, and Chris Kelly. Thank you to Bryan Stuart and Jeff Beane with the North Carolina Herpetological Society for their help and advice.

Agencies who provided permit approvals and site access include: the Cherokee and Pisgah National Forests, the North Carolina Wildlife Resources Commission, the

North Carolina Division of Parks and Recreation, and the Tennessee Wildlife Resources Agency. Special thanks to William Ellison with the Unaka Ranger District, and Luke Appling with the North Carolina State Parks (Grandfather Mountain State Park). Very special thanks to the Jesse and Kerm at Grandfather Mountain for all of their assistance over the years. Salamander research was conducted under approval from the Duke University Institutional Animal Care and Use Committee (A281-12-11 and A215-15-08).

Thank you to those who helped with computational resources, data analysis, and data production, especially: Tom Milledge, Olivier François, Robin Waples, Paul Hohenlohe, Matt Fuller, and (especially) Tom Schultz. Special thanks to Meg Stephens for administrative help and moral support. For stimulating conversations and collaborations, thank you to my colleagues Andy Bunn, Kim Andrews, Stéphanie Manel, Amanda Stahlke, Lisette Waits, Amanda Xuereb, and Stéphane Joost. And a special thank you to Renee LaCroix and Sue Madsen for their mentorship and friendship, and for encouraging me to continue my graduate career.

Finally, thank you to my friends and family: Karen, Danica, Ingrid, Claire and Jake, Kayleigh and Matt, Irene, Stella, and Satellite. Thank you Mom and Barry for your unflagging support over the years. And biggest thanks of all to my incredible husband, David LoSchiavo, whose patience, empathy, sense of humor, and unconditional love helped make this dissertation a reality.

1. Landscape genomics and the importance of conserving genetic diversity under global change

The primary driver of the ongoing biodiversity crisis is human-mediated global environmental change, which includes habitat loss and fragmentation, climate change, the introduction of invasive species, disrupted biogeochemical cycles, emerging diseases and pathogens, and overexploitation (Butchart *et al.* 2010; Dirzo *et al.* 2014; Waters *et al.* 2016). An underappreciated component of biodiversity loss is the extirpation of populations, and the erosion of genetic diversity within those that remain (Hughes *et al.* 1997; Pauls *et al.* 2013; Miraldo *et al.* 2016). In the context of biodiversity conservation, genetic factors have been underappreciated, despite the fact that they are essential to ensuring the persistence of species in changing and stressful conditions (Reed & Frankham 2003; Spielman *et al.* 2004; Frankham 2005; Bijlsma & Loeschcke 2012). The field of conservation genetics, which involves efforts to minimize the impact of deleterious genetic factors in small, declining populations, has been the primary focus of genetic interventions for conservation over the past several decades. However, more recent applications of genetics to conservation in the relatively new field of landscape genetics have been focused on restricting biodiversity loss within populations and species before they reach the point of high extinction risk (Segelbacher *et al.* 2010; McMahon *et al.* 2014).

Landscape genetics integrates population genetics, landscape ecology, and spatial statistics to investigate how recent global change has affected the distribution of genetic variation across heterogeneous landscapes (Manel & Holderegger 2013; Balkenhol *et al.* 2016). Integrating three disparate fields of inquiry into a unified framework has not been a simple task (Richardson *et al.* 2016). Despite these difficulties, landscape genomics has made important contributions to understanding how the loss of intraspecific genetic diversity influences ecological and evolutionary processes. These contributions include assessing functional connectivity in heterogeneous landscapes, linking processes such as land use change and degradation to patterns of genetic variation, and, more recently, linking environmental variation to potentially adaptive genetic variation (Manel & Holderegger 2013).

This latter endeavor, landscape genomics, has been identified as a subfield of landscape genetics that involves the use of larger genetic data sets (though not necessarily entire genome sequences) to investigate how environmental heterogeneity influences the distribution of both neutral and adaptive genetic variation. The development of this field has come as a direct result of advances in sequencing technologies that allow for dense genotyping at reasonable costs in any organism (Davey *et al.* 2011; Andrews *et al.* 2016), the availability of environmental predictors at high spatial and temporal resolution (Schoville *et al.* 2012), and increased computational power that allows for the efficient analysis of these high-dimensional data sets.

Landscape genomics, and genomics more generally, have shown significant promise to advance conservation and stem biodiversity loss (McMahon *et al.* 2014; Hoffmann *et al.* 2015). The major advantage of landscape genomics for investigating adaptive genetic variation in species of conservation concern is that it does not require prior genomic information or the use of manipulative experiments, such as reciprocal transplants or common gardens (Sork *et al.* 2013). The ability to identify potentially adaptive genetic variation and the drivers of local adaptation can allow conservation managers to quantify adaptive potential and manage for evolutionary resiliency in wild populations in the face of complex and interacting environmental changes (Sgro *et al.* 2011; Funk *et al.* 2012; Harrison *et al.* 2014). These insights into adaptive variation can inform conservation genetic restoration efforts (e.g. genetic rescue), as well as allow for the proactive management of species in the face of stressors such as climate change or disease outbreaks (e.g. Steane *et al.* 2014; Schwabl *et al.* 2016).

Two of the fundamental challenges in landscape genomics are detecting local adaptation from large genomic data sets, and integrating these data into conservation applications. The meaningful application of landscape genomics to conservation hinges on our ability to successfully partition neutral from adaptive genetic variation. This is because these two sets of genetic variation provide different insights into population processes. Neutral markers allow us to estimate population structure, levels of inbreeding, genetic drift, effective population size, and gene flow. In a landscape

genetics context, we can examine neutral genetic variation and landscape heterogeneity in order to address questions such as the effect of landscape features on gene flow and levels of genetic variability, the relative importance of contemporary and historical landscape change on gene flow, the evaluation of source-sink dynamics, and invasive species and disease spread across landscapes (Storfer *et al.* 2010). By contrast, analysis of potentially adaptive genetic variation provides insight into evolutionary history and local adaptation. Landscape genomics provides a means of identifying this adaptive variation while explicitly testing environmental factors that are expected to shape natural selection across populations (called genotype-environment association or environmental association analysis, Rellstab *et al.* 2015).

We face a number of difficulties when using statistical tests to partition neutral and adaptive genetic markers, including distinguishing neutral demographic signals from signals of selection, detecting selection across heterogeneous landscapes, and detecting signals of selection that are derived from multilocus adaptive processes (Hoban *et al.* 2016). Because wild populations live in complex landscapes and are subject to diverse selection pressures, it is imperative that the statistical approaches we use for this task are thoroughly tested in a controlled framework. To address these issues, I use landscape genetic simulations to investigate the effect of environmental heterogeneity, dispersal ability, and selection on the strength of local adaptation. I then test a set of genotype-environment association (GEA) methods for their ability to detect selection

across this large parameter space, which includes a strong demographic signal that is highly correlated with the selection surface (Chapter 2).

The simulations in Chapter 2 use a single-locus selection framework. However, many important adaptive processes result in weak, multilocus molecular signatures. These processes, including selection on standing genetic variation, are frequently the source of contemporary adaptation to changing environmental conditions, and so are especially important to identify in species of conservation concern (Savolainen *et al.* 2013). However, it can be difficult for GEA methods to identify the relevant patterns, e.g. coordinated shifts in allele frequencies across many loci. I follow up on the univariate selection framework in Chapter 2 with an analysis of GEA detection of multilocus selection in Chapter 3. I assess the performance of a set of multivariate and machine learning methods that should, in theory, be better suited to detecting weak signals of multilocus selection (Rellstab *et al.* 2015). I find that a subset of these GEA methods are particularly effective at detecting adaptive processes that result in weak, multilocus signatures, providing an important tool for investigating the genetic basis of local adaptation and informing management actions to conserve the evolutionary potential of species of conservation concern (Chapter 3).

Finally, I apply these rigorously tested GEA methods to a reduced representation genomic data set developed for an endemic species of conservation concern, Weller's salamander (*Plethodon welleri*, Chapter 4). I describe a simple index of "adaptive

dissimilarity” that can be used to characterize the scope of adaptive variation across a species range. In combination with other metrics including neutral genetic variation, population differentiation, and effective population size, the adaptive dissimilarity index can be used to inform a range of conservation management scenarios that are improved by the explicit consideration of differences in adaptive genetic variation among populations. These scenarios include: (1) site prioritization to ensure evolutionary resiliency; (2) genetic rescue to increase genetic diversity and population fitness while minimizing the risk of outbreeding depression; and (3) assisted gene flow to maximize adaptive potential in response to rapid climate change.

In the final chapter, I build a case for the continuing importance of genetic data in conservation planning and management, and suggest next steps for improvement in landscape genomics. Advances in conservation and landscape genomics must be part of the broader effort to stem the biodiversity crisis by conserving not just genetic diversity, but also the ecological and evolutionary processes that sustain it.

2. Detecting spatial genetic signatures of local adaptation in heterogeneous landscapes

2.1 Introduction

Understanding the role of the environment in driving spatial patterns of biodiversity is a central goal in evolutionary biology and ecology. Local adaptation to environmental conditions is a major source of such spatial patterns. The extent of local adaptation is largely shaped by the interaction between selection and gene flow along selective gradients (Haldane 1930; Mayr 1963; Slatkin 1973; Nagylaki 1975; Felsenstein 1976; García-Ramos & Kirkpatrick 1997; Lenormand 2002). When selection is weak relative to gene flow, local adaptation may be inhibited due to migration load (Lenormand 2002). Conversely, when selection is strong local adaptation may occur under a migration-selection balance due to selection against maladapted migrants (Yeaman & Whitlock 2011). However, at low levels of dispersal when genetic variance within populations limits adaptation, increasing dispersal may increase genetic variance and favor local adaptation (Barton 2001; Bell & Gonzalez 2011). Many theoretical approaches to studying spatial patterns of biodiversity have tended to be in systems that are spatially implicit or have a one-dimensional linear environmental gradient (e.g., Holt & Gaines 1992; Kirkpatrick & Barton 1997; Mouquet & Loreau 2003). However, the geometry, or spatial structure, of environmental gradients may play an important role in determining spatial patterns of biodiversity (Felsenstein 1977; Palmer 1992; Lenormand

2002; Holt & Barfield 2011; Frea *et al.* 2013; Schiffers *et al.* 2014).

The spatial configuration of the landscape (i.e., arrangement of, and distance between habitat patches) can affect the probability of gene flow between habitats and therefore have important implications for the generation and maintenance of local adaptation (reviewed in Hedrick 1986, 2006; Lenormand 2002; Kawecki & Ebert 2004). For a given strength of selection gradient, local adaptation may be facilitated in landscapes with a high level of habitat aggregation (e.g., shallow continuous environmental gradients, Figure 1a, and large homogenous habitat patches, Figure 1c-d) because migrants will often disperse into similar environments (Endler 1973; Slatkin 1973). By contrast, in landscapes with low levels of habitat aggregation (e.g., highly heterogeneous habitats, Figure 1b), local adaptation may be weaker as gene flow between these habitats overwhelms selection (Garant *et al.* 2007). Importantly, these outcomes largely depend on the interaction of habitat configuration with levels of dispersal and selection strength (Slatkin 1973; Garant *et al.* 2007). For example, empirical studies have demonstrated patterns of fine-scale local adaptation (i.e., microgeographic adaptation) to heterogeneous habitats when dispersal is low (Tack & Roslin 2010; Paccard *et al.* 2013). To provide insight into the expected frequency and strength of local adaptation in nature, we must characterize how habitat heterogeneity, dispersal, and selection interact (Richardson *et al.* 2014). However, there have been few studies conducted on heterogeneous landscapes with a multi-scale structure approaching the

spatial continuum common in nature (Schiffers *et al.* 2014). Studying the effects of migration, selection and spatial structure is essential in realistic landscapes given that increasing complexity in the spatial structure of environments may generate counter-intuitive effects on local adaptation (Holt & Barfield 2011).

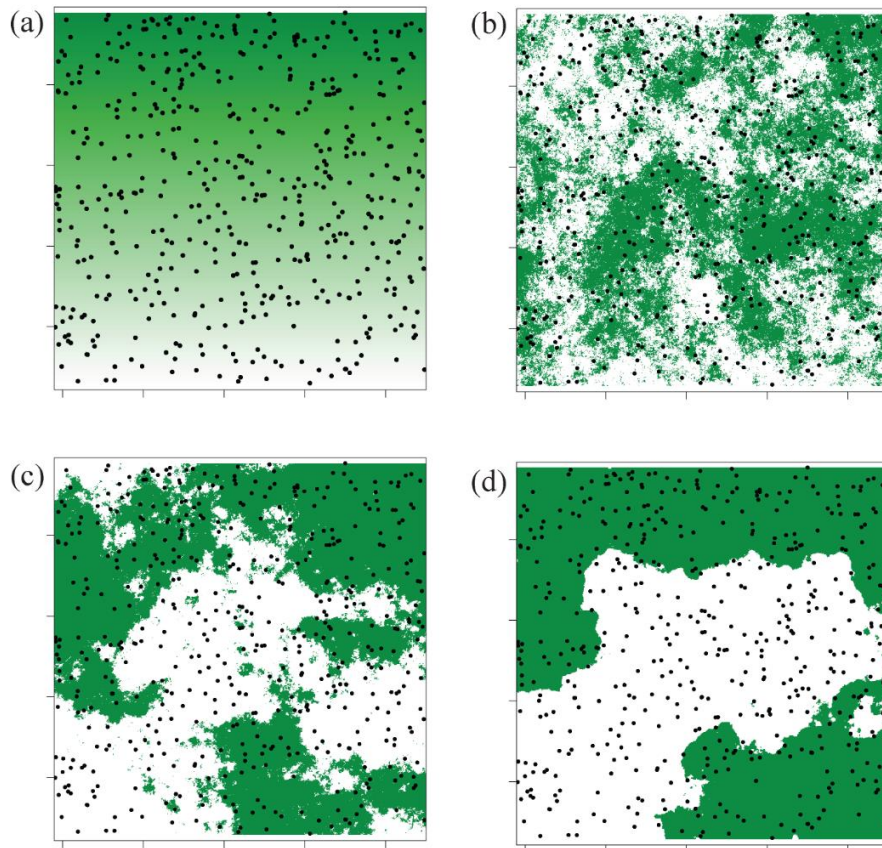


Figure 1. Landscape selection configurations used for simulations. (a) Continuous selection gradient representing selection for AA genotypes in the North (dark) and aa genotypes in the South (light). Examples of discrete selection landscapes, from least to most aggregated: (b) H1, (c) H5, and (d) H9. Dark areas represent AA habitat and light areas represent aa habitat. Points represent the 500 sampled individuals.

One approach to characterizing empirical patterns of local adaptation is to examine the extent to which spatial environmental variation coincides with genotypic variants (Hedrick *et al.* 1976; Mitton *et al.* 1977), i.e., genotype-environment association (GEA) methods (e.g., Joost *et al.* 2007, 2013; Coop *et al.* 2010; Frichot *et al.* 2013; Rellstab *et al.* 2015). GEA methods can be used to detect selection in cases where environmental gradients are continuous and when populations are not clearly distinguishable (Jones *et al.* 2013). This is an advantage when studying species that do not group into discrete populations or habitat types, or when studying species for which there is little prior ecological or genetic information (Joost *et al.* 2013; Jones *et al.* 2013). Simulation studies have examined the ability of GEA methods to detect selection under different scenarios of selection intensity, population structure, and sampling schemes (De Mita *et al.* 2013; Jones *et al.* 2013; de Villemereuil *et al.* 2014; Lotterhos & Whitlock 2015). However, to date, few simulation studies have addressed the effect of spatially heterogeneous selection surfaces on the performance of GEA methods. Additionally, no simulation studies have addressed how the interactions between landscape heterogeneity, dispersal, and selection affect our ability to detect local adaptation using GEA approaches.

Here, we explore the effects of environmental heterogeneity, dispersal ability, and selection on the strength of local adaptation through simulations. A simulation framework is valuable because it allows for stochastic demography and evolution, and

also makes the study of complex landscapes more tractable compared with analytical models (Bridle *et al.* 2010). We test a suite of GEA methods in the simulation parameter space to determine how these factors impact our ability to detect patterns of local adaptation. A major difficulty in any approach to detect selection in the genome is distinguishing between patterns of selection and population history or structure (e.g., population expansions, population bottlenecks, isolation by distance). Patterns resulting from population history can generate genotype-environment correlations similar to those underlying local adaptation, resulting in high false positive rates (i.e., incorrectly identifying a locus as under selection when it is not, Jensen *et al.* 2005; Meirmans 2012). One way to overcome this problem is to control for genome-wide patterns of variation, assumed to reflect population history. Several univariate mixed-model based GEA approaches have been used to limit false positives (e.g., generalized linear and additive mixed models, Jones *et al.* 2013; models using an empirical covariance matrix, Günther & Coop 2013; and latent factor mixed models, LFMM, Frichot *et al.* 2013). However, univariate approaches, which test one locus and one predictor variable at a time, are not ideal because in reality selection affects many loci and is driven by many variables simultaneously (Hahn 2008; Orsini *et al.* 2012). Some multivariate methods, which take high dimensional multi-locus genetic data and reduce it into a lower dimensional space, may be able to account for the joint action of selection and demography across the genome. For instance, ordination methods, which have a long history in plant and

community ecology (Whittaker 1967; van den Wollenberg 1977; ter Braak 1987; Austin 1987; Fitzpatrick & Keller 2015) extract trends from multivariate data by summarizing these data into a reduced set of uncorrelated axes (Jombart *et al.* 2009; Legendre & Legendre 2012). The similarities between community ecology and genomic data, namely a large number of variables (species or loci) observed at a set of sampling locations (sites or individuals/demes), implies that these analytical techniques could be effectively applied to large genomic data sets (e.g., Fitzpatrick & Keller 2015).

In a GEA framework, we can potentially distinguish outliers by looking for loci that show unique or unusual patterns in the ordination space. Because the ordination is explaining covariation in the data, we expect it to model patterns that affect the majority of the loci, such as those that arise due to population history. While principal components analysis, a common ordination technique, has been used to detect population structure in genetic data for nearly 50 years (Cavalli-Sforza 1966), only recently has it been used to correct for population structure in genome-wide association studies (akin to GEA, Price *et al.* 2006; Patterson *et al.* 2006). In a novel use of ordination for multivariate outlier detection, Lasky and colleagues (2012) used redundancy analysis to quantify SNP variation in georeferenced *Arabidopsis* accessions with reference to geography and climate variables. We build on this and other recent empirical work using ordination methods for outlier detection (Galinsky *et al.* 2016; Duforet-Frebourg *et al.* 2016) by assessing a suite of ordination methods and a computationally efficient

correlative mixed model approach for their ability to detect selected loci under various spatial selection regimes.

2.2 Methods

2.2.1 Simulation framework

We conducted simulations in the program CDPOP v1.2 (Landguth & Cushman 2010), which models population genetic change across a landscape surface as a function of mutation, mating, gene flow, drift, and selection. Our simulations consisted of 5,000 diploid individuals with 100 bi-allelic loci; one of these loci was subject to selection (except for “no selection” runs; see details below). All loci experienced a 0.0005 mutation rate per generation, free recombination, and no physical linkage. We ran 10 Monte Carlo replicates of each simulation for a total of 1,250 generations, discarding the first 250 generations as burn-in (no selection imposed) to establish a spatial genetic pattern prior to initiating the landscape selection configurations. Three of the simulations were run with a zero mutation rate in order to assess the impact of mutation rate on detection results (Table A1, Appendix A).

2.2.2 Simulation scenarios

We generated simulations under different combinations of landscape selection configuration, selection strength, and dispersal capacity. We tested two types of

landscape selection configurations: a continuous selection gradient landscape and discrete selection landscapes (Figure 1). In the continuous selection gradient landscape (referred to as “G” landscapes), selection acted in a continuous clinal fashion along an environmental gradient with different homozygous genotypes (AA and aa) favored at different ends of the gradient (referred to as North and South), reflecting a pattern of antagonistic pleiotropy (Figure 1a; Jones *et al.* 2013). Discrete selection landscapes included discrete habitat types (type “AA” or “aa”, Figure 1b-d) in which AA and aa genotypes were favored in their respective habitat patches. For the discrete selection scenarios, we used the neutral landscape model QRULE (Gardner 1999) to simulate binary landscape maps (1024 x 1024 pixels). Habitat fragmentation was controlled with the H parameter, which affects the aggregation of habitat pixels; higher values of H lead to higher levels of aggregation. The discrete landscapes consisted of 50% of each habitat type and aggregation levels of H = 0.1 (“H1”, Figure 1b), 0.5 (“H5”, Figure 1c), and 0.9 (“H9”, Figure 1d). We produced 10 replicate landscapes for each H value in order to average across stochastic variation among simulated landscapes.

Across these different spatial selection configurations, we tested the effects of varying selection strength, mediated through density-independent (i.e., environment-driven) mortality (s) determined by genotypes at the selected locus. Selection strengths included $s = 0.01$ or “1%”, $s = 0.05$ or “5%”, $s = 0.10$ or “10%”, and $s = 0.50$ or “50%”. We also included simulations with “no” selection ($s = 0$) as a null model. In the continuous

selection gradient scenario, AA experienced 0% mortality in the North and s mortality (either 1%, 5%, 10%, or 50%) in the South, while the aa genotype was given the opposite selection gradient surface (0% mortality in the South and s mortality in the North). The Aa genotype experienced uniform density-independent mortality across the surface equal to the mean mortality of the two homozygotes at the extreme ends of the gradient ($s/2$; e.g., 25% density-independent mortality for 50% selection). For the discrete selection landscape scenarios, AA individuals had no mortality in “AA” patches, and experienced 1%, 5%, 10%, or 50% mortality if they occurred in “aa” patches. Individuals with aa genotypes at the locus under selection experienced the opposite selection gradient. The Aa genotypes again experienced uniform selection ($s/2$) across the entire surface.

Finally, we tested the effects of six dispersal levels (3%, 5%, 10%, 15%, 25%, and 50%) that represent the maximum percentage of the landscape surrounding an individual that is available for movement and mating. These dispersal levels represent a range of biologically realistic dispersal distances per generation, from minimal dispersal (3%, e.g., terrestrial salamanders or gravity-dispersed seeds) to long-distance dispersal (50%, e.g., passerine birds or wind-dispersed seeds). Mating pairs of individuals and dispersal locations of offspring were chosen based on a random draw from the inverse-square probability function of distance, truncated with the specified maximum distance.

Mating parameters represented a population of unisexual individuals with females and males mating with replacement. The number of offspring produced from mating was determined from a Poisson distribution ($\lambda = 4$), which produced an excess of individuals each generation to maintain a constant population size of 5,000 individuals at every generation. Carrying capacity of the simulation surface was 5,000 individuals. Excess individuals were discarded once all 5,000 locations became occupied, which is equivalent to forcing out emigrants once all available home ranges are occupied (Balloux 2001; Landguth & Cushman 2010).

2.2.3 Isolation by distance and local adaptation

We sampled 500 randomly selected individuals from the 5,000 available individuals in the simulation space. This same set of 500 individuals were sampled from each simulation for all subsequent analyses (plotted in Figure 1). We did not vary sample size or sampling scheme in this analysis, although assessing the impact of sample size and sampling approaches will be an important area for follow-up (see “Future Directions”). We measured isolation by distance (IBD) across all loci in each simulation using spatial eigenfunction analysis and multivariate linear regression, as proposed by Diniz-Filho *et al.* (2013) and Legendre *et al.* (2015). First we applied a principal coordinate analysis (PCoA, details below) to the pairwise multivariate genetic distance matrix, which was calculated using Bray-Curtis distance (Bray & Curtis 1957).

We retained PCoA axes based on the broken-stick criterion (Legendre & Legendre 2012); retained axes were used as the response data in the subsequent redundancy analysis (multivariate linear regression, or RDA, details below). Spatial eigenfunctions (distance-based Moran's eigenvector maps, dbMEMs) were calculated from the coordinates of the samples and used as predictors in the RDA. Forward selection was used to reduce the number of dbMEMs (Blanchet *et al.* 2008). We calculated adjusted R² statistics (R²_{adj}) and assessed significance using 1000 permutations. These analyses used the packages "vegan" (Oksanen *et al.* 2013), "PCNM" (Legendre *et al.* 2012), "boot" (Canty & Ripley 2012), and "packfor" (Dray *et al.* 2011) in R v. 2.15.2 (R Development Core Team 2012). These results were compared to r² values derived from simple Mantel's tests of Bray-Curtis genetic distances and the log of geographic distance, using the "ecodist" package (Goslee & Urban 2007). Mantel r values were squared to facilitate comparison with R²_{adj} statistics from spatial eigenfunction and redundancy analysis (Table A2, Appendix A).

To assess the strength of local adaptation, we quantified the relationship between allele frequencies and selection gradients. To do so, we converted the allele frequency at the locus under selection to the number of "A" alleles, and arbitrarily converted selective gradients to numerical values: for continuous landscapes we used the value of the continuous habitat (ranging between 0 and 1) occupied by each individual; for discrete landscapes we used the value of the discrete habitat (0 or 1, corresponding to

“aa” or “AA” habitat) occupied by each individual. Local adaptation was then determined by Pearson correlation between the allele frequency and selective gradient.

2.2.4 Genotype-environment association methods

We used both multivariate and univariate GEAs to assess the genetic signature of local adaptation. Multivariate ordination methods take two main forms: indirect ordinations, which use internal patterns of association in the genetic data to explain as much genetic variability as possible in the smallest number of axes; and constrained ordinations, which use a similar approach but restrict the ordination axes to be combinations of supplied explanatory variables. We used two indirect ordinations and two constrained ordinations to detect covariation between allele frequencies and environmental variables (described below). More details of ordination methods can be found in Legendre & Legendre (2012), with representative applications to genetic data in Jombart *et al.* (2009).

Principal components analysis (PCA) is an indirect ordination that constructs a new set of axes for a multivariate dataset that maximally explain the variance in the data. This approach uses linear combinations of the original axes and preserves the Euclidean distance among objects. Principal coordinate analysis (PCoA) is an indirect ordination similar to PCA. However, PCoA is an eigenanalysis of the distance (or any distance-based metric) among observations. Where PCA uses linear combinations of the

original axes, PCoA axes are influenced by the chosen distance metric, producing a representation of objects in Euclidean space while preserving the chosen distance metric. For example, PCoA of a Euclidean distance matrix would yield a PCA solution.

Redundancy analysis (RDA) is a constrained ordination that extends linear regression to multivariate response data in order to maximize the proportion of the response variable that is explained. Linear combinations of the response variable (in this case, genetic data) are modeled as a function of linear combinations of the predictors (in this case, environmental data). Redundancy analysis involves a two-step process in which a multivariate linear regression is computed between genetic and environmental data to produce a matrix of fitted values, then a PCA of the fitted values produces canonical axes, which are linear combinations of the original explanatory variables. Distance-based redundancy analysis (dbRDA) is the constrained version of PCoA and the analogue of an RDA based on a dissimilarity matrix. In this case, genetic data are subject to PCoA and the resulting eigenvectors are used as the response variable in RDA, producing the dbRDA ordination.

We compared these ordination methods to latent factor mixed models (LFMMs), which use a hierarchical Bayesian mixed modeling approach to identify allele-environment correlations while modeling residual population structure with “latent factors” (Frichot *et al.* 2013). Latent factors are similar to principal components; in fact, when the number of latent factors (K) equals the number of loci in the data set, it is

analogous to a PCA (Frichot *et al.* 2013). The computational efficiency of LFMMs comes from the flexibility to use a smaller latent factor value than the total number of loci. The value of K can have a large impact on LFMM results: larger values of K increase false negative rates while smaller values of K increase false positive rates. For this reason, we used two approaches to determine the value of K (see below).

Genetic data were coded as the number of “A” alleles at each locus (monomorphic loci were removed). We standardized genetic and environmental data (i.e., scaled to unit standard deviation and centered on the mean) for PCA and RDA and calculated multivariate Bray-Curtis distances for PCoA and dbRDA. For continuous selection gradient analyses, we standardized two independent environmental variables: the x-coordinate location of an individual (“x”) and the y-coordinate location of an individual (“y”). For discrete selection simulations, a third standardized habitat variable (“habitat”) was also used, which describes whether an individual was located in an “AA” or “aa” patch (calculated using the “raster” package, Hijmans 2015).

For all ordinations, outlier loci were identified on each of the first three ordination axes as those loci with a “locus score” that was ± 3 SD from the mean score for that axis. Locus scores are the coordinates of each locus in the ordination space (called “species scores” in the “vegan” package). For PCoA, where locus scores are not automatically calculated, we computed weighted average scores for each locus using the ordination score and SNP allele frequency (function “wascores” in “vegan”). Once

outlier loci were identified, they were then tested for association with environmental variables by calculating the correlation between the allele frequencies at that locus and each environmental variable. Significant relationships had a p-value < 0.001 . All ordinations were conducted using the “vegan” package.

For LFMMs, we used two methods to determine the value of K: the Patterson method (also called the Tracy-Widom test, Patterson *et al.* 2006) and the Minimum Average Partial Test (MAP, Shriner 2012) While the Patterson approach tends to overestimate the number of significant principal components, resulting in larger values of K, the MAP approach tends to estimate smaller values of K (Table A3, Appendix A). Values of K were calculated using the “RMTstat” package (Johnstone *et al.* 2009) and code provided by Daniel Shriner (2012). Results were comparable across both K selection methods, however the Patterson approach generally resulted in lower false positive rates. LFMM results using the Patterson K are presented here, with MAP K results presented in Table A4, Appendix A. We ran LFMMs using the command line version (1.2) for Linux, downloaded from <http://membres-timc.imag.fr/Eric.Frichot/lfmm/software.htm>. We used 1,200 iterations and a burn-in period of 200 and tested a subset of models to ensure results converged at this run length. LFMM outliers were detected as those loci with a p-value < 0.001 after Bonferroni correction.

For each GEA method, we calculated the following metrics and averaged across ten replicates for each simulation scenario: true positive rate (TPR, the number of correct positive detections out of one possible), false positive rate (FPR, the number of incorrect positive detections out of 99 possible), and a “GEA index” that assesses parameter estimation for each method (i.e., correctly identifying the driving environmental variable). The GEA index ranges between 3 (best performance) and 0 (worst performance) and was coded as follows for continuous selection gradients, where the locus under selection was driven by y : 3 = the correct identification: y is the most significant variable identified; 2 = y is significant but less significant than x ; 1 = y is not detected as significant, but x is detected; and 0 = no environmental variable is detected. Similarly, the GEA association index for discrete selection simulations was coded as follows: 3 = the correct identification: habitat is the most significant variable identified; 2 = habitat is significant but less so than y or x , 1 = habitat is not detected as significant, but y or x are detected; and 0 = no environmental variable is detected as significantly associated with the locus under selection. Spurious correlations (GEA index = 1) were distinguished from “no detection” (GEA index = 0) since we expect that the spatial dependence of environmental predictors will sometimes result in correct identification of a locus under selection but incorrect detection of the driving predictor (Wagner & Fortin 2005).

2.3 Results

2.3.1 Isolation by distance and local adaptation

We assessed genome-wide IBD using spatial eigenfunction analysis and RDA. As expected, dispersal distance primarily shaped patterns of IBD across simulations. IBD increased with decreasing dispersal distance, ranging from a minimum $R^2_{adj} = 0.01$ at 50% dispersal capacity to a maximum $R^2_{adj} = 0.36$ at 3% dispersal capacity (Figure 2a). By contrast, increasing selection strength and increasing aggregation of habitat (i.e., factors that increase the strength of local adaptation) led to only small increases in patterns of genome-wide IBD (Figure 2a). Detection of IBD via spatial eigenfunction/RDA analysis and Mantel's tests were comparable, though the strength of the relationship was always weaker for Mantel's tests (Table A2, Appendix A; Diniz-Filho *et al.* 2013).

The strength of local adaptation was determined by quantifying the relationship between the allele frequency of the selected locus and selection gradients. Habitat configuration had a major effect on the strength of local adaptation. Overall, local adaptation increased with increasing levels of habitat aggregation (i.e., lowest for H1 and highest for continuous gradient habitats, Figure 2b and Figure 3). The effect of habitat configuration on the strength of local adaptation was weakest under high dispersal and weak selection, and became stronger as dispersal decreased and selection increased (Figure 3). All landscape configurations showed a pattern of larger increases

in local adaptation from 1% to 5% selection and 10% to 50% selection, with a much smaller increase from 5% to 10% selection (Figure 3).

Dispersal level had the strongest effect on patterns of local adaptation under moderate (5% and 10%) selection strengths (Figure 3). The average increase in the strength of local adaptation from the highest (50%) to the lowest (3%) dispersal level was nearly two times greater under 5% and 10% selection compared to 1% and 50% selection (Figure 3). At the highest dispersal levels (25-50%), the strength of local adaptation remained high under 50% selection (Figure 3), indicating that selection was strong enough to maintain local adaptation despite high gene flow.

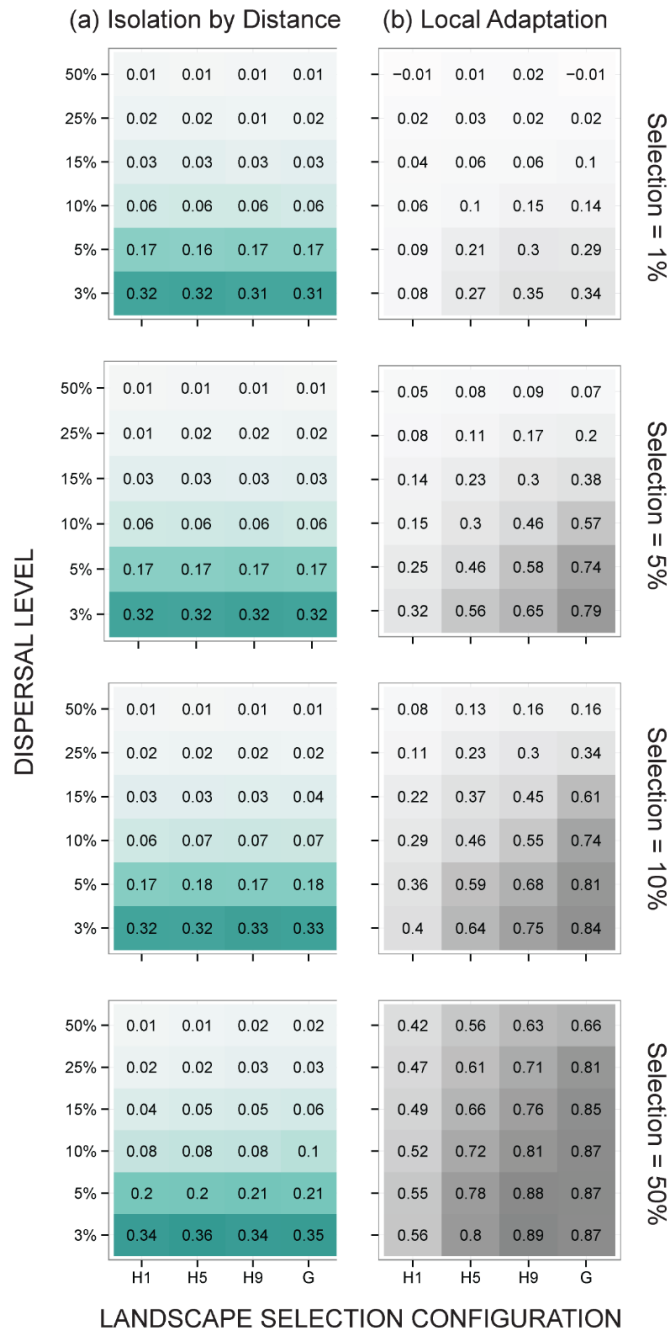


Figure 2. Isolation by distance, assessed by spatial eigenfunction and redundancy analysis, averaged across ten replicates of each simulation scenario (a). The strength of local adaptation, assessed by correlation between the selected locus and environment, averaged across ten replicates of each simulation scenario (b).

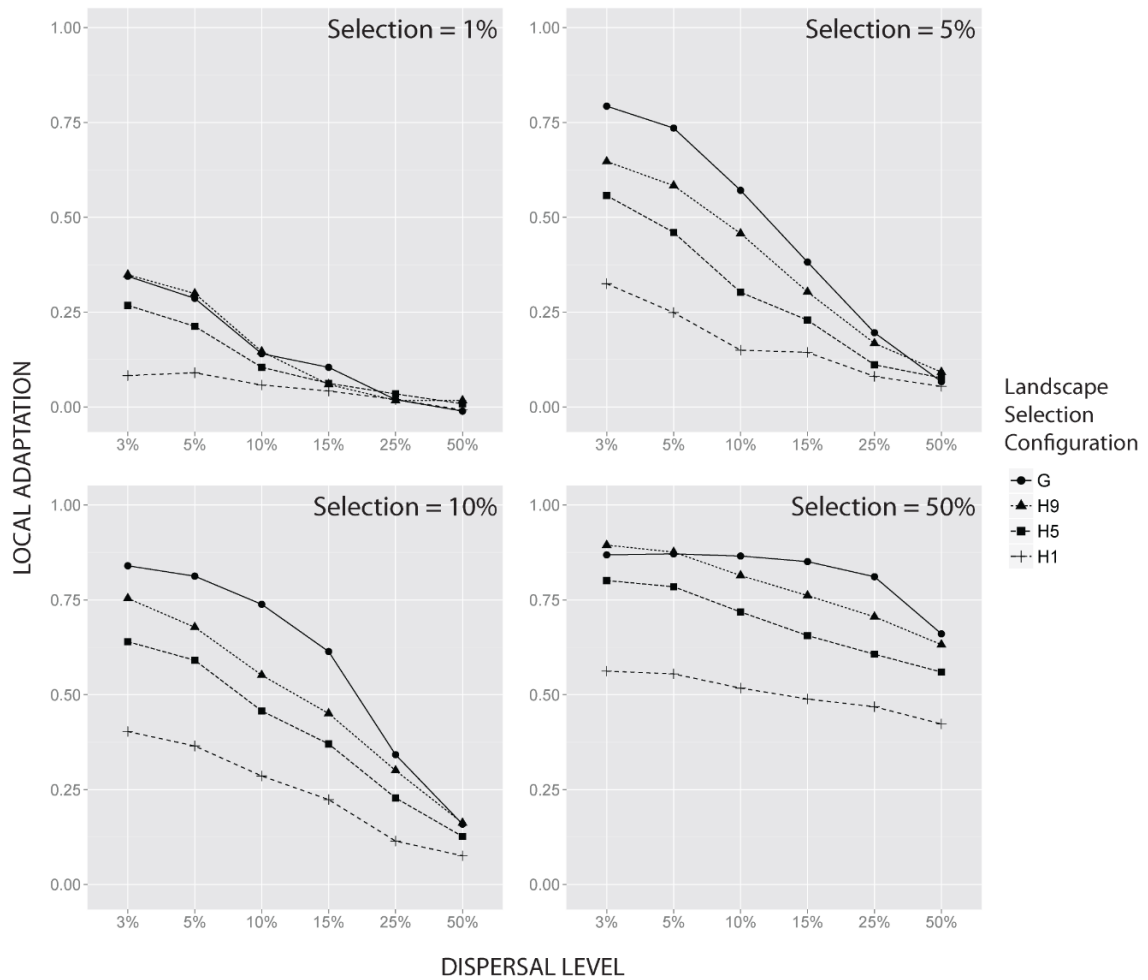


Figure 3. Strength of local adaptation across dispersal levels and landscape selection configurations, with one plot per selection strength. Local adaptation is assessed by correlation between the selected locus and environment, averaged across ten replicates of each simulation scenario.

2.3.2 Effects of landscape, selection, and dispersal on detection probability

We found that highly aggregated selection landscapes (continuous selection gradients, highly aggregated discrete habitats) produced stronger local adaptation (Figure 2b and Figure 3) and correspondingly detection methods were generally more powerful (higher TPRs, Figure 4) and better able to detect the driving environmental variable (stronger GEA indices, Figure 5).

Under 1% selection the selected locus was rarely detected by most methods, regardless of dispersal level (Figure 4). Under 5% and 10% selection, TPRs were negatively associated with dispersal capacity, with the highest dispersal values inhibiting detection of the selected locus. However, with 50% selection TPRs for most methods were high regardless of dispersal capacity. Generally, lower dispersal rates resulted in higher levels of IBD and local adaptation (Figure 2), accompanied by higher TPRs (Figure 4) and stronger GEA indices (Figure 5).

2.3.3 Method comparison

False positive rates across ordination methods were uniformly low (0-2%, Figure 6a-d) and unaffected by habitat configuration, selection strength, or dispersal capacity. The univariate method we tested, LFMM (using Patterson K), had much higher FPRs compared to ordination methods at low to moderate dispersal levels (3-15%). Average

FPRs greater than 40% were common for LFMM with 3% and 5% dispersal, with a maximum average FPR of 55% on gradient selection surfaces (Figure 6e). Although LFMMs had the highest power under weak selection/low dispersal simulations (Figure 4e), FPRs for these scenarios averaged 40% (Figure 6e). Ordinations had uniformly low TPRs and FPRs across weak selection scenarios. FPRs for no selection simulations (used as a null model) were nearly identical to FPRs in selection simulations (Figure A1, Appendix A).

Of the four ordination methods, constrained ordinations (RDA and dbRDA) had the highest TPRs (Figure 4) and strongest GEA indices (Figure 5) across all scenarios when compared to indirect methods (PCA and PCoA). TPRs and GEA indices were generally high across most dispersal levels for constrained ordinations, while indirect methods showed a pattern of stronger TPRs and GEA indices at intermediate dispersal levels.

2.3.4 Effect of mutation rate

A subset of the simulations were run with a zero mutation rate in order to assess the impact of the chosen mutation rate (0.0005 per generation) on detection results. Differences in detection rates, IBD, and local adaptation were assessed with paired t-tests. There were few significant differences at $\alpha=0.05$: four cases for FPRs and two cases for IBD (Table A1, Appendix A).

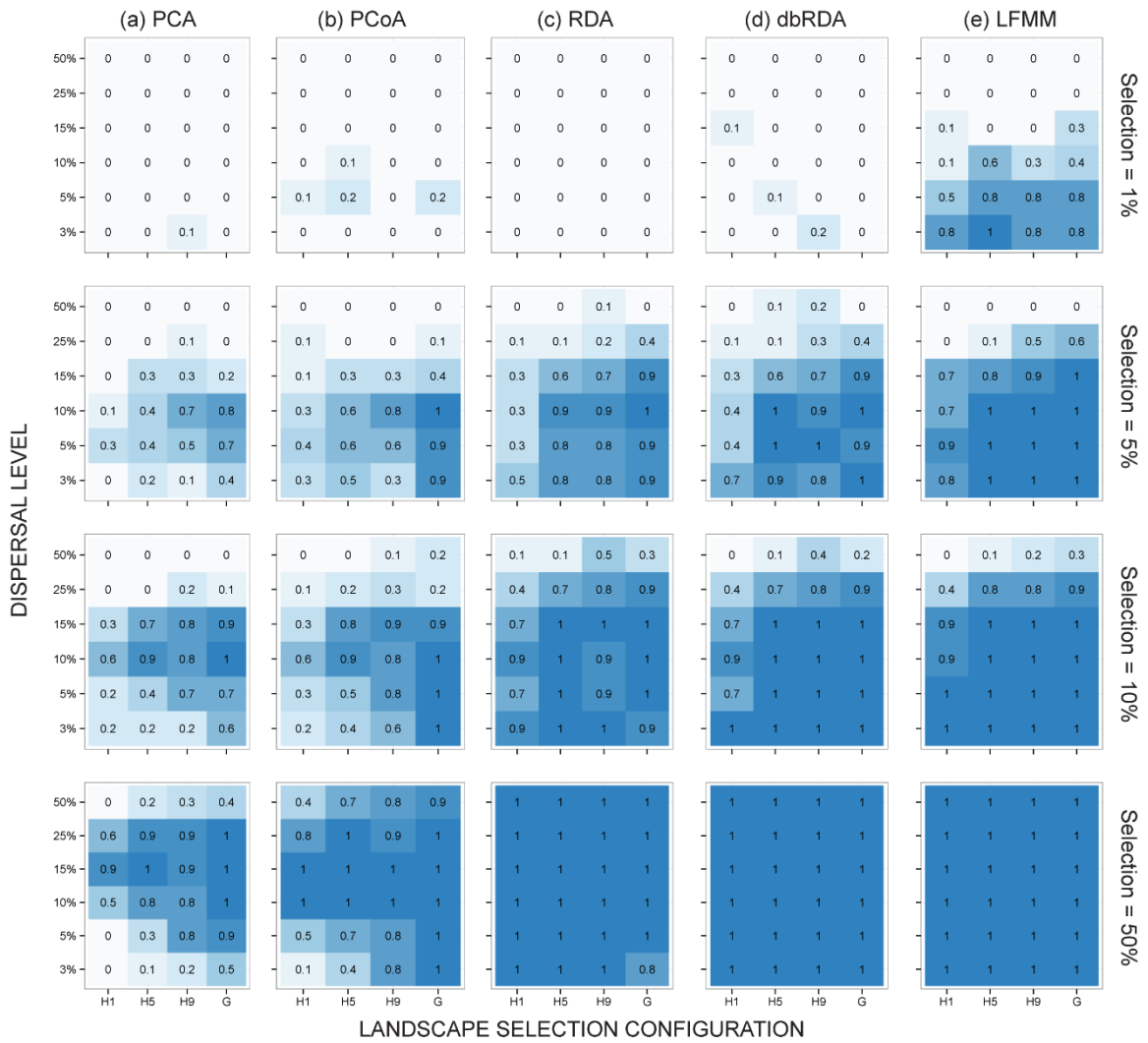


Figure 4. Average true positive rate (TPR) across ten replicates of each simulation scenario. TPR scales from 0 (worst performance, 0% TPR, light shades) to 1 (best performance, 100% TPR, dark shades). Results for (a) principal components analysis, (b) principal coordinates analysis, (c) redundancy analysis, (d) distance-based redundancy analysis, and (e) latent factor mixed models.

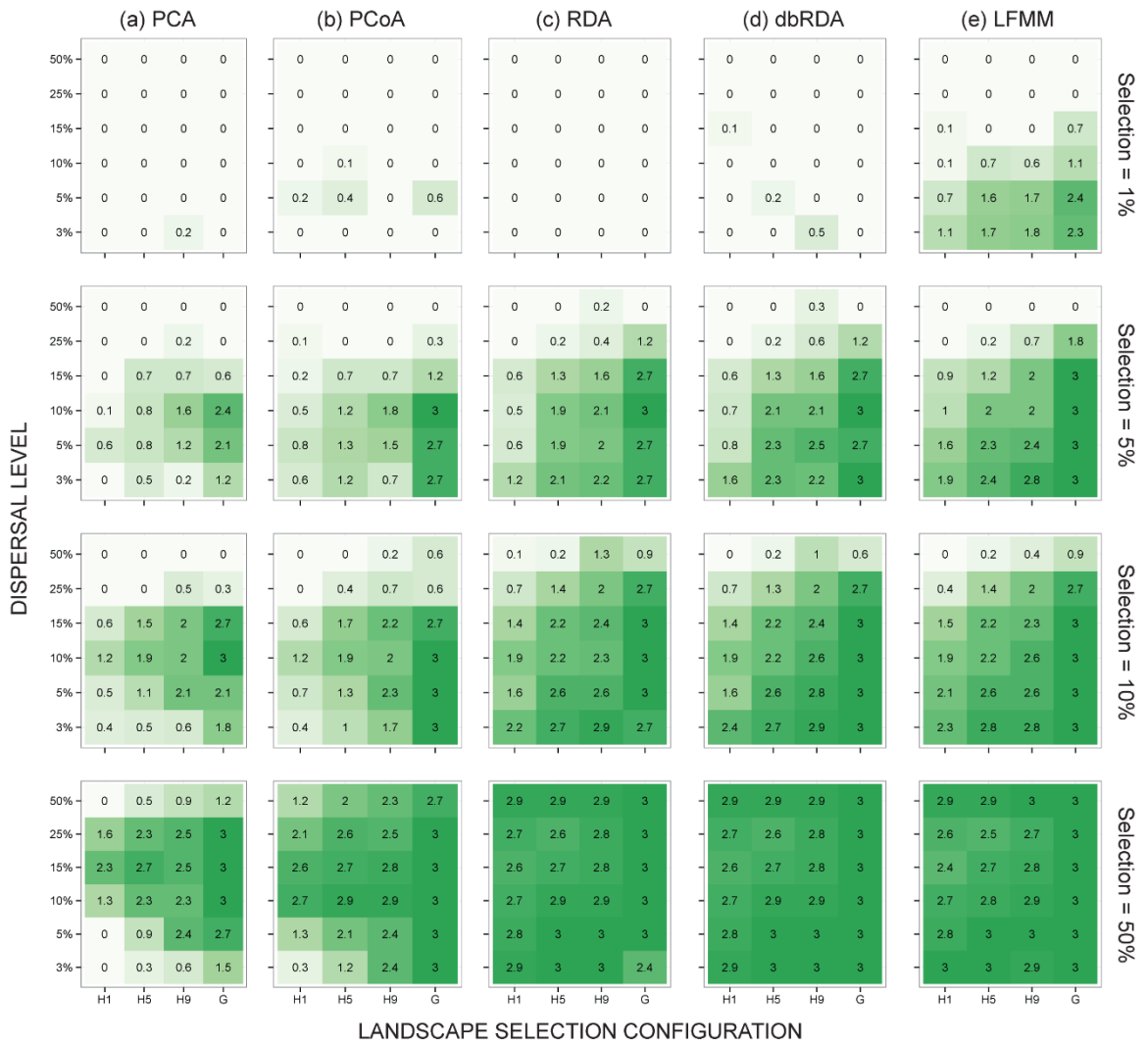


Figure 5. Average genotype-environment association (GEA) index across ten replicates of each simulation scenario. Correct detection (3) has dark shading, with no detection (0) in light shading. Results for (a) principal components analysis, (b) principal coordinates analysis, (c) redundancy analysis, (d) distance-based redundancy analysis, and (e) latent factor mixed models.

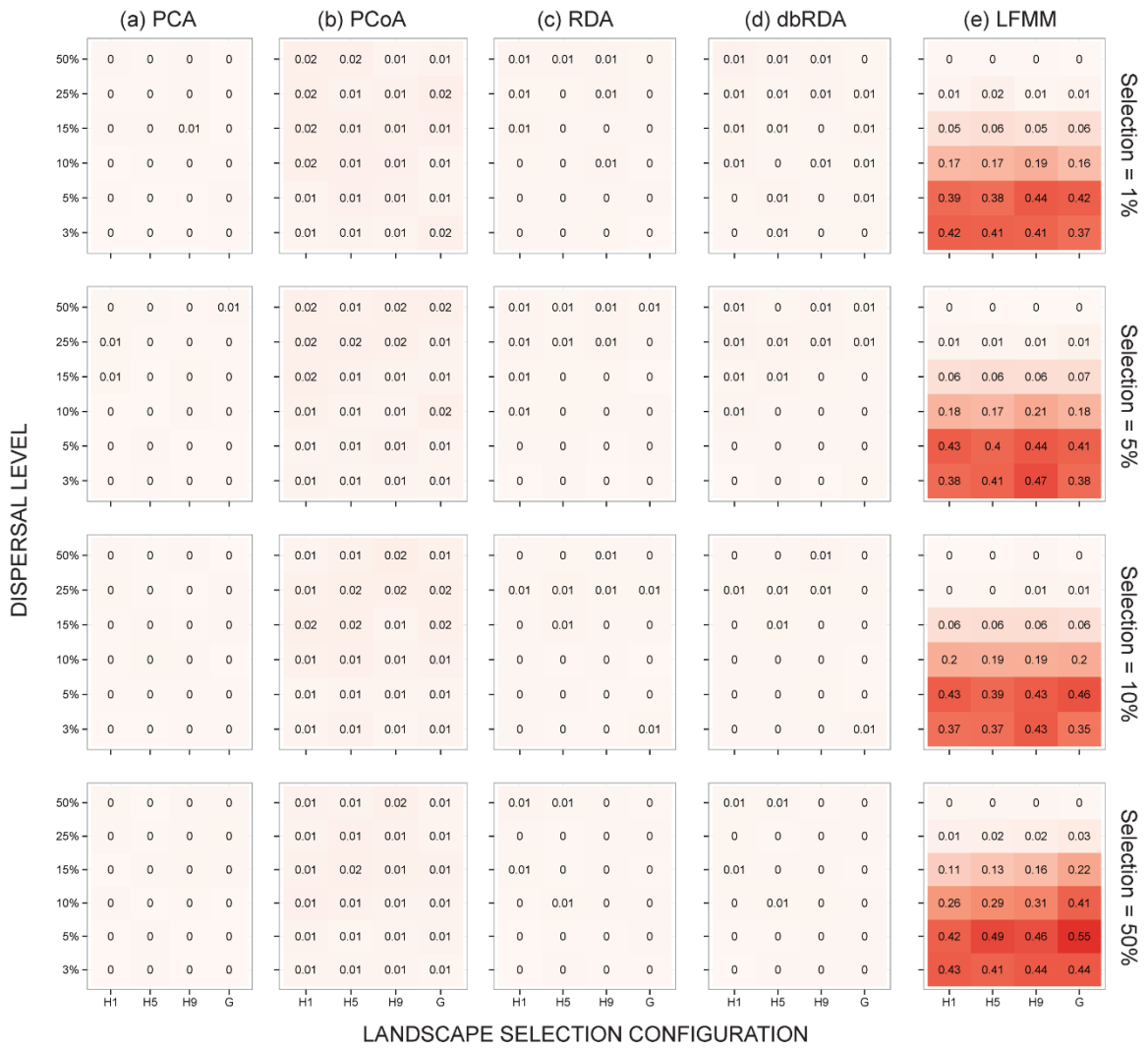


Figure 6. Average false positive rate (FPR) across ten replicates of each simulation scenario. FPR scales from 0 (best performance, 0% FPR, light shades) to 1 (worst performance, 100% FPR, dark shades). Results for (a) principal components analysis, (b) principal coordinates analysis, (c) redundancy analysis, (d) distance-based redundancy analysis, and (e) latent factor mixed models.

2.4 Discussion

Spatial environmental variation plays a central role in maintaining spatial patterns of biodiversity, many of which are due to local adaptation. However, many populations fail to adapt along environmental gradients, partly due to the interaction between dispersal and the spatial structure of the environment. Existing knowledge of the relationship between spatial environmental structure and local adaptation has been largely based on the study of linear or monotonic environmental gradients (e.g., Holt & Gaines 1992; Kirkpatrick & Barton 1997), with few studies considering how the complexity of realistic landscapes may affect patterns of local adaptation (Holt & Barfield 2011; Schiffers *et al.* 2014). Our understanding of the geographic mosaic of selection depends on our ability to detect genomic signatures of selection in realistic landscapes. To this end, we examined how the interplay between environmental heterogeneity, dispersal ability, and selection affects the strength of local adaptation and our ability to detect selection in continuously distributed populations. Our study provides a quantitative assessment of the spatial, dispersal, and selective conditions that favor the generation and maintenance of local adaptation, and may guide more accurate predictions regarding the strength of local adaptation in nature.

We found strong effects of habitat configuration on local adaptation (supporting previous work by Lotterhos & Whitlock (2014)). The strength of local adaptation increased as habitat was more aggregated and as dispersal levels decreased (Figure 2b

and Figure 3). This pattern is a product of the interplay of habitat patchiness and the chance a dispersing individual will end up in a suitable habitat patch (i.e., the flow of alleles across environmental gradients, Lenormand 2002). As habitat aggregation increases, the spatial autocorrelation in selective gradients also increases, decreasing the probability of gene flow between different selective regimes. Additionally, the effect of habitat configuration on local adaptation was greater under limited dispersal and stronger selection (Figure 3). The lack of an effect of configuration under high dispersal and weak selection may be explained by the theoretical result of Slatkin (1973), who found that local adaptation will not occur below the “characteristic length” (equal to the average dispersal distance divided by the square root of the selection differential). That is, when dispersal is high and selection weak, the characteristic length is very high, potentially higher than even our most aggregated landscapes. Indeed, in more spatially aggregated landscapes (H5, H9, and continuous gradient), weak selection was largely ineffective in generating a pattern of local adaptation, suggesting that when selection is weak the extent of landscape heterogeneity is of minor importance in shaping or preventing local adaptation. We did not find evidence that habitat aggregation mediated non-linear effects of dispersal on local adaptation via effects on genetic variance (Barton 2001), likely because evolution in our simulations was not limited by genetic variance. Our findings closely parallel results from stochastic spatially explicit simulations of both population genetics (Behrman & Kirkpatrick 2011; Schiffers *et al.* 2014) and ecological

communities (Palmer 1992; Lasky & Keitt 2013), where dispersal and the spatial structure of environmental gradients interact to determine the importance of the environment in driving spatial biodiversity.

We found that local adaptation in our simulated fine-grained landscapes (H1) occurred even in the face of substantial gene flow when selection was moderate to strong (10%-50%, Figure 2b and Figure 3). Our findings support results from empirical case studies of local adaptation to small, patchily distributed habitats, known as microgeographic adaptation (Allen & Sheppard 1971; Tack & Roslin 2010; Richardson *et al.* 2014), which requires very strong selective gradients or very restricted gene flow (Slatkin 1975). Additionally, the more pronounced decline in local adaptation with increasing gene flow for moderate selection strengths (5% to 10%) illustrates a shift in the migration-selection balance response across selection levels; while weak (1%) and strong (50%) selection show only modest changes in local adaptation across dispersal levels (very low and very high levels of local adaptation for 1% and 50% selection, respectively), moderate selection strengths are much more sensitive to increasing gene flow (Figure 3).

We found evidence for modest genomic divergence driven by limitations on gene flow due to selection (i.e., “isolation by environment”, Barton 1979; Wang & Bradburd 2014). Specifically, changes in habitat aggregation and the strength of selection had small effects on spatial structure at neutral sites (Figure 2a). The weak effect of

selection on neutral sites here was likely due to the lack of physical linkage between loci in our simulations (i.e., high recombination) and monogenic local adaptation (Barton 1979).

We did not explore several factors that may play an important role in determining the strength of local adaptation and our ability to detect it, such as carrying capacity and genetic architecture. Carrying capacity can interact with dispersal to affect local adaptation, as lower carrying capacity increases the chance of population extinction under high migration load (Bridle *et al.* 2010). Additionally, polygenic architecture may interact with spatial structure of the environment. Schiffers *et al.* (2014) found that the effects of the spatial structure of selective gradients on local adaptation are contingent on the genetic architecture of traits under selection, such that under some scenarios local adaptation is weaker for polygenic traits in highly aggregated habitats. In general, migration load may be higher for polygenic traits (Lenormand 2002), due to swamping of many alleles with small fitness effects. The loci underlying polygenic local adaptation will be considerably more challenging to detect statistically (Yeaman 2015).

2.4.1 Evaluation of detection methods

In order to leverage information contained in population genomic datasets, it is essential to develop statistical approaches capable of robustly detecting loci underlying local adaptation in complex landscapes. This is a major challenge because the factors

that facilitate local adaptation (e.g., limited dispersal) may also produce genome-wide patterns that confound the detection of loci under selection (e.g., population structure and IBD). As expected, detection methods generally had their poorest performance under combinations of weak (1%) selection, high dispersal (25% to 50%), and high habitat heterogeneity (H1). Increasing selection from 1% to 5% resulted in pronounced overall improvement to detection rates, especially for ordination methods (Figure 4 and Figure 5).

The most striking result from our methods comparison is the ability of ordination techniques to effectively control for population structure due to IBD, a major contributor to high false positive rates when testing for loci under selection (Meirmans 2012). Ordination methods produced uniformly low FPRs (0-2%, Figure 6a-d), in contrast to LFMMs, which produced very high FPRs (up to 55%, Figure 6e) under low dispersal scenarios. Low dispersal generates high levels of IBD (Figure 2a), contributing to spurious genotype-environment correlations (Meirmans 2012). However, under weak (1%) selection and limited dispersal, there is a tradeoff between power to detect local adaptation and controlling for IBD. Ordinations have uniformly low power under weak selection, while LFMM have higher power under weak selection/low dispersal scenarios (Figure 4), which comes at the cost of high false positive rates (39-44%, Figure 6e). While LFMMs incorporate latent factors in an effort to control for population structure, we find that this approach is insufficient for the strong signals of IBD generated with low

dispersal. This is likely due to the ambiguity in determining the number of latent factors (K) at low dispersal levels in our individual-based framework (Table A3, Appendix A). In low dispersal simulations there was large disagreement between the two assessments of K (the Patterson and MAP approaches), whereas in higher dispersal simulations the two methods converged on a similar value (Table A3, Appendix A). The reasons for divergence in estimating K under high IBD scenarios is unclear. However, even when using the more conservative Patterson method to assign K, FPRs were high in cases of strong IBD (Figure 6e and Figure 2a).

Ordinations take a different approach to controlling for population structure that does not require the a priori assignment of structure. Generally, the ordinations tested here take the multidimensional scatter of genetic data and create a reduced set of axes that maximize the variability explained (Legendre & Legendre 2012). Because processes that produce population structure are expected to affect all neutral loci in a similar manner, these loci will tend not to show unique or unusual patterns in the ordination space; instead, the first few ordination axes will capture these main drivers of structure.

Among the four ordination methods, we found two interesting patterns: (1) constrained ordinations have the highest TPRs (Figure 4) and strongest GEA indices (Figure 5) across all scenarios when compared to indirect methods; and (2) indirect methods show a pattern of stronger GEA indices and TPRs at intermediate dispersal levels. The better performance of constrained over indirect ordinations is related to

differences in how the ordination axes are derived between the two approaches. Constrained ordinations find combinations of multiple predictor variables that explain multiple response variables. The inclusion of predictor variables that are thought to drive selection essentially reorders the ordination axes to prioritize trends explained by those variables. In the case of our simulations, this means that the locus under selection will tend to be detected on one of the first three constrained axes (since we used three explanatory variables, Figure 7c-d). By contrast, indirect ordinations, which proceed based solely on internal patterns of variability in the genetic data (with no reference to environment), are unlikely to detect the locus under selection within the first few ordination axes. This is because the anomalous pattern created by that locus is unlikely to have a signal that is strong enough to load on the first few axes (Figure 7a-b).

This difference in how the ordination axes are prioritized between indirect and constrained methods may also explain why the adaptive signals detected by indirect ordinations were strongest at intermediate dispersal levels (Figure 4a-b, Figure 5a-b). When dispersal was very high, gene flow resulted in the selected locus being common in areas where it was maladaptive, weakening the signal of local adaptation (Figure 2b, García-Ramos & Kirkpatrick 1997; Lenormand 2002, Garant *et al.* 2007). When dispersal was limited, the adaptive signal was relegated to minor axes (with low overall explanatory power) since the first few ordination axes were dominated by explaining the high IBD signal in the data (Figure 2a, Figure 7a-b). Searching through all of the

minor axes (in this case 100 axes total) for the outlier signal would likely result in a very high false positive rate.

These results make a strong case for constrained ordinations as an important GEA analytical tool due to their high power under moderate to strong selection (5% to 50%) combined with very low false positive rates (0-1%). Additionally, these methods can reveal genetic structure varying from clusters to clines, have no underlying population genetic assumption (e.g., Hardy-Weinberg equilibrium), and are computationally efficient (Jombart *et al.* 2009). Their low power under weak (1%) selection, however, points to the utility of taking an ensemble detection approach, using multiple methods and looking for agreement across approaches (Jones *et al.* 2013). However, there is additional evidence from other simulation work (e.g., Tiffin & Ross-Ibarra 2014) that weak selection is difficult to detect no matter what methods are used; this will be an important area for further research (see below).

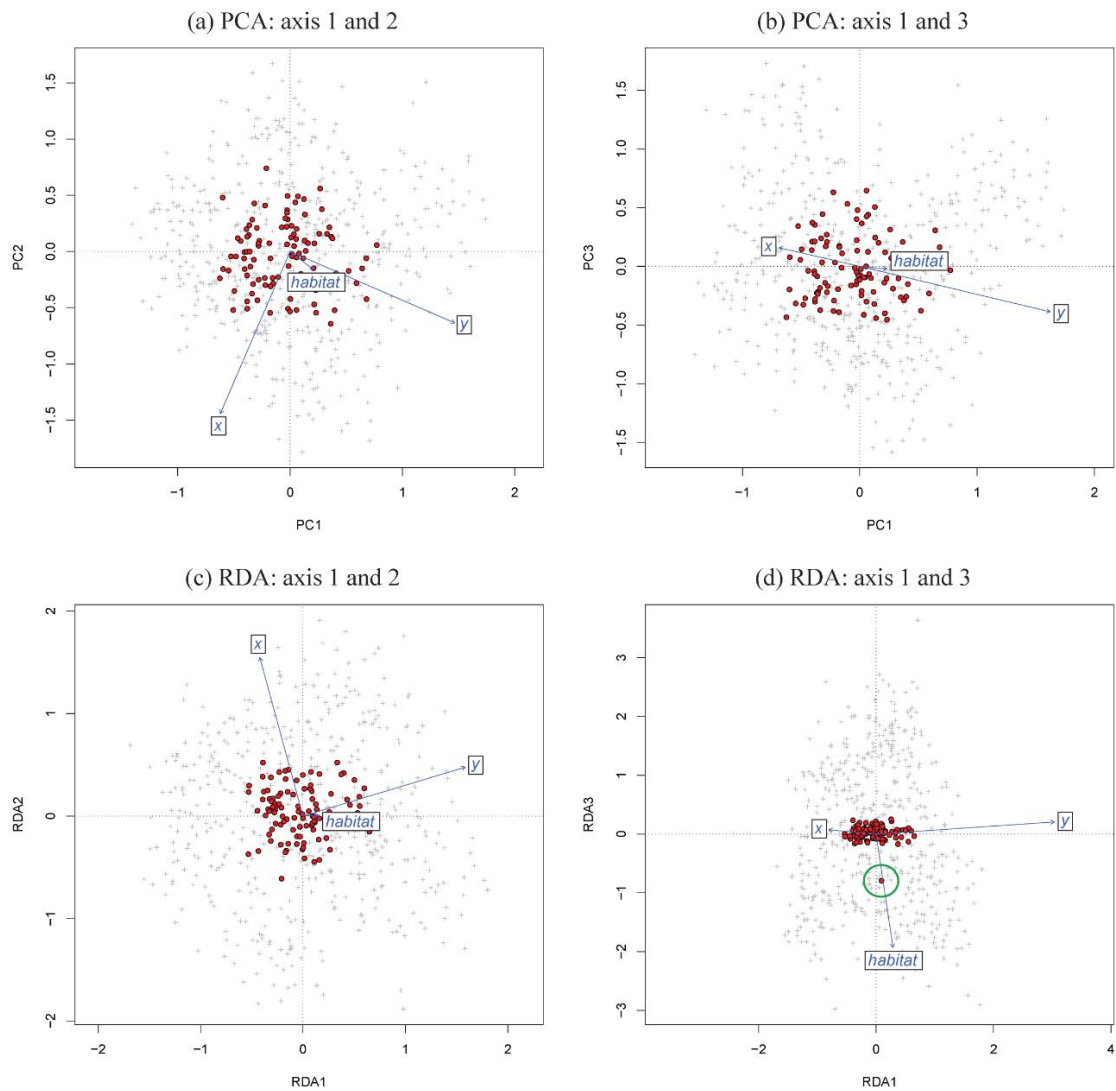


Figure 7. Examples of ordination plots for PCA (top row) and RDA (bottom row). Simulation plotted is replicate 10 from the H1 landscape configuration, strong (50%) selection, and 5% dispersal. Plots show the distribution of loci (red circles) and individual genotypes (gray pluses) in the ordination space. The correlation of the predictor variables with the axes is shown with the blue vectors. In this case, PCA did not detect the selected locus on the first three axes (a-b), while RDA did detect the selected locus (circled in green) on axis 3, correctly correlated with habitat (d). Note how x and y load strongly on the first two RDA axes (c), while habitat loads strongly on RDA axis 3 (d). This is in contrast to PCA, where habitat fails to load strongly on any of the first three axes (a-b).

2.4.2 Future directions

The number of simulation parameters we tested was necessarily limited in order to examine how combinations of habitat aggregation, dispersal capacity, and selection strength affected local adaptation and detection performance. Many variables remain to be tested including the effects of conditional neutrality (Tiffin & Ross-Ibarra 2014), temporally fluctuating selection, new mutation vs. standing variation, trait dominance, complex demographic scenarios (e.g., population expansions along environmental gradients), population size, and sampling scheme (following up on work by Lotterhos & Whitlock 2015). The ability of GEA methods to detect multi-locus selection in a controlled framework also remains untested. This is an important element for future research because adaptation often occurs via coordinated shifts in allele frequencies across large numbers of loci, many of small effect (Imhof & Schlötterer 2001; Kassen & Bataillon 2006; Le Corre & Kremer 2012; Harrisson *et al.* 2014; Yeaman 2015). A recent empirical investigation showed the promise of multivariate methods for detecting these polygenic signals of local adaptation (Bourret *et al.* 2014), while other studies suggest detecting these loci may be inherently challenging (Yeaman 2015). Studies that address the above issues will further our understanding of the conditions that shape local adaptation in wild populations and how our ability to detect selection changes under these conditions.

3. Using genotype-environment associations to identify multilocus local adaptation

3.1 Introduction

Analyzing genome scan data for loci underlying local adaptation has become common practice in evolutionary and ecological studies (Hoban *et al.* 2016). These analyses can provide insight into the mechanisms of local adaptation and inform management decisions for agricultural, natural resources, and conservation applications. Genotype-environment association (GEA) approaches are particularly promising for detecting these loci (Rellstab *et al.* 2015). Unlike differentiation outlier methods, which identify loci with strong allele frequency differences among populations, GEA approaches identify adaptive loci based on associations between genetic data and a set of environmental variables hypothesized to drive selection. Benefits of GEA include the option of using individual-based (as opposed to population-based) sampling and the ability to make explicit links to the ecology of organisms by including relevant predictors. The inclusion of predictors can also improve power and allows for the detection of selective events that do not produce high genetic differentiation among populations (De Mita *et al.* 2013; de Villemereuil *et al.* 2014; Rellstab *et al.* 2015).

Univariate statistical methods have dominated GEA since their first appearance (Mitton *et al.* 1977). These methods test one locus and one predictor variable at a time, and include generalized linear models (e.g., Joost *et al.* 2007; Stucki *et al.* 2016), variations

on linear mixed effects models (e.g., Coop *et al.* 2010; Frichot *et al.* 2013; Yoder *et al.* 2014; Lasky *et al.* 2014), and non-parametric approaches (e.g. partial Mantel, Hancock *et al.* 2011). While these methods perform well, they can produce elevated false positive rates in the absence of correction for multiple comparisons. Corrections such as Bonferroni can be overly conservative (potentially removing true positive detections), while alternative correction methods, such as false discovery rate (FDR, Benjamini & Hochberg 1995), rely on an assumption of a null distribution of p-values, which may often be violated for empirical data sets. While none of these issues should discourage the use of univariate methods (though corrections should be chosen carefully, see François *et al.* (2016) for an excellent overview), other analytical approaches may be better suited to the high dimensionality of modern genomic data sets.

In particular, multivariate and machine learning approaches, which analyze many loci simultaneously, are well suited to data sets comprising hundreds of individuals sampled at many thousands of genetic markers. Compared to univariate methods, these approaches are thought to more effectively detect multilocus selection since they consider how groups of markers covary in response to environmental predictors (Rellstab *et al.* 2015). This is important because many adaptive processes are expected to result in weak, multilocus molecular signatures. These processes include selection on standing genetic variation, recent/contemporary selection that has not yet led to allele fixation, conditional neutrality, and the quantitative basis of many adaptive

traits (Yeaman & Whitlock 2011; Le Corre & Kremer 2012; Savolainen *et al.* 2013; Tiffin & Ross-Ibarra 2014). Identifying the relevant patterns (e.g. coordinated shifts in allele frequencies across many loci) that underlie these adaptive processes is essential to both improving our understanding of the genetic basis of local adaptation, and conserving the evolutionary potential of species threatened by anthropogenic effects such as habitat fragmentation and climate change (Savolainen *et al.* 2013; Harrisson *et al.* 2014). While multivariate and machine learning methods may, in theory, be better suited to detecting these shared patterns of response, they have not yet been tested on common data sets simulating multilocus adaptation, limiting confidence in their effectiveness on empirical data.

Here we evaluate a set of these methods, as well as a popular univariate approach, using published simulations of multilocus selection (Lotterhos & Whitlock 2014, 2015). We assess detection rates across methods using a common rank-based metric, and also present results based on cutoffs used in empirical studies. We then evaluate whether explicit correction for population structure improves performance. We follow up with a test of two of these methods on their ability to detect weak multilocus selection, as well as an assessment of two approaches to combining detections across different tests. We find that constrained ordinations maintain the best balance of true and false positive rates across a range of demographies, sampling designs, sample sizes, and selection levels.

3.2 Methods

3.2.1 Statistical approaches to GEA

Multivariate statistical techniques, including ordinations such as principal components analysis (PCA), have been used to analyze genetic data for over fifty years (Cavalli-Sforza 1966). Indirect ordinations like PCA (which do not use predictors) use patterns of association within the genetic data to find orthogonal axes that fully decompose the genetic variance. Constrained ordinations extend this analysis by restricting these axes to combinations of supplied predictors (Jombart *et al.* 2009; Legendre & Legendre 2012). When used as a GEA, a constrained ordination is essentially finding sets of loci that covary with multivariate environmental patterns. By contrast, a univariate GEA is testing for single locus relationships with single environmental predictors. The use of constrained ordinations in GEA goes back as far as Mulley *et al.* (1979), with more recent applications to genomic data sets in Lasky *et al.* (2012) and Forester *et al.* (2016). In this analysis, we test two promising constrained ordinations, redundancy analysis (RDA) and distance-based redundancy analysis (dbRDA). We also test an extension of RDA that uses a preliminary step of summarizing the genetic data into sets of covarying markers (Bourret *et al.* 2014). We do not include canonical correspondence analysis, a constrained ordination that is best suited to modeling unimodal responses, although this method has been used to analyze microsatellite data sets (e.g. Angers *et al.* 1999; Grivet *et al.* 2008).

Random Forest (RF) is a machine learning algorithm that is designed to identify structure in complex data and generate accurate predictive models. It is based on classification and regression trees (CART), which recursively partition data into response groups based on splits in predictors. CART models can capture interactions, contingencies, and nonlinear relationships among variables, differentiating them from linear models (De'ath & Fabricius 2000). RF reduces some of the problems associated with CART models (e.g. overfitting and instability) by building a "forest" of classification or regression trees with two layers of stochasticity: random bootstrap sampling of the data, and random subsetting of predictors at each node (Breiman 2001). This provides a built-in assessment of predictive accuracy (based on data left out of the bootstrap sample) and variable importance (based on the change in accuracy when variables are permuted). For GEA, variable importance is the focal statistic, where the predictor variables used at each split in the tree are molecular markers, and the goal is to sort individuals into groups based on an environmental category (classification) or to predict an environmental response (regression). Markers with high variable importance are best able to sort individuals or predict responses. RF has been used in a number of recent GEA and GWAS studies (Holliday *et al.* 2012; Briec *et al.* 2015; Pavey *et al.* 2015; Laporte *et al.* 2015, 2016), but has not yet been tested in a GEA simulation framework. Finally, we compare these multivariate and machine-learning methods to a popular univariate method, latent factor mixed models (LFMM, Frichot *et al.* 2013).

3.2.1.1 Constrained ordinations

We tested redundancy analysis (RDA) and distance-based redundancy analysis (dbRDA) as implemented by Forester *et al.* (2016). RDA is a two-step process in which genetic and environmental data are analyzed using multivariate linear regression, producing a matrix of fitted values. Then PCA of the fitted values is used to produce canonical axes, which are linear combinations of the predictors. We scaled genotypes for RDA. Distance-based redundancy analysis is similar to RDA but allows for the use of non-Euclidian dissimilarity indices. Whereas RDA can be loosely considered as a PCA constrained by predictors, dbRDA is analogous to a constrained principal coordinate analysis (PCoA, or a PCA on a non-Euclidean dissimilarity matrix). For dbRDA, we calculated the distance matrix using Bray-Curtis dissimilarity (Bray & Curtis 1957), which quantifies the dissimilarity among individuals based on their multilocus genotypes. For both methods, SNPs are modeled as a function of predictor variables, producing as many constrained axes as predictors. We identified outlier loci on each constrained ordination axis based on their “locus score”, which represents the coordinates/loading of each locus in the ordination space. We use *rda* for RDA and *capscale* for dbRDA in the *vegan*, v. 2.3-5 package (Oksanen *et al.* 2013) in R v. 3.2.3 (R Development Core Team, 2015) for this and all subsequent analyses.

3.2.1.2 Redundancy analysis of components

This method, described by Bourret *et al.* (2014), differs from the approach described above in using a preliminary step that summarizes the genotypes into sets of covarying markers, which are then used as the response in RDA. The idea is to identify from these sets of covarying loci only the groups that are most strongly correlated with environmental predictors. We began by ordinating SNPs into principal components (PCs) using *prcomp* in R on the scaled data, producing as many axes as individuals. Following Bourret *et al.* (2014), we used parallel analysis (Horn 1965) to determine how many PCs to retain. Parallel analysis is a Monte Carlo approach in which the eigenvalues of the observed components are compared to eigenvalues from simulated data sets that have the same size as the original data. We used 1,000 random data sets and retained components with eigenvalues greater than the 99th percentile of the eigenvalues of the simulated data using the *hornpa* package, v. 1.0 (Huang 2015).

Next, we applied a varimax rotation to the PC axes, which maximizes the correlation between the axes and the original variables (in this case, the SNPs). Note that once a rotation is applied to the PC axes, they are no longer “principal” components (i.e. axes associated with an eigenvalue/variance), but simply components. We then used the retained components as dependent variables in RDA, with environmental variables used as predictors. Next, components that were significantly correlated with at least one of the two constrained RDA axes were retained. Significance was based on a cutoff ($\alpha =$

0.05) corrected for sample sizes using a Fisher transformation as in Bourret *et al.* (2014).

Finally, SNPs were correlated with these retained components to determine outliers. We call this approach redundancy analysis of components (cRDA).

3.2.1.3 Random Forest

The Random Forest approach implemented here builds off of work by Goldstein *et al.* (2010), Holliday *et al.* (2012), and Briec *et al.* (2015). This three-step approach is implemented separately for each predictor variable. The variables used in this study were continuous, so RF models were built as regression trees. For categorical predictors (e.g. soil type) classification trees would be used, which require a different parameterization (important recommendations for this case are provided in Goldstein *et al.* 2010).

First, we tuned the two main RF parameters, the number of trees (*ntrees*) and the number of predictors sampled per node (*mtry*). We tested a range of values for *ntrees* in a subset of the simulations, and found that 10,000 trees were sufficient to stabilize variable importance (note that variable importance requires a larger number of trees for convergence than error rates, Goldstein *et al.* 2010). We used the default value of *mtry* for regression (number of predictors/3, equivalent to ~3,330 SNPs in this case) after checking that increasing *mtry* did not substantially change variable importance or the percent variance explained. In a GEA/GWAS context, larger values of *mtry* reduce error rates,

improve variable importance estimates, and lead to greater model stability (Goldstein *et al.* 2010).

Because RF is a stochastic algorithm, it is best to use multiple runs, particularly when variable importance is the parameter of interest (Goldstein *et al.* 2010). We begin by building three full RF models using all SNPs as predictors, saving variable importance as mean decrease in accuracy for each model. Next, we sampled variable importance from each run with a range of cutoffs, pulling the most important 0.5%, 1.0%, 1.5%, and 2.0% of loci. These values correspond to approximately 50/100/150/200 loci that have the highest variable importance. For each cutoff, we then created three additional RF models, using the average percent variance explained across runs to determine the best starting number of important loci for step 3. This step removes clearly unimportant loci from further consideration (i.e. “sparsity pruning”, Goldstein *et al.* 2010).

Third, we doubled the best starting number of loci from step 2; this is meant to accommodate loci that may have low marginal effects (Goldstein *et al.* 2010). We then built three RF models with these loci, and recorded the mean variance explained. We removed the least important locus in each model, and recalculated the RF models and mean variance explained. This procedure continues until two loci remain. The set of loci that explain the most variance are the final candidates. Candidates are then combined

across runs to identify outliers. Locus rankings used average variable importance for each locus across the three runs.

3.2.1.4 Latent factor mixed models

Latent factor mixed models are hierarchical Bayesian mixed models that account for population structure using latent factors (K), which are similar to principal components (Frichot *et al.* 2013). We tested values of K ranging from one to 25 using a sparse nonnegative matrix factorization algorithm (Frichot *et al.* 2014), implemented as function *snmf* in the R package LEA, v. 1.2.0 (Frichot & François 2015). We plotted the cross-entropy values and selected K based on the inflection point in these plots; when the inflection point was not clear, we used the value where additional cross-entropy loss was minimal.

We parameterized LFMM models with this best estimate of K , and ran each model ten times with 5,000 iterations and a burnin of 2,500. We used the median of the squared z -scores to rank loci and calculate a genomic inflation factor (GIF) to assess model fit (Frichot & François 2015; François *et al.* 2016). The GIF is used to correct for inflation of z -scores at each locus, which can occur when population structure or other confounding factors are not sufficiently accounted for in the model (François *et al.* 2016). The GIF is calculated by dividing the median of the squared z -scores by the median of

the chi-squared distribution. We used the LEA and qvalue, v. 2.2.2 (Storey *et al.* 2015) packages in R. Full K and GIF results are presented in Table B1.

3.2.2 Correction for population structure

To determine if explicit modeling of population structure improved the performance of ordinations and RF, we repeated those analyses after accounting for population structure using spatial eigenvectors (for RDA, dbRDA, and cRDA) and regression with ancestry coefficients (for RF). The spatial eigenvector procedure uses Moran eigenvector maps (MEM) as spatial predictors in partial RDA and dbRDA analysis. MEMs provide a decomposition of the spatial relationships among sampled locations based on a spatial weighting matrix (Dray *et al.* 2006; Wagner *et al.* 2017). We used spatial filtering to determine which MEM variables to include in the partial analyses (Dray *et al.* 2012). Briefly, this procedure begins by applying a principal coordinate analysis (PCoA) to the genetic distance matrix, which we calculated using Bray-Curtis dissimilarity. We used the broken-stick criterion (Legendre & Legendre 2012) to determine how many genetic PCoA axes to retain. Retained axes were used as the response in a full RDA, where the predictors included all MEMs. Forward selection (Blanchet *et al.* 2008) was used to reduce the number of MEMs, using the full RDA adjusted R^2 statistic as the threshold. Finally, retained MEMs that were significantly correlated with environmental predictors were removed ($\alpha = 0.05/\text{number of}$

MEMs). The final set of significant MEMs were used as conditioning variables in RDA and dbRDA. We used the *spdep*, v. 0.6-9 (Bivand *et al.* 2013) and *adespatial*, v. 0.0-7 (Dray *et al.* 2016) packages to calculate MEMs.

For RF, we followed Briec *et al.* (2015) and used individual ancestry coefficients to correct both allele counts and environmental variables (Zhao *et al.* 2012). We used function *snmf* to estimate individual ancestry coefficients, running five replicates using the best estimate of K , and extracting individual ancestry coefficients from the replicate with the lowest cross-entropy. For genotypes, we used the residuals from logistic regression of SNP counts against ancestry coefficients. For environmental variables, we used the residuals from linear models of the variables against ancestry coefficients. These residuals were used as inputs into the RF framework described above.

3.2.3 Simulations

We used a subset of simulations published by Lotterhos & Whitlock (2014, 2015). Briefly, four demographic histories are represented in these data, each with three replicated environmental surfaces (Figure B1, Appendix B): an equilibrium island model (IM), equilibrium isolation by distance (IBD), and nonequilibrium isolation by distance with expansion from one (1R) or two (2R) refugia. In all cases, demography was independent of selection strength, which is analogous to simulating soft selection (Lotterhos & Whitlock 2014). Haploid, biallelic SNPs were simulated independently,

with 9,900 neutral loci and 100 under selection. The mean of the environmental/habitat parameter had a selection coefficient equal to zero and represented the background across which selective habitat was patchily distributed (Figure B1, Appendix B). Selection coefficients represent a proportional increase in fitness of alleles in response to habitat, where selection is increasingly positive as the value increases from the mean, and increasingly negative as the environmental value decreases from the mean (Lotterhos & Whitlock 2014, Figure B1, Appendix B). This landscape emulates a weak cline, with a north-south trend in the selection surface (Lotterhos & Whitlock 2014, Figure B1, Appendix B). Of the 100 adaptive loci, most were under weak selection. For the IBD scenarios, selection coefficients were 0.001 for 40 loci, 0.005 for 30 loci, 0.01 for 20 loci, and 0.1 for 10 loci. For the 1R, 2R, and IM scenarios, selection coefficients were 0.005 for 50 loci, 0.01 for 33 loci, and 0.1 for 17 loci. Note that realized selection varied across demographies, so results across demographic histories are not directly comparable (Lotterhos & Whitlock 2015).

We used the following sampling strategies and sample sizes from Lotterhos & Whitlock (2015): random, paired, and transect strategies, with 90 demes sampled, and 6 or 20 individuals sampled per deme. Overall, 72 simulations were used for testing. We assessed trend in neutral loci using linear models of allele frequencies within demes as a function of coordinates. We evaluated the strength of local adaptation using linear models of allele frequencies within demes as a function of environment.

The original simulation data assigned individual genotypes in a non-random fashion within populations. Because we were conducting individual-based analyses, we randomized allele counts for SNPs among individuals, within populations (K. Lotterhos, pers. comm.). We prepared two environmental predictors: habitat, which imposed a continuous selective gradient on the non-neutral loci, and the value for the x-coordinate of each population. We included the x-coordinate as a spurious predictor, analogous to an environmental variable hypothesized to drive selection that covaries with longitude. We scaled both variables prior to use. We did not use the y-coordinate as a second spurious predictor because it was highly correlated with habitat ($r > 0.7$) in the majority of simulations (Table B2).

3.2.4 Evaluation statistics

In order to equitably compare the output from these methods, we used locus rankings to calculate the number of correct detections out of the number of selected loci in each simulation (i.e. a common cutoff for all methods). We ranked loci based on the relevant (scaled) test statistics across both predictors, i.e. loadings and correlations for ordinations, variable importance for RF, and z-scores for LFMM. For example, in a simulation with 100 loci under selection and 90 true positive detections in the top 100 ranked loci, the true positive rate (TPR) would be 90/100, while the false positive rate (FPR) would be 10/100.

Since cutoffs (e.g. thresholds for statistical significance) are frequently used in empirical analyses for null hypothesis testing, we also provide detection results for commonly used cutoffs. We calculated a cutoff TPR as the number of correct positive detections out of the number possible. The cutoff FPR was the number of incorrect positive detections out of 9900 possible. For the main text, we present results from the “best” cutoff for each method; full results for all cutoffs tested are presented in the Supplemental Information. For constrained ordinations (RDA and dbRDA) we identified outliers as SNPs with a locus score +/- 2.5 and 3 SD from the mean score of each constrained axis. For cRDA, we used cutoffs for SNP-component correlations of $\alpha = 0.05, 0.01, \text{ and } 0.001$, corrected for sample sizes using a Fisher transformation as in Bourret *et al.* (2014). For LFMM, we compared two Bonferroni-corrected cutoffs (0.05 and 0.01) and a FDR cutoff of 0.1.

For both ranked and cutoff evaluation statistics, we calculated TPRs separately for different selection coefficients. In all cases, detection rates were averaged across the three replicate environments. Note that the number of selected loci ranged from 89-100, since some loci were removed by the original simulation authors due to low heterozygosity (Lotterhos & Whitlock 2015).

3.2.5 Weak selection

We compared RDA and cRDA for their ability to detect signals of weak selection ($s = 0.005$ and $s = 0.001$). All tests were performed as described above, with no additional corrections for population structure, after removing loci under strong ($s = 0.1$) and moderate ($s = 0.01$) selection from the simulation data sets. The number of loci under selection in these cases varied from 43 to 76.

3.3 Results

3.3.1 Population corrections

We found that explicitly accounting for population structure did not improve the performance of ordinations and was detrimental to the performance of RF. Spatial filtering had very little to no impact on true and false positive rates of ordination methods (Table B3 and B4). No corrections were applied to IM scenarios for ordination methods, due to low spatial structure (i.e. no PCoA axes were retained based on the broken-stick criterion). Regression of ancestry coefficients on RF inputs dramatically reduced TPRs (Table B3 and B4). All results presented here do not use population corrections; full results for runs with correction are presented in Table B3 and B4.

3.3.2 Ranked results

The three ordinations performed comparably in terms of locus rankings, and tended to outperform RF and LFMM (Figure 8). Ordinations performed best in IBD, 1R, and 2R demographies. Ordination results were relatively insensitive to sample size and sampling design (with the IM random sample being the exception, with lower TPRs). Within ordination techniques, RDA and cRDA had slightly higher detection rates compared to dbRDA. RF had very low TPRs across all simulations. LFMM was more sensitive than ordinations to demography, sampling design, and sample size. Detection rates for LFMM were better with smaller sample sizes (6 individuals/deme), and generally higher for the paired sampling design.

All methods performed well on loci under strong selection, with all methods but RF detecting 100% of these loci (Figure 9 for 20-individual sample size and Figure B2, Appendix B, for 6-individual sample size). Detection rates for loci under moderate and weak selection were comparable across ordination methods, with RDA and cRDA having the overall highest detection. RF had very low detection rates for moderate and weakly selected loci, while LFMM had lower detection rates than ordinations in non-equilibrium demographies. For ordinations, selection level detection rates were mostly comparable across sample sizes, except IM, where detection was better with the larger sample size. RF and LFMM had better detection with smaller sample sizes.

3.3.3 Cutoff results

The best performing cutoffs were: RDA/dbRDA, ± 3 SD; cRDA, $\alpha = 0.001$; and LFMM, FDR = 0.1. Full cutoff results are presented in the Supplementary Information (Figures B5, B6, and B7, Appendix B).

Cutoff TPRs (Figure 10) generally reflected ranked TPRs (Figure 8), with ordinations performing best in most cases, RF having low detection rates overall, and LFMM performing well depending on the scenario. False positive rates were low for all methods except cRDA (IBD, 1R, and 2R demographies). Selection level detection rates using cutoffs were generally higher than ranked results for cRDA, RF, and LFMM (Figures B3 and B4, Appendix B). RF had better selection level detection rates with the smaller sample size.

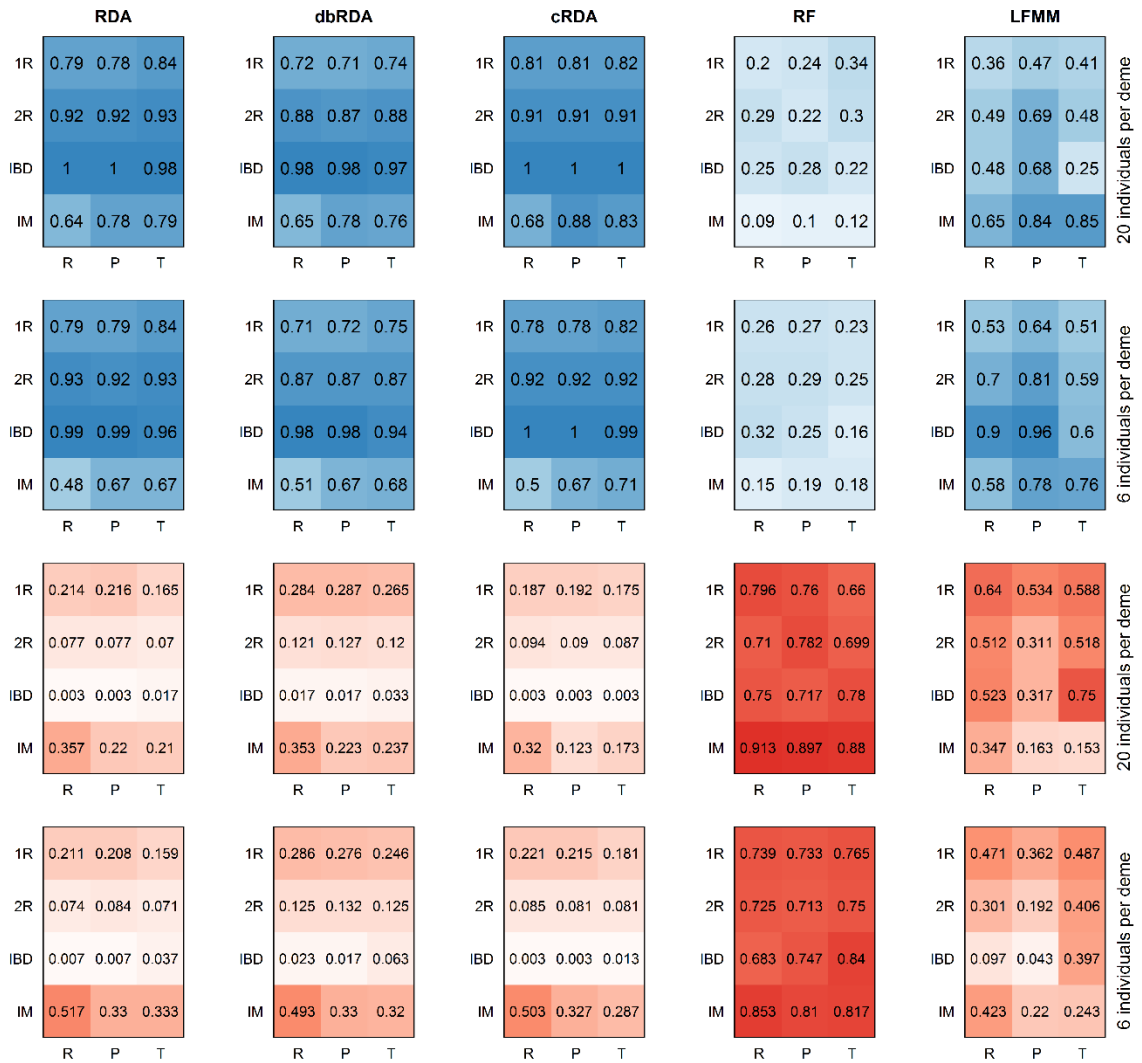


Figure 8. Average true positive (blue) and false positive (red) rates for all loci under selection from five methods (columns) using locus rankings (i.e. number of positive detections out of number of loci under selection). Each method shows results for different sampling strategies (R = random, P = pairs, T = transects), demographies (1R and 2R = refugial expansion, IBD = equilibrium isolation by distance, IM = equilibrium island model), and sample sizes (rows).

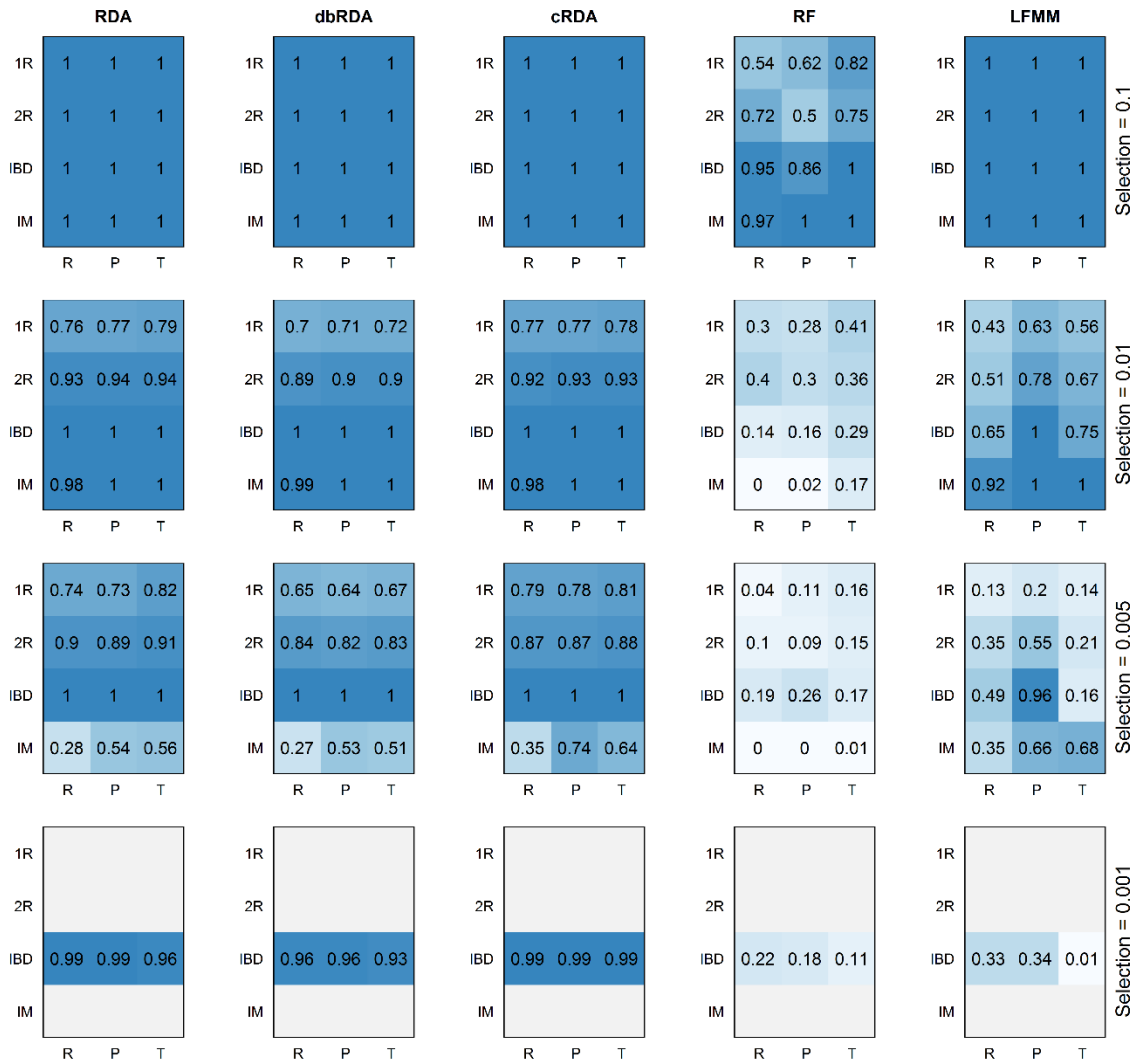


Figure 9. Average true positive rates for different levels of selection (rows) from five methods (columns) using locus rankings and a sample size of 20 individuals per deme. Each method shows results for different sampling strategies (R = random, P = pairs, T = transects) and demographies (1R and 2R = refugial expansion, IBD = equilibrium isolation by distance, IM = equilibrium island model). Only the IBD demography included very weak selection (s=0.001).

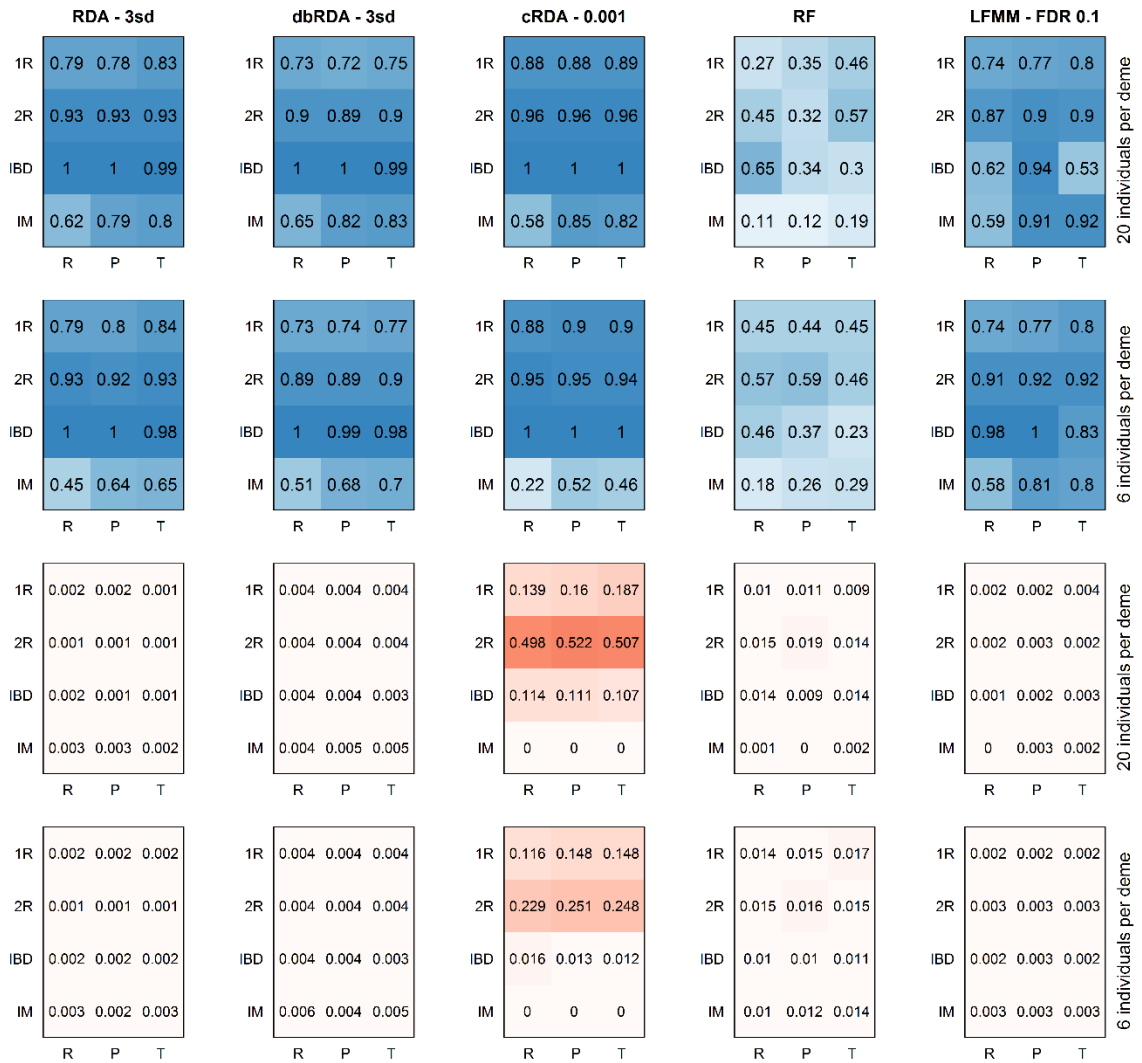


Figure 10. Average true positive (blue) and false positive (red) rates from five methods (columns) using the best cutoff for each method. Each method shows results for different sampling strategies (R = random, P = pairs, T = transects), demographies (1R and 2R = refugial expansion, IBD = equilibrium isolation by distance, IM = equilibrium island model), and sample sizes (rows).

3.3.4 Weak selection

We compared RDA and cRDA for their ability to detect only weak loci in the simulations. Using locus rankings, RDA had more consistent performance across scenarios, and had overall higher TPRs and lower FPRs compared with cRDA (Figure 11, first and second columns). cRDA had low detection rates in the 1R demography with the larger sample size, and in the IM demography, regardless of sample size (no detections at all with 6 individuals/deme). Using cutoffs, RDA had more consistent performance across all scenarios (Figure 11, third column). Detection was better using cRDA in the 1R demography when sampling 6 individuals per deme, but was much worse when sampling 20 individuals per deme (Figure 11, fourth column). Overall, cRDA had the same detection problems noted with the ranked results, in addition to high FPRs under 1R, 2R, and IBD demographies.

3.3.5 Combining detections

We compared the univariate LFMM and multivariate RDA cutoff results for overlap and differences in their detections (Figure 12). The methods had greater commonality in the loci they correctly identified as true positives than in the loci they incorrectly identified (false positives), indicating that mutual detections could be an effective way of reducing FPRs. In some cases, however, RDA detected a large number of selected loci that were not identified by LFMM (Figure 12, second column), indicating

that power would be lost when using only overlapping results. Significant true positive contributions from LFMM were found only in the IM demography. Overall, LFMM had greater numbers of unique false positive detections compared to RDA. Few unique true positive detections and many unique false positive detections limit the utility of combining LFMM and RDA.

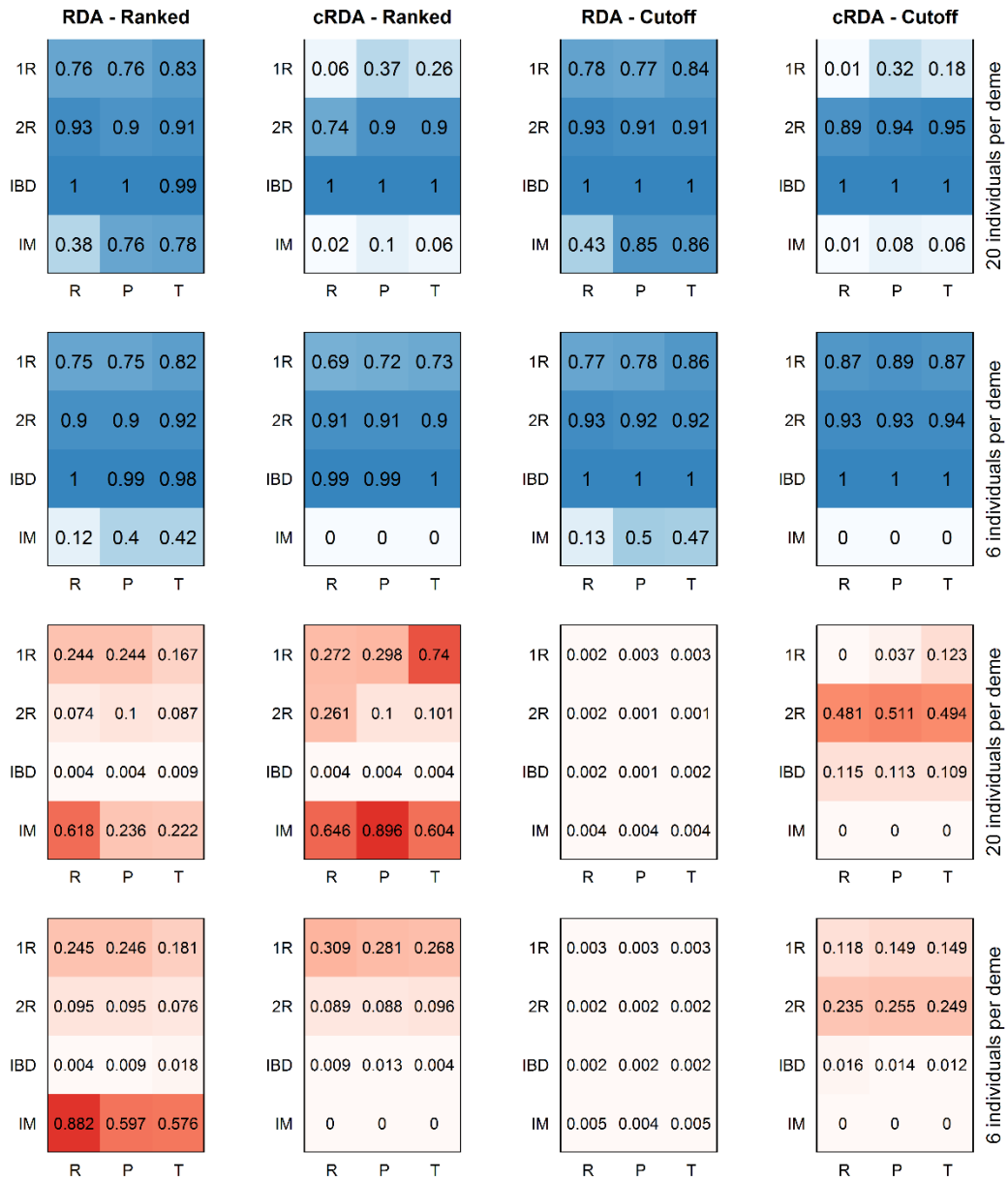


Figure 11. Average true positive (blue) and false positive (red) rates for RDA and cRDA (columns) on simulations with weak selection only. The first two columns show results for locus rankings, while the third and fourth columns show results for the best cutoff for each method. Results are presented for different sampling strategies (R = random, P = pairs, T = transects), demographies (1R and 2R = refugial expansion, IBD = equilibrium isolation by distance, IM = equilibrium island model), and sample sizes (rows).

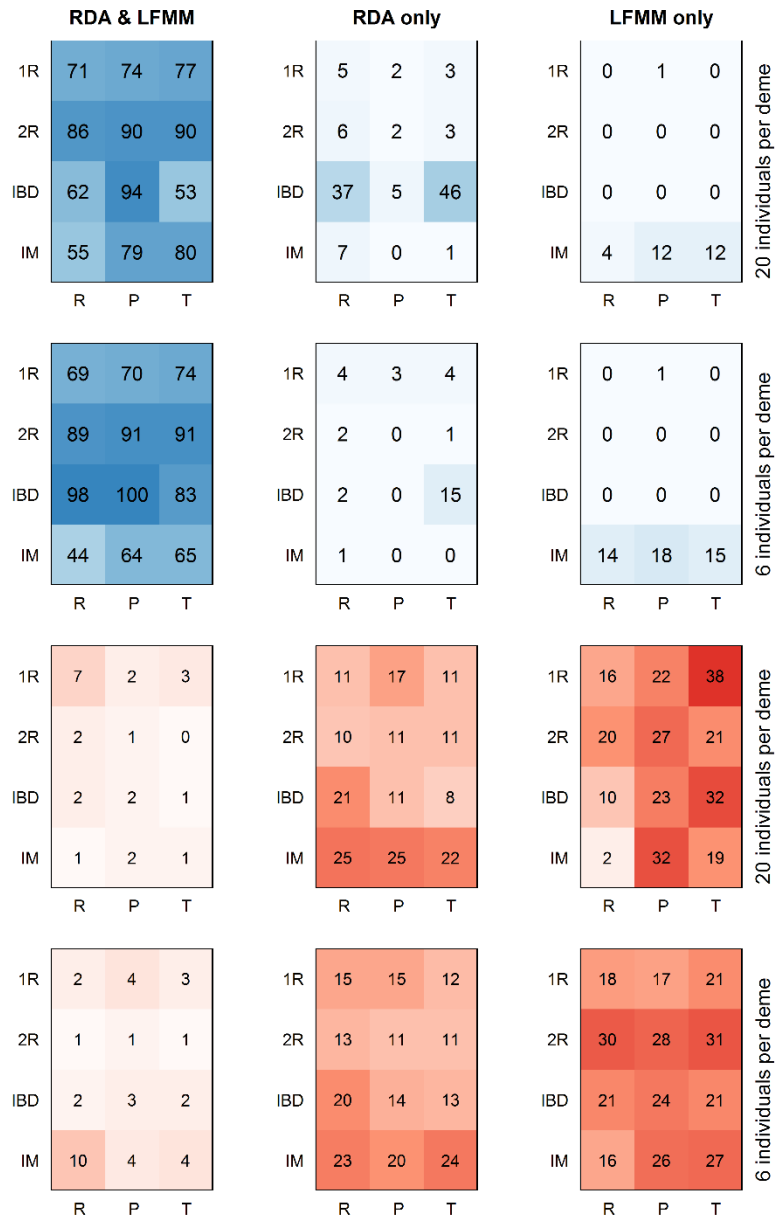


Figure 12. Average counts of true positive (blue) and false positive (red) detections for two methods, RDA and LFMM. The first column shows the average number of loci detected by both methods. The second and third columns show the average number of detections that are unique to RDA and LFMM, respectively. Results are presented for different sampling strategies (R = random, P = pairs, T = transects), demographies (1R and 2R = refugial expansion, IBD = equilibrium isolation by distance, IM = equilibrium island model), and sample sizes (rows).

3.4 Discussion

Multivariate and machine learning genotype-environment association (GEA) methods have been noted for their ability to detect multilocus selection (Rellstab *et al.* 2015; Hoban *et al.* 2016), although there has been no controlled assessment of the effectiveness of these methods in detecting multilocus selection to date. Since these approaches are increasingly being used in empirical analyses (e.g. Bourret *et al.* 2014; Brieuc *et al.* 2015; Pavey *et al.* 2015; Hecht *et al.* 2015; Swaegers *et al.* 2015; Laporte *et al.* 2016; Brauer *et al.* 2016), it is important that these claims are evaluated to ensure that the most effective GEA methods are being used, and that their results are being appropriately interpreted.

Here we compare a suite of GEA approaches in a simulation framework to assess their ability to correctly detect multilocus selection under different demographic and sampling scenarios. We found that constrained ordinations had the best overall performance across the demographics, sampling designs, sample sizes, and selection levels tested here. The univariate LFMM method also performed well, though power was scenario-dependent. Random Forest, by contrast, had very low detection rates overall. In the following sections we address these methods by category and discuss reasons for method performance and provide suggestions for their use on empirical data sets.

3.4.1 Constrained ordinations

The three constrained ordination methods all performed well (Figure 8 and Figure 9). They were relatively insensitive to sample size (6 vs 20 individuals sampled per deme), in agreement with Xuereb *et al.* (In review) who found that reducing sampling from 500 to 100 individuals had only moderate effects on TPRs for RDA and dbRDA and no effect on FPRs. The one exception was the IM demography, where larger sample sizes consistently improved TPRs, as previously noted by De Mita *et al.* (2013) and Lotterhos & Whitlock (2015) for univariate GEA methods. Power was lowest in the IM demography, which is typified by a lack of spatial autocorrelation in allele frequencies and a reduced signal of local adaptation (Table B4), making detection more difficult. Detection rates were highest for IBD, followed by the 2R and 1R demographies. All three methods were relatively insensitive to sampling design, with transects performing slightly better in 1R and random sampling performing worst in IM. Otherwise results were consistent across designs, in contrast to the univariate GEA methods tested by Lotterhos and Whitlock (2015), most of which had higher power with the paired sampling strategy. Ordinations are likely less sensitive to sampling design since they take advantage of covarying signals of selection, making them more robust to sampling that does not maximize environmental differentiation (e.g. random or transect designs). All methods performed similarly in terms of detection rates across selection strengths. As expected, weak selection was more difficult to detect than moderate or

strong selection, except for IBD, where detection levels were high regardless of the strength of selection (Figure 9, and Figures B2-B4, Appendix B).

High TPRs were maintained when using cutoffs for all three ordination methods. False positives were universally low for RDA and dbRDA. By contrast, cRDA showed high FPRs for all demographies except IM, tempering its slightly higher TPRs. These higher FPRs are a consequence of using component axes as predictors. Across all scenarios and sample sizes, cRDA detected component 1, 2, or both as significantly associated with the constrained RDA axes (Table B5). Most selected loci load on these components (keeping true positive detections high), but neutral markers also load on these axes, especially in cases where there are strong trends in neutral loci (i.e. maximum trends in neutral markers reflect FPRs for cRDA, Tables B2, Figure 10). Given these results, we hypothesized that it might be challenging for cRDA to detect weak selection in the absence of a covarying signal from loci with stronger selection coefficients. If the selection signature is weak, it may load on a lower-level component axis (i.e. an axis that explains less of the genetic variance), or it may load on higher-level axes, but fail to be significantly associated with the constrained RDA axes. Note that although cRDA contains a step to reduce the number of components, parallel analysis resulted in retention of all axes in every simulation tested here (Table B5). This meant that cRDA could search for the signal of selection across all possible components.

When tested on simulations with loci under weak selection only, RDA, which uses the genotype matrix directly, maintained similar detection patterns as in the full data set, indicating that selection signals can be detected with this method in the absence of loci under strong selection (Figure 11). Using a cutoff, RDA maintained very low FPRs across all simulation scenarios and sample sizes. By contrast, cRDA detection was more variable, ranging from comparable detection rates with the full data set, to no/poor detections under certain demographies and sample sizes (Figure 11). In these latter cases, poor performance is reflected in the component axes detected as significant (Table B5); instead of identifying the signal in the first few axes, a variable set of lower-variance axes are detected (or none are detected at all). This indicates that the method is not able to “find” the selected signal in the component axes in cases where that signal is not driven by strong selection. This result, in addition to higher FPRs for cRDA, builds a case for using the genotype matrix directly with a constrained ordination such as RDA or dbRDA, as opposed to a preliminary step of data conversion with PCA.

RDA plots illustrate how loci under selection can be distinguished from neutral loci using constrained ordinations (Figure 13). RDA shows a negative relationship between habitat and the selected loci, and is clearly able to distinguish the signal of selection from the spurious x-coordinate predictor. Depending on where the cutoff is placed (i.e. how many deviations from the mean score), false negatives can be seen in the IM, 1R, and 2R demographies as the pink selected loci that are not well-differentiated

from the “cloud” of gray neutral loci. This is particularly noticeable in the IM demography, where many of the loci under weak selection do not differentiate from the neutral signal. Data from natural systems likely lie somewhere among these demographic extremes, and successful differentiation in the presence of IBD and non-equilibrium conditions indicate that ordinations should work well across a range of natural systems.

Finally, our results suggest that additional correction for population structure is not needed for these methods, at least within the range of population structure present here (Table B3 and B4). This indicates that constrained ordinations are effectively accounting for the joint action of selection (modeled on the constrained axes) and demography (residual variance not explained by environment that is modeled on the unconstrained axes). Biplots of the first two unconstrained (PC) axes (Figure B9, Appendix B) and screeplots of the variance explained by the first 15 unconstrained axes (Figure B10, Appendix B) reflect how demographies with different levels of population structure are modeled in the unconstrained axes by RDA. Testing these methods in simulation scenarios with more significant population structure would be a helpful follow-up to confirm the generality of these results.

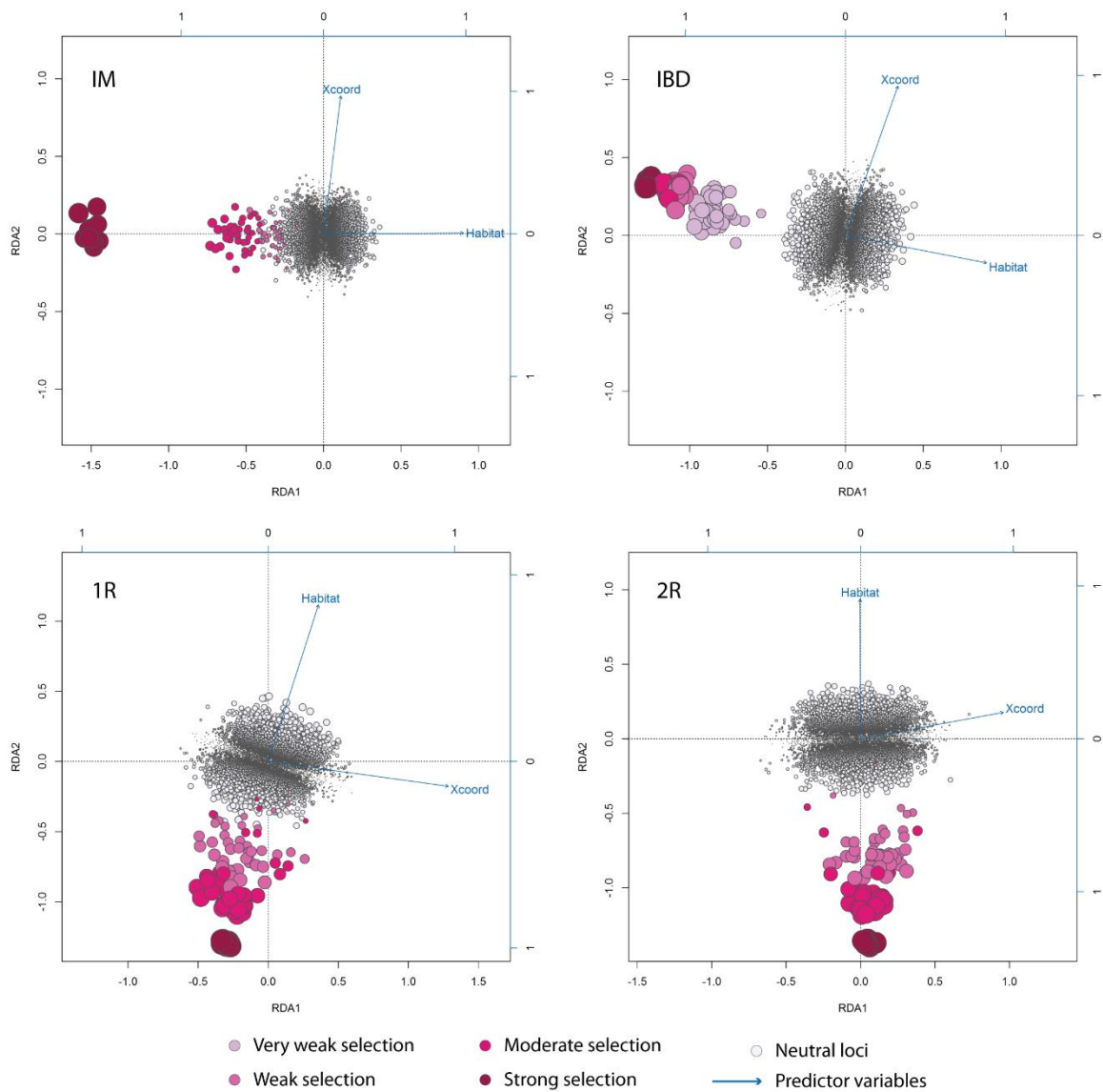


Figure 13. Redundancy analysis plots showing loci with point size scaled by their correlation with the driving environmental variable (“Habitat”), and correlation of predictor variables with the constrained RDA axes (arrows). Plots are shown for an equilibrium island model (IM), equilibrium isolation by distance model (IBD), and non-equilibrium one- and two- refugial expansion models (1R and 2R) for paired sampling (6 individuals/deme) on environmental surface “453”.

3.4.2 Random Forest

Random Forest performed very poorly in detecting loci under moderate and weak selection. These results indicate that RF is not a good GEA approach for large genomic data sets. Poor performance is caused by the “sparsity” of the genotype matrix (i.e. most SNPs are not under selection), which results in detection that is dominated by strongly selected loci (i.e. loci with strong marginal effects, Figure 9). This issue has been documented in other simulation and empirical studies (Goldstein *et al.* 2010; Winham *et al.* 2012; Wright *et al.* 2016) and indicates that RF is not suited to identifying weak multilocus selection or interaction effects in these cases. Empirical studies that have used RF as a GEA have likely identified a subset of loci under strong selection, but are unlikely to have identified loci underlying more complex genetic architectures. Note that the amount of environmental variance explained by the RF model can be high (i.e. overall percent variance explained by the detected SNPs), while still failing to identify most of the loci under selection (Table B6). Removing strong associations from the genotypic matrix can potentially help with the detection of weaker effects (Goldstein *et al.* 2010), but this approach has not been tested on large matrices. Combined with the computational burden of this method (taking 10-14 days for the larger data sets), as well as the availability of fast and accurate alternatives such as RDA (which takes ~3 minutes on the same data), it is clear that RF is not a viable option for GEA analysis of genomic data.

Random Forest does hold promise for the detection of interaction effects in much smaller data sets (e.g. tens of loci, Holliday *et al.* 2012). However, this is an area of active research, and the capacity of RF models in their current form to both capture and identify SNP interactions has been disputed (Winham *et al.* 2012; Wright *et al.* 2016). New modifications of RF models are being developed to more effectively identify interaction effects (e.g. Li *et al.* 2016), but these models are computationally demanding and are not designed for large data sets. Overall, extensions of RF show potential for identifying more complex genetic architectures, but caution is warranted in using them on empirical data prior to rigorous testing on realistic simulation scenarios (Wright *et al.* 2016).

3.4.3 Latent factor mixed models

The univariate LFMM method performed well, especially considering that it does not take advantage of covariation in allele frequencies to detect loci. Still, as expected, detection rates were lower overall for loci under moderate and weak selection when compared with ordinations. This is in agreement with LFMM results from de Villemereuil *et al.* (2014), who also found a reduction in power when detecting polygenic selection. Additionally, the performance of LFMM was more dependent on sampling design, sample size, and demography than ordinations. Our results clearly demonstrated that Bonferroni corrections are too conservative for LFMM (Figure B7,

Appendix B), and that FDR-based approaches for multiple testing are much better suited to genomic data when the GIF indicates the test is well-calibrated (François *et al.* 2016, Table B1).

3.4.4 Should results from different tests be combined?

A common approach in local adaptation studies is to run multiple tests (GEA only, or a combination of GEA and differentiation methods) and look for duplicate detections across methods. This ad hoc approach is thought to increase confidence in true positive detections, while minimizing false positives. The problem with this approach is that it can bias detection toward strong selective sweeps to the exclusion of other adaptive mechanisms which may be equally important in shaping phenotypic variation (Le Corre & Kremer 2012; François *et al.* 2016). If the goal is to detect other forms of selection such as recent selection or selection on standing genetic variation, this approach will not be effective since most methods are unlikely to detect these weak signals.

This issue is illustrated by using two different combinations of RDA and LFMM detections: keeping only mutual detections and keeping all detections. Agreement on true positives is high, while agreement on false positives is low (Figure 12, first column). Keeping only loci detected by both RDA and LFMM may therefore seem to be an effective way to reduce FPRs while maintaining good TPRs. However, depending on the

scenario, RDA has a large number of true positive detections that are unique to that method (Figure 12, second column). These unique true positive detections, all of which are under moderate and weak selection (e.g. Figure 9), would be discarded using a duplicates-only criterion, limiting our inference to those loci with the strongest adaptive signal. This effect was also noted by Lotterhos & Whitlock (2015) when looking at detection overlap in the methods tested in their analysis. Alternatively, keeping all detections from both methods would dramatically increase FPRs, while providing very little improvement in TPRs since multiple unique detections by LFMM are found only in the IM demography (Figure 12, third column).

The decision of whether and how to combine results from different tests will be specific to the study questions, the tolerance for false negative and false positive detections, and the capacity for follow-up analyses on detected markers. For example, if the goal is to detect loci with strong effects while keeping false positive rates as low as possible, running multiple GEA and/or differentiation-based methods and considering only duplicate detections could be a suitable strategy. However, if the goal is to detect selection on standing genetic variation or a recent selection event, combining detections from multiple tests would be too conservative. In this case, the best approach would be to use a single GEA method, such as RDA, that can effectively detect covarying signals arising from multilocus selection, while being robust to selection strength, sampling design, and sample size.

3.4.5 Conclusions and recommendations

Random Forest performed very poorly as a GEA method on the simulations tested here. True positive rates were limited due to strong marginal effects created by the subset of loci under strong selection. Still, RF may be useful for follow-up analyses of the genomic architecture of smaller sets of candidate loci. However, the effectiveness of RF for identifying interactions and other complex genetic architectures is currently disputed, and practitioners should proceed cautiously until new extensions of RF are rigorously tested under realistic simulation scenarios. The univariate method we tested, LFMM, performed well, but was more sensitive to sampling designs and sample sizes than RDA and dbRDA. Additionally, since this method cannot detect covarying signals of selection, overall detection of loci under moderate and weak selection was reduced.

We found that constrained ordinations, especially RDA, show a superior combination of low false positive rates and high true positive rates across weak, moderate, and strong multilocus selection. These results were robust across the demographic histories, sampling designs, and sample sizes tested here. Additionally, RDA outperformed an alternative ordination-based approach, cRDA, especially (and importantly) when the multilocus selection signature was completely derived from loci under weak selection. It is important to note that constrained ordinations require complete data sets (no missing values). Fortunately, recent work has indicated that RDA and dbRDA are robust to even high levels (50%) of randomly missing data when using

simple imputation methods such as the mean value across individuals (Xuereb *et al.* In review). Additionally, RDA and dbRDA can be used on both individual and population-based samples. It will be important to continue testing these promising methods in simulation frameworks that include genetic architectures that are more complex than the multilocus selection response modeled here. This includes locus interaction effects (i.e. epistasis) and more complex polygenic architectures. However, this study indicates that constrained ordinations are an effective means of detecting adaptive processes that result in weak, multilocus molecular signatures, providing a powerful tool for investigating the genetic basis of local adaptation and informing management actions to conserve the evolutionary potential of species of agricultural, forestry, fisheries, and conservation concern.

4. Conserving adaptive capacity in a Southern Appalachian salamander threatened by climate change

4.1 Introduction

Landscape genomics is an emerging field that investigates how landscape features and environmental conditions shape patterns of neutral and adaptive genetic variation (Schoville *et al.* 2012; Manel & Holderegger 2013). It is particularly valuable for the study of adaptive variation in species of conservation concern, since it does not require prior genomic information or the use of manipulative experiments, such as reciprocal transplants and common gardens (Sork *et al.* 2013). For this reason, landscape genomics, and genomic methods more generally, are increasingly being used to help quantify adaptive potential and manage for evolutionary resiliency in wild populations (Funk *et al.* 2012; Harrison *et al.* 2014; McMahon *et al.* 2014; Hoffmann *et al.* 2015).

The increasing tractability of landscape genomic studies is a direct consequence of advances in high-throughput sequencing technologies that can be used to cost-effectively genotype many individuals at thousands of markers across the genome (Davey *et al.* 2011; Andrews *et al.* 2016). These markers can be partitioned into neutral and potentially adaptive genetic variation using a variety of statistical approaches (Hoban *et al.* 2016). Analysis of neutral genetic variation provides insight into population structure, genetic variability, inbreeding depression, effective population size, and landscape effects on gene flow. Analysis of potentially adaptive genetic

variation, made accessible with these genomic technologies, provides insight into local adaptation and the evolutionary potential of wild populations. From a conservation perspective, analysis of adaptive genetic variation provides a novel means of informing management actions to maximize the adaptive capacity of species in response to climate change and other anthropogenic impacts and stressors.

In this paper, we will lay out the benefits of landscape genomic studies for species of conservation concern using a case study of an endemic salamander species. We will illustrate an analytical approach called “adaptive dissimilarity” that can be used to inform a variety of management actions. Adaptive dissimilarity is a measure of the (dis)similarity of populations based on their potentially adaptive genetic markers. This metric is inspired by the population adaptive index (PAI) described by Bonin *et al.* (2007). The PAI identifies the percentage of adaptive loci that have significantly different allele frequencies when compared to all other populations (Bonin *et al.* 2007). Adaptive dissimilarity improves upon the PAI by using a pairwise, multivariate measure to calculate how (dis)similar populations are based on their multilocus allele frequencies at loci potentially under selection (or loci linked to these selected regions). When combined with a multivariate technique for detecting loci under selection (Forester *et al.* In review, 2016), the adaptive dissimilarity metric provides an integrated assessment of how covarying adaptive markers differ (or are similar) across many populations, offering an intuitive means to identify complementary sets of adaptive genetic variation.

Our focal species is the endemic Weller's salamander (*Plethodon welleri*), a high-elevation Southern Appalachian Mountain species of conservation concern (Figure 14, photo). Its small range (Figure 14) is located in a global center for forest and freshwater systems biodiversity (Stein *et al.* 2000), including a global hotspot for salamander biodiversity (Milanovich *et al.* 2010). Weller's and other terrestrial, forest-dwelling salamanders have limited dispersal capabilities, narrow physiological tolerances, and are highly sensitive to changes in climate, especially the interaction of temperature and moisture (Bernardo & Spotila 2006). Appalachian salamanders are under threat from a diversity of causes, most of which are not well understood (Highton 2005; Gratwicke 2008; Caruso & Lips 2013; Martel *et al.* 2014). Major concerns are habitat fragmentation and degradation, forest alteration (e.g. acidification due to acid rain and fog and tree loss due to invasive pests), population isolation, disease impacts, development and recreation pressures, and climate change. Weller's salamander is characteristic of many species in need of conservation: due to ethical concerns and biological and ecological traits (such as long generation times), reciprocal transplants and common garden/lab experiments are not an option for studying adaptive variation. It is in these species that landscape genomics can offer an unprecedented window into local adaptation and evolutionary potential.

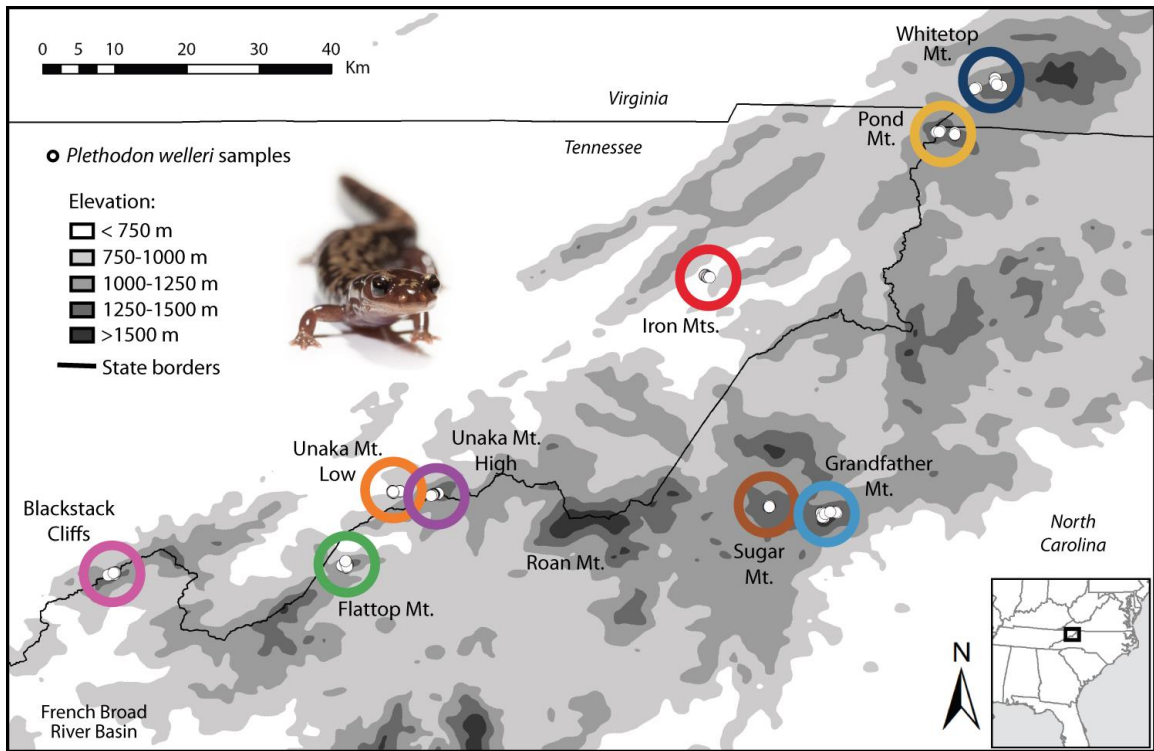


Figure 14. Location of sampled Weller’s salamander populations in the Southern Appalachian Mountains. Inset photo of Weller’s salamander by Katherine Cain.

The southern Appalachian Mountains show a large range of variation in temperature and moisture at fine spatial scales (Fridley 2009). The patchy distribution of Weller’s salamander on mountain peaks provides a naturally replicated temperature gradient (via elevation) for distinguishing local adaptation (Figure 14). The presence of warm-adapted genotypes at low elevations has important consequences for the potential of montane salamanders to adapt to rapid warming, since this genetic variation could improve the adaptive capacity of cold-adapted populations at higher elevations.

Substantial changes in climate are expected for this region in the coming decades (Figure 15), and are of particular concern since much of the endemism in flora and fauna for this region is derived from the patchy, high elevation (“sky island”) habitats which have no nearby climatic analogue. In combination with finer scale habitat fragmentation, which can impede the ability of populations to exchange adaptive migrants, it is unlikely that many of these species, including terrestrial salamanders, will be able to shift their ranges to track changing conditions. Many populations of these endemic species will be left to adapt to these changing conditions in place or face local extinction. Understanding and having options for the proactive management of the evolutionary potential of these species is therefore of high priority in determining conservation needs and strategies.

The goals of this analysis are to integrate information derived from neutral and potentially adaptive genetic variation to develop a set of management recommendations for Weller’s salamander under current conditions and projected climate change.

Specifically, our goals are to assess genetic variation within and between Weller’s salamander populations, determine if populations are locally adapted to environmental conditions, and estimate population sizes. We will provide an example of how this information can be used in three different conservation scenarios: (1) site prioritization, (2) management of small, isolated populations through genetic rescue, and (3) assisted migration to support evolutionary potential.

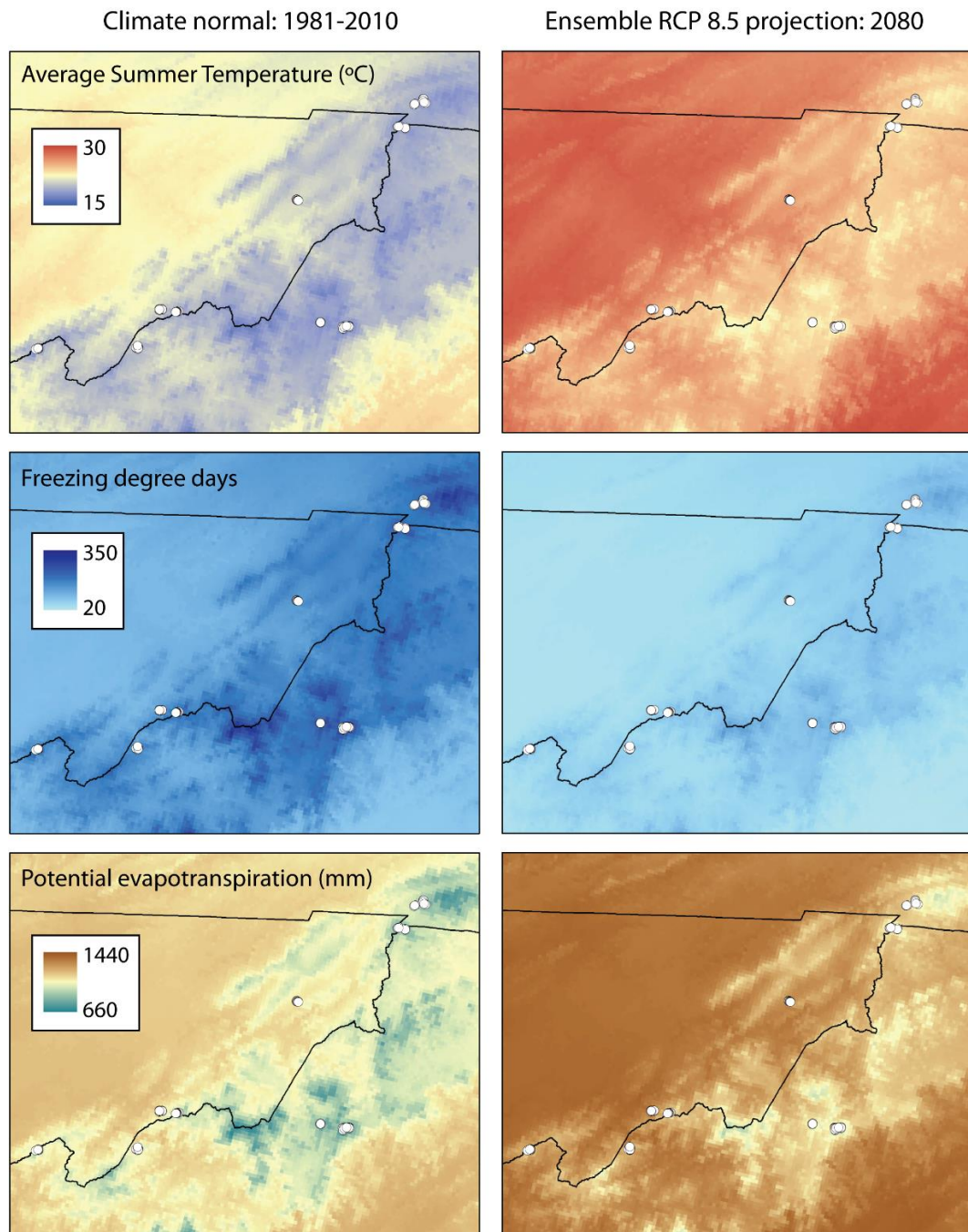


Figure 15. Three climatic parameters relevant to terrestrial salamander biology and ecology across the Weller's salamander range, with sampled populations for this study shown as white circles. Climate normals (1981-2010) at left and ensemble projections (CMIP5) for 2080 under the RCP 8.5 (high emissions) scenario at right. Climate data from (AdaptWest Project 2015; Wang *et al.* 2016).

4.2 Methods

4.2.1 Overview

In the following sections we describe field data collection, environmental models, laboratory protocols, bioinformatics processing (including data quality filtering), data analysis, and finally, the conservation scenarios employed (refer to Figure 16 for an overview of these steps and use of data products).

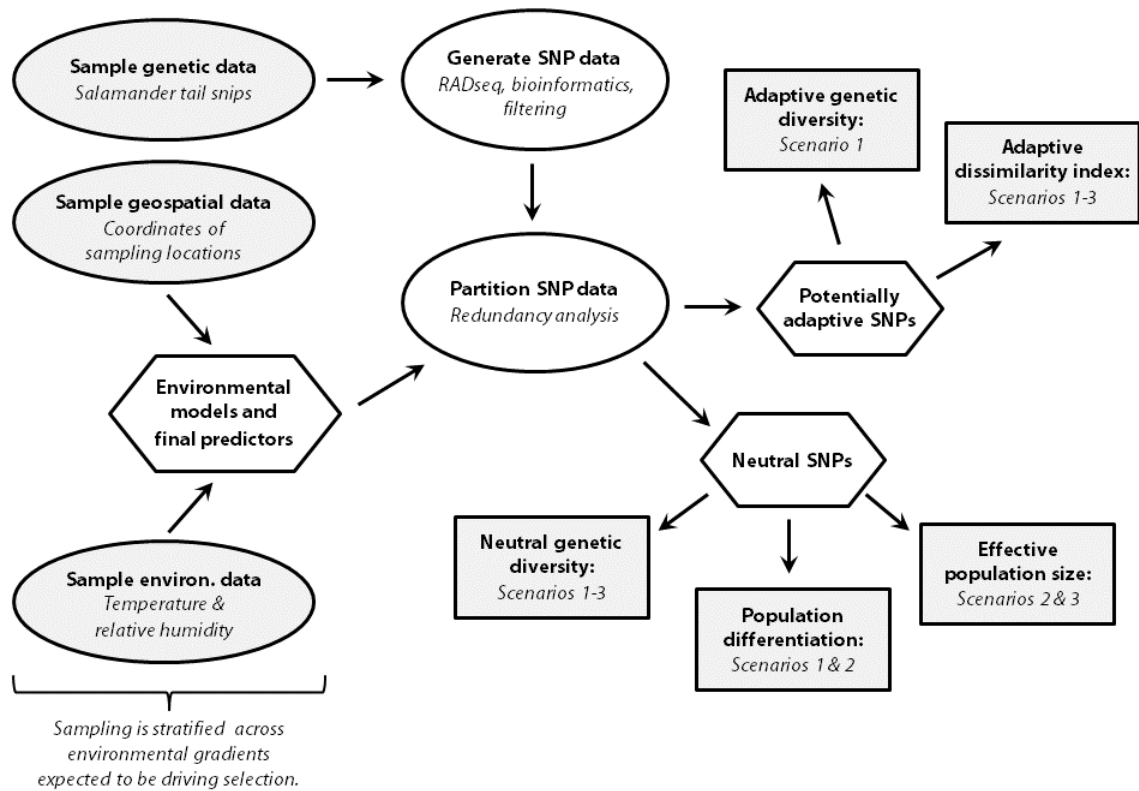


Figure 16. Flowchart of methods. Gray ovals are field data collection; white ovals are data analysis; hexagons are intermediate data products; gray rectangles are final outputs, showing data used for the three conservation scenarios.

4.2.2 Data collection

Weller's salamander (*Plethodon welleri*) is a fully terrestrial salamander in the family Plethodontidae. Members of this genus lack lungs and so must keep their skin moist to maintain cutaneous gas exchange. These salamanders are therefore sensitive to temperature and humidity conditions. Weller's salamander is generally found above 1,300 m in elevation, and is often affiliated with spruce-fir forests at the highest elevations. Populations are also found in mesic hardwood forests at lower elevations (down to 650 m, Figure 14, Table 1).

We sampled nine of the ten known Weller's salamander populations between 2013 and 2016. An eleventh, historically occupied site (ca. 1984) in Watauga County, NC has been repeatedly resurveyed without locating any Weller's salamanders. Development at this site may have extirpated this population. Salamanders were discovered by actively seeking individuals within a focal area (e.g. by turning over logs, bark, and branches). Sample size was 30–32 individuals per site. We recorded basic salamander and habitat data (snout-vent length, weight, cover object description, GPS coordinates, etc.) before taking 3–5 mm tail snips using an aseptic technique. Salamanders were then released at their point of capture.

We built models for temperature and relative humidity across the study area based on data loggers stratified across elevation and aspect at two mountain sites, with validation loggers installed at three additional sites (Figure C1, Appendix C). Data

loggers (Onset Hobo U23-004) recorded temperature and relative humidity every 15 minutes at 5 cm above the ground surface. Details on model production, validation, and verification are provided in Appendix C. From these modeled data we calculated a variety of metrics aimed at separating various aspects of the thermal regime including seasonal means, minima, and maxima as well as cumulative heat sums and metrics incorporating both temperature and humidity. We selected predictor variables based on their ecological and biological relevance, their distribution across populations, and correlation structure (highly correlated variables, i.e. $|r| > 0.7$, were removed).

Table 1. Average elevation and environmental conditions (March-November) of Weller’s salamander populations sampled across the range.

Population name	Population abbreviation	Elevation (m)	Mean daily minimum temperature (°C)	Vapor pressure deficit
Iron Mts.	IM	700	10.8	0.191
Unaka Mt. Low	UL	738	11.3	0.324
Blackstack Cliffs	BC	1334	8.4	0.232
Flattop Mt.	FT	1370	8.3	0.231
Whitetop Mt.	WT	1449	7.9	0.183
Pond Mt.	PM	1459	7.5	0.141
Sugar Mt.	SM	1497	7.6	0.178
Unaka Mt. High	UH	1566	7.3	0.166
Grandfather Mt.	GM	1678	6.5	0.131

4.2.3 RADseq library construction and sequencing

We used a reduced-representation sequencing approach called double digest restriction-site associated DNA sequencing (RADseq) to reduce genome complexity and provide genome-wide coverage of genetic markers (Etter *et al.* 2011; Peterson *et al.* 2012). RADseq does not require any prior genomic information, and can be used to produce cost-effective single nucleotide polymorphism (SNP) marker data sets across a large number of individuals (Andrews *et al.* 2016).

We produced RADseq libraries for Illumina sequencing following published protocols (Peterson *et al.* 2012). Briefly, we extracted total genomic DNA from tail tissues using Wizard SV Genomic DNA Extraction Kits following manufacturer protocols (Promega). We quantified total DNA concentrations using Qubit dsDNA BR Assays (Life Technologies) and verified DNA quality using restriction digests followed by electrophoresis on agarose gels. We digested 1µg of total DNA per individual with the 8-cutter restriction enzyme *SbfI* and the 4-cutter restriction enzyme *msp1*. Digested DNA products were bound to Sera-Mag SpeedBeads and washed to remove proteins, salts, and residual restriction enzyme. We then ligated barcoded P1 adaptors onto the *SbfI* restriction site and P2 adaptors onto the *msp1* restriction site. DNA fragments containing both P1 and P2 adaptors were specifically amplified using Phusion High Fidelity PCR Master Mix (NEB). We purified the PCR products using the Ampure XP Purification System (Agencourt) and quantified them using Qubit dsDNA BR Assays (Life

Technologies). The purified PCR products (the RAD library) was then sequenced (50bp single end) on an Illumina HiSeq-2000 instrument at the Duke Center for Genomic and Computational Biology Sequencing and Genomic Technologies Shared Resource core facility. Four individuals from two populations were run as duplicates (using different barcodes) to facilitate Stacks parameter testing (see below).

4.2.4 Bioinformatics

We analyzed sequence data using Stacks v. 1.43 (Catchen *et al.* 2011, 2013) for de novo SNP discovery and genotyping. We used `process_radtags` to demultiplex the raw data, and the default sliding window settings on Phred33 scores to discard sequencing reads of low quality. Using a subset of the individuals, we conducted multiple Stacks runs to optimize four Stacks parameters: minimum stack depth (`-m`), distance between stacks (`-M`), the upper bound on the error rate for the SNP model (`--bound_high`), and the distance between catalog loci (`-n`). Parameter optimization used two individuals from each of two populations, including two duplicate samples from each population. Three samples from a third, more geographically distant population were also analyzed, for a total of 11 samples. Sixteen combinations of `-m` (3-5), `-M` (3-5), and `--bound_high` (0.05, 0.10) in `ustacks`, and `-n` (3-5) in `cstacks` were tested on these samples across the entire pipeline: `ustacks`, `cstacks`, `rxstacks`, `cstacks`, `sstacks`, and `populations`. Parameter optimization considered the number of RAD tags (short sequence reads) and SNPs

retained and population/duplicate clustering using multidimensional scaling plots from PLINK v. 1.07, (Purcell *et al.* 2007).

After optimizing Stacks parameters, we ran the full Stacks pipeline on all samples using the following settings: `ustacks: -m 4, -M 4, --bound_high 0.05, -r` (drop highly repetitive stacks), `-d` (enable the deleveraging algorithm to resolve overmerged RAD tags); `cstacks: -n 3`; `rxstacks: --bound_high 0.05, --lnl_lim -10` (minimum log likelihood quality score required to keep a catalog locus), `--conf_lim 0.25` (proportion of loci that must be confounded relative to the catalog locus), and `--prune_haplo` (prune non-biological haplotypes).

4.2.5 Filtering

The purpose of data filtering is to ensure high data quality by removing errors, artifacts, and excessive amounts of missing data. We started by removing failed individuals, characterized by extremely low genotyping (> 90% missing data). We then applied the following filters to the genotypic data frame across all populations: (1) exclude RAD tags with more than 4 SNPs (which may represent low quality tags), (2) use only one SNP per tag (to minimize linkage); where there are 2-4 SNPs in a tag, select the SNP with the highest minor allele frequency to maximize information content, (3) exclude loci genotyped in less than 70% of all individuals, (4) exclude loci with an overall minor allele frequency < 3%, (5) exclude loci with observed heterozygosity > 0.5

(the expected maximum for biallelic loci), and (6) remove individuals with > 60% missing data. Using this data set, we identified and removed individuals within populations that were related at the half-sib level or greater using KING v. 2.0 (Manichaikul *et al.* 2010). We used diagnostic tools, including identity-by-missingness analysis, in the R package stackr v 0.4.6 (Gosselin & Bernatchez 2016) to assess patterns of missing data among the samples in R v. 3.2.3 (R Development Core Team 2015).

For effective population size (N_e) estimation, the goal was to maximize the number of individuals retained for the analysis while minimizing missing data. We began by removing failed individuals as above. We then applied the following filters within each population (as opposed to across all individuals as we did above): (1) exclude RAD tags with more than 4 SNPs, (2) use only one SNP per tag; where there are 2-4 SNPs in a tag, select the SNP with the highest minor allele frequency to maximize information content, (3) exclude loci genotyped in less than 75% of individuals within each population, (4) exclude loci with an overall minor allele frequency < 5%, (5) exclude loci with observed heterozygosity > 0.5, (6) remove related individuals (from above analysis) and individuals with > 50% missing data within their population, and (7) remove loci detected as potentially under selection (see Data analysis, below).

4.2.6 Data analysis

Once the data were screened and filtered, the next step was to determine which loci were potentially under selection. We used a multivariate genotype-environment association method, redundancy analysis (RDA), to detect potentially adaptive loci (or, more likely, loci linked to adaptive regions). Redundancy analysis is a constrained ordination that extends linear regression to multivariate response data in order to maximize the proportion of the response variable that is explained (Legendre & Legendre 2012). Linear combinations of the response variable (in this case, genetic data) are modeled as a function of linear combinations of the predictors (in this case, environmental data). Redundancy analysis involves a two-step process in which a multivariate linear regression is computed between genetic and environmental data to produce a matrix of fitted values, then a principal components analysis of the fitted values produces canonical axes, which are linear combinations of the original explanatory variables. The result, in this instance, is a set of axes that summarize the genomic information that can be explained by environmental predictors.

Redundancy analysis requires a complete data frame (no missing values). To impute missing genotypes, we used the mean allele count of genotyped individuals at each SNP within populations. We then took the global mean (across all typed individuals) for SNPs that were completely untyped within a population. This simple imputation method has been shown to work well when RDA is used on incomplete data

sets with random missing data (Xuereb *et al.* In review). We scaled the genetic data (coded as allele counts) and environmental predictors for use in RDA. We identified potentially adaptive loci on each of the two constrained ordination axes as those loci with a “locus score” that was ± 2.5 SD from the mean score for that axis. The locus score represents the coordinates of each locus in the ordination space. This approach essentially identifies sets of SNPs that show an extreme association with the environmentally defined RDA axes. We used the function *rda* in the *vegan* (v. 2.3-5) package (Oksanen *et al.* 2013) for this analysis.

Loci detected as potentially under selection with RDA were removed from the data sets used for neutral analyses and effective population size estimation. We used *Stacks* to calculate observed and expected heterozygosity (variant sites only) and nucleotide diversity (π , variant and fixed sites) within populations for both neutral and potentially adaptive SNPs. We calculated pairwise *F_{ST}* in *Stacks*, using the approach applicable to bi-allelic SNP data (Weir & Cockerham 1984). We visualized population structure in both sets of markers using discriminant analysis of principal components (DAPC) implemented in *adegenet* v. 2.0.1 (Jombart 2008; Jombart & Ahmed 2011). DAPC is an extension of both PCA and discriminant analysis that focuses on among group variation, while minimizing within group variation (Jombart *et al.* 2010). For DAPC plots, we imputed missing data using the most frequent genotype within populations.

We estimated effective population sizes using the linkage disequilibrium method (LDNe) in NeEstimator v.2.01 (beta) (Do *et al.* 2014). Effective population size (N_e) is the evolutionary equivalent of a population's census size; whereas census size is more closely tied to ecological processes (e.g. competition, demography), N_e is related to evolutionary processes such as genetic drift and selection (Waples *et al.* 2014). The premise behind estimating N_e based on linkage disequilibrium (LD, the non-random association of alleles at different loci) is that smaller populations will have increased LD due to the larger influence of genetic drift. To estimate N_e in LDNe, we used the random mating model with a critical value of 0.05. Due to our use of a large number of SNP loci in estimating N_e , we applied a correction factor to the results based on the diploid chromosome number (14) for Weller's salamander (Waples *et al.* 2016).

4.2.7 Conservation scenarios

Finally, we used output from these analyses to address three conservation scenarios for Weller's salamander. All three make use of the "adaptive dissimilarity" (AD) index, a measure of (dis)similarity of populations based on allele frequencies at potentially adaptive markers. The input is a matrix of population allele frequencies at a set of loci detected as potentially under selection. We used the R package *vegan* to calculate chord distances among populations based on this input matrix. We chose chord distance because it produces a bounded result (between 0 and 1.41), although

Euclidean distance could also be used. This produces a full matrix of dissimilarities among all populations; averaging across columns or rows provides an index of overall dissimilarity for each population.

Scenario 1: Site prioritization for conservation. There is a large literature devoted to the delineation of management and conservation units using genetic data (e.g. (Moritz 1994; Crandall *et al.* 2000; Fraser & Bernatchez 2001; Ottewell *et al.* 2016). While our goal is not to review this literature (see Funk *et al.* 2012 for a recent review) we present here an example of how an assessment of adaptive dissimilarity can inform simple site prioritization plans based on maximizing the protection of genetic diversity and evolutionary potential. We contrast this plan to one based only on information from neutral markers. Inputs for this analysis are population differentiation, neutral genetic diversity, adaptive genetic diversity, and adaptive dissimilarity.

Scenario 2: Genetic rescue. The aim of genetic rescue is to improve the fitness of small populations by increasing genetic diversity through the movement of individuals between populations (Whiteley *et al.* 2015). While the focus for this scenario is on neutral genetic diversity and effective population size, here we provide an illustration of how adaptive dissimilarity can be used to minimize the risks of outbreeding depression (a reduction in fitness due to the mixing of divergently adapted genotypes and/or the disruption of co-adapted gene complexes).

Scenario 3: Assisted gene flow. Assisted gene flow is the movement of individuals within the species range from an adaptively divergent source population that has alleles that are predicted to be adaptive under future environmental conditions (Aitken & Whitlock 2013). The goal is to maximize evolutionary potential by moving “pre-adapted” alleles into populations that are expected to experience dramatic changes in environmental conditions. Inputs for this scenario will include effective population size and adaptive dissimilarity as well as consideration of neutral population divergence.

4.3 Results

Our starting sample size for genomic analysis was 263 individuals sampled across nine populations (Figure 14). These populations represent nine of the ten known populations of Weller’s salamander across the range. After discarding low quality sequencing reads, `process_radtags` produced an average of 7,188,722 RAD tags per individual. After filtering, the data set included 237 individuals genotyped at 6,070 loci. Seven failed individuals (> 90% missing data) were removed, as well as 15 individuals with < 60% genotyping and four individuals that were related at the half sib level or greater. Mean read depth per locus (averaged across all samples) ranged from 10 to 40, with a median of 16. Identity-by-missingness analysis showed some clustering of Sugar Mountain samples (Figure C2, Appendix C), indicating that caution should be used in

interpreting results from that population since heterozygosity levels may be underestimated.

To investigate potential selection pressures, we developed a set of environmental predictors including seasonal sets of mean daily maximum and minimum temperature and relative humidity, cumulative heat sums, and vapor pressure deficit. The models used to develop these metrics performed well based on verification and validation (Appendix C). We selected two environmental variables that were relevant to the seasonal activity and physiological constraints of terrestrial salamanders and were not highly correlated ($r = 0.66$): vapor pressure deficit and mean daily minimum temperature, both averaged over the activity season for Weller's salamander (March-November, Table 1). Vapor pressure deficit provides a measure of evaporative water loss, a primary control on activity levels for terrestrial salamanders (Feder 1983). Temperature is also important, since terrestrial salamanders can alter their metabolic rate to accommodate temperature changes, directly affecting rates of energy assimilation and production (Gifford 2016). We used minimum daily temperatures, since these occur at night, when terrestrial salamanders are most likely to be active on the surface. During the day, these animals retreat to microclimate refugia under cover objects or underground, buffering them from daily temperature maxima.

We then used these two predictors and the filtered genomic data set to identify loci potentially under selection using RDA. We identified 66 loci as potentially under

selection based on a 2.5 SD cutoff for SNP loadings on the two constrained ordination axes (Figure C3, Appendix C). All of these loci were significantly correlated ($p < 0.0001$) with mean daily minimum temperature, while 19 loci were also significantly correlated with vapor pressure deficit. DAPC plots of these 66 markers illustrate how the two low-elevation populations, Iron Mts. (IM) and Unaka Mt. Low (UL), drive adaptive patterns at these detected loci (Figure 17b, c). These populations are at much lower elevation and are much warmer than the other Weller's populations (Table 1). These two sites differ in vapor pressure deficit, however, with the more southwestern populations, including UL, having higher VPD, which would result in higher overall water stress for resident salamanders.

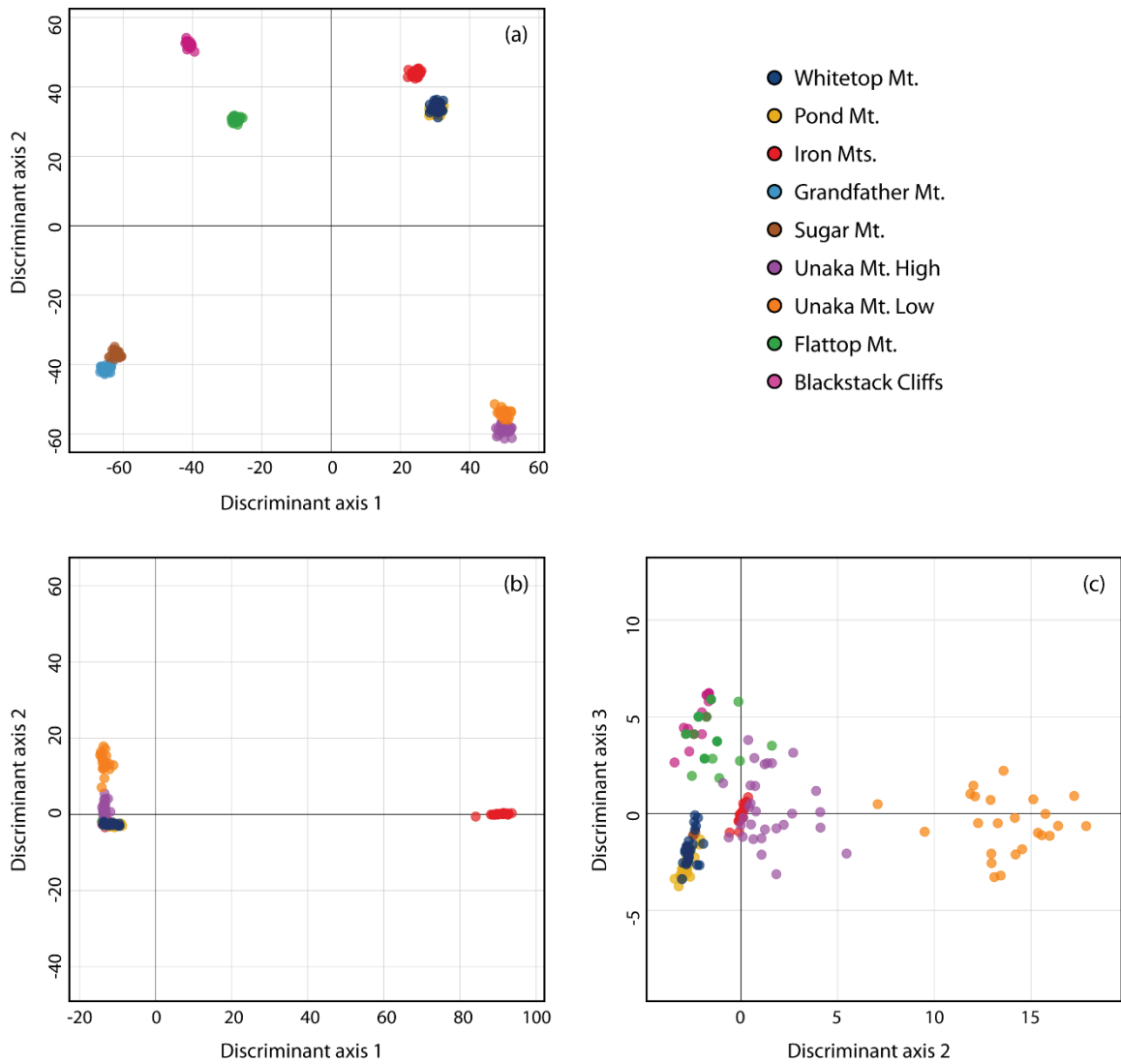


Figure 17. Discriminant analysis of principal components of 6004 neutral SNPs (a) and 66 potentially adaptive SNPs (b, c) from nine Weller's salamander populations. Adaptive DAPC shows axes 1 and 2 (b), and axes 2 and 3 (c). Colors match populations in range map (Figure 14).

We calculated observed heterozygosity (H_o), expected heterozygosity (H_e), and nucleotide diversity (π) for the set of adaptive (66 total) and neutral (6004 total) markers within each population (Table 2), as well as F_{ST} from the neutral markers (Table 3). We calculated effective population size (N_e) from neutral markers filtered to maximize individual sample sizes while minimizing missing data (to improve estimation of N_e). Estimates of N_e with a 95% confidence interval including infinity (e.g. Sugar Mt. and Unaka Low, Table 2) indicate that sampling error explains more than genetic drift at the upper bound of the estimate (Do *et al.* 2014). The populations with infinite estimates correspond to those with smaller sample sizes (number of individuals and number of markers). Rankings of populations based on levels of H_e and π were concordant for both neutral and adaptive variation, while H_o showed some variation. As expected, F_{ST} was high between most populations, ranging from 0.03 to 0.48 (median = 0.32). F_{ST} values largely reflected geographic proximity of populations (compare with Figure 14 and neutral DAPC plot, Figure 17a), and high values were not unexpected given the fragmentation of high mountain habitats and limited dispersal of terrestrial salamanders. Neutral and adaptive gene diversity were not highly correlated (average r across diversity metrics = 0.24). Estimates of N_e were not strongly correlated with either neutral or adaptive genetic diversity metrics (average r across diversity metrics = -0.25).

Table 2. Observed heterozygosity (H_o), expected heterozygosity (H_e), and nucleotide diversity (π) of adaptive and neutral markers within each population. Effective population size (N_e) was estimated from neutral markers filtered to maximize retained individuals while minimizing missing data. Salamander sample sizes are provided for diversity statistics and N_e estimation.

Pop.	Adaptive (66 loci)			Neutral (6004 loci)			N_e (95% confidence intervals)	Sample Sizes	
	H_o	H_e	π	H_o	H_e	π		Diversity statistics	N_e
BC	0.014	0.016	0.0004	0.044	0.054	0.0012	132 (72-617)	23	27
FT	0.015	0.016	0.0004	0.086	0.095	0.0022	868 (701-1137)	23	24
UL	0.066	0.119	0.0028	0.057	0.107	0.0024	462 (164-∞)	28	28
UH	0.043	0.057	0.0013	0.076	0.112	0.0025	622 (539-735)	29	29
SM	0.005	0.004	0.0001	0.052	0.072	0.0016	4269 (763-∞)	24	27
GM	0.001	0.001	0.0000	0.070	0.083	0.0019	675 (535-913)	30	30
IM	0.030	0.042	0.0010	0.059	0.083	0.0019	635 (443-1114)	30	30
PM	0.027	0.030	0.0007	0.105	0.128	0.0029	150 (147-152)	25	25
WT	0.021	0.022	0.0005	0.089	0.122	0.0028	264 (249-281)	25	25

Table 3. Pairwise F_{ST} of Weller's salamander populations, shaded from low values (light gray) to high values (dark gray).

	BC	FT	UL	UH	SM	GM	IM	PM	WT
BC		0.36	0.39	0.36	0.47	0.43	0.48	0.37	0.40
FT	0.36		0.28	0.27	0.33	0.31	0.36	0.28	0.30
UL	0.39	0.28		0.03	0.34	0.33	0.34	0.26	0.28
UH	0.36	0.27	0.03		0.32	0.31	0.32	0.25	0.27
SM	0.47	0.33	0.34	0.32		0.06	0.40	0.30	0.33
GM	0.43	0.31	0.33	0.31	0.06		0.38	0.29	0.32
IM	0.48	0.36	0.34	0.32	0.40	0.38		0.20	0.22
PM	0.37	0.28	0.26	0.25	0.30	0.29	0.20		0.06
WT	0.40	0.30	0.28	0.27	0.33	0.32	0.22	0.06	

The adaptive dissimilarity matrix provides information on multilocus differentiation across populations in their potentially adaptive genetic variation. The average dissimilarity across columns (or rows) indicates which populations are the most different in terms of their adaptive genetic variation. In agreement with the DAPC visualization of potentially adaptive genetic variation (Figure 17b, c), it is the Iron Mts. and Unaka Low populations which are most dissimilar from all others. The Unaka populations represent low and high elevation sampling of what is likely a continuously distributed population (distance between these sites is about 4 km and is completely forested). This is reflected in low F_{ST} (0.03) between these sites. Nevertheless, we see high differentiation between these two sites based on adaptive markers due to substantial differences in environmental conditions (Table 1), indicating local adaptation. In fact, the Unaka High population is more similar to the geographically distant but environmentally similar Grandfather, Sugar, Pond, and Whitetop Mountains (Table 4, Figure 14). The western populations, which share higher VPD with the Unaka Low site, are more similar to that site in term of adaptive markers, despite high F_{ST} on neutral markers (Table 3).

Table 4. Adaptive dissimilarity of Weller’s salamander populations, shaded from low values (light gray) to high values (dark gray). Average adaptive dissimilarity for each population is provided in the bottom row.

	BC	FT	UL	UH	SM	GM	IM	PM	WT
BC		0.29	1.16	0.78	1.03	1.09	1.26	1.07	1.06
FT	0.29		1.09	0.67	1.11	1.17	1.28	1.15	1.14
UL	1.16	1.09		0.90	1.34	1.36	1.36	1.35	1.35
UH	0.78	0.67	0.90		0.79	0.84	1.25	0.82	0.82
SM	1.03	1.11	1.34	0.79		0.09	1.25	0.20	0.15
GM	1.09	1.17	1.36	0.84	0.09		1.26	0.20	0.14
IM	1.26	1.28	1.36	1.25	1.25	1.26		1.19	1.20
PM	1.07	1.15	1.35	0.82	0.20	0.20	1.19		0.21
WT	1.06	1.14	1.35	0.82	0.15	0.14	1.20	0.21	
Avg.	0.97	0.99	1.24	0.86	0.74	0.77	1.26	0.77	0.76

4.3.1 Scenario 1: Site prioritization for conservation

Here, for simplicity, we will assume a scenario where we are interested in identifying the three most important populations for conservation action (e.g. land purchase or restoration) based on information from genetic markers. When neutral genetic data are available, the goal is most often to prioritize populations that maximize the within and between group variability of the species (e.g. Ottewell *et al.* 2016; Pierson *et al.* 2016). For Weller’s salamander, this would mean either the Pond Mt. or Whitetop

Mt. populations first (highest neutral diversity, but low population differentiation, based on F_{ST}), a Unaka Mt. site second (both high and low elevation populations have high neutral diversity and low F_{ST}), and Flattop Mt. third (Tables 2, 3, and 5). If we consider rankings based on the amount of potentially adaptive genetic diversity, we would also want to include the Iron Mt. site, in addition to Unaka and Pond Mts. (Table 5, center column).

Rankings of the amount of adaptive variation, however, do not take full advantage of the information content provided by these potentially adaptive markers. Unlike neutral diversity, the type of variation (not just the overall amount) is of importance. If the goal is to prioritize sites not just in an effort to maximize overall genetic variation, but also to conserve the evolutionary potential of the species, we would want to ensure that we include as broad of a suite of the available adaptive variation as possible. For example, with Weller's salamander, we would be interested in conserving both warm and cool-adapted genotypes. We would not necessarily achieve a goal of maximizing evolutionary potential by only considering rankings based on the amount of adaptive variation.

Table 5. Weller’s salamander population rankings based on different input criteria (columns). Sites are sorted from highest to lowest ranked.

Neutral <i>He/π/FST</i>	Adaptive <i>He/π</i>	Adaptive Dissimilarity
PM or WT	UL	IM
	UH	UL
UH or UL	IM	GM
	PM	FT
FT	WT	BC
IM	BC	SM
GM or SM	FT	WT
	SM	UH
BC	GM	PM

A straightforward approach to this problem of conserving complementary sets of adaptive genetic variation uses the adaptive dissimilarity index as a greedy heuristic algorithm. These algorithms are used extensively in site prioritization and reserve planning to maximize the number of species protected based on various metrics such as species richness, rarity, and habitat connectivity (Margules & Pressey 2000; Urban 2002). In this case, we are using the adaptive dissimilarity index as an iterative (heuristic) algorithm that finds a parsimonious (greedy) solution based on adding complementary sets of adaptive genetic variation. We could start by prioritizing the population that is most unique in terms of adaptive genetic variation, found by identifying the population most different, on average, across multi-locus adaptive genotypes (Table 4). That site is

the warm-adapted Iron Mts. population (average dissimilarity of 1.26). The next most dissimilar is Unaka Low (found by looking for the largest value in the Iron Mt. column, 1.36, Table 4). If we combine the adaptive markers from these populations and recalculate the adaptive dissimilarity index, the next most dissimilar site is the cool, high elevation Grandfather Mt. population. We can continue this process until we have ranked the populations based on their adaptive dissimilarity and the complementarity of their multilocus genotypes with previously identified populations (Table 5, third column). Comparison of these three approaches for site prioritization (Table 5) illustrate how different components of genetic variation change our understanding of what is unique, complementary, and most essential to maximizing the protection of genetic diversity and evolutionary potential across a species range.

4.3.2 Scenario 2: Genetic rescue

Target populations for genetic rescue are generally characterized by small population size, isolation, and low genetic diversity. Reduced fitness and reduced phenotypic variation can also be typical characteristics (Whiteley *et al.* 2015; Frankham 2015). By these criteria, Blackstack Cliffs would be a possible candidate for genetic rescue, due to its low levels of neutral genetic diversity, small effective population size, and isolation (at least according to surveys to date). The closest known populations are Flattop and Unaka Mt., which both show high differentiation (F_{ST}) from Blackstack

Cliffs, indicating no recent gene flow. The major concern with genetic rescue is outbreeding depression, which is the reduced fitness of offspring produced by resident and source individuals, due to genetic divergence and/or the disruption of co-adapted gene complexes (Frankham *et al.* 2011). Despite their relatively close geographic location, the high *FST* values between Blackstack Cliffs and Unaka Low and Flattop Mt. could be of concern for genetic rescue of this population. However, comparison of adaptive dissimilarity (Table 4) clearly indicates that Flattop Mt. is the most similar based on genotyped adaptive variation, indicating that this source population would be least likely to result in outbreeding depression. Given the clear benefits of genetic rescue for isolated populations (Whiteley *et al.* 2015; Frankham 2015), this proactive management approach should be considered for Weller's salamander and other isolated, high elevation species in the Southern Appalachian Mountains.

4.3.3 Scenario 3: Assisted gene flow

Unlike genetic rescue, the target population for assisted gene flow should have a large effective population size (to maximize the effectiveness of selection and minimize the impact of genetic drift), and the source and target populations should be divergent based on their adaptive genotypes. The goal is to introduce "pre-adapted" genotypes into a target population that is expected to see dramatic changes in environmental conditions (Aitken & Whitlock 2013). The source population should have adaptive

variation that is expected to be advantageous under future conditions in the target population. Based on these parameters, Grandfather and Flattop Mts. would be good candidates as targets for assisted gene flow, since their populations are large and forecasted climate change impacts are high (Figure 15). Unaka Low and the Iron Mts. would both be potential source options. Specifically, the best source for assisted gene flow to Flattop Mt. would likely be the Unaka Low population. While the Iron Mt. population has greater adaptive dissimilarity, the Unaka Low population has more variation related to vapor pressure deficit, which is already relatively high at the Flattop site. By contrast, the best source for Grandfather Mt. would likely be the Iron Mt. population, which shows a stronger temperature signal. At high elevation, climate change is expected to have a greater impact on temperature for the Grandfather Mt. population, rather than dramatic increases in vapor pressure deficit. Another option for these target sites would be to include individuals from both low elevation source populations (the “portfolio effect” or “composite provenancing”) to maximize available variation and cover a broader range of future climate conditions (Sgro *et al.* 2011; Weeks *et al.* 2011; Aitken & Whitlock 2013).

4.4 Discussion

Our analysis of RAD-sequencing derived genomic data for Weller’s salamander reinforced our expectation of high levels of population structure in this dispersal-

limited, habitat-restricted species. However, despite the clear isolation of these sites, the resident populations show relatively high estimates of effective population size, which tend to be low for amphibian species overall (Wang *et al.* 2011). These relatively high N_e estimates are especially encouraging, given that we would expect them to be downwardly biased due to random sampling across multiple age cohorts (Robinson & Moyer 2013; Waples *et al.* 2014). Additionally, despite their characterization as high elevation specialists, Weller's salamander can clearly occupy habitats at much lower elevations that have warmer and drier conditions than those higher elevation sites more frequently occupied by the species (Table 1). This variability in environmental regimes provides an indication that the species has the adaptive capacity required to successfully occupy habitats that are environmentally dissimilar to their more typical high-elevation habitat. Given projected changes in climate for the region, and the isolation and lack of additional suitable habitat (i.e. no ability to expand the range upward in elevation or latitude), this environmental and genetic variation across populations could be very important in ensuring the persistence of the species into the future.

Here, we describe a simple, multilocus adaptive dissimilarity (AD) index that can be used to characterize the (dis)similarity of populations based on their potentially adaptive genetic markers. This index provides an intuitive way to integrate potentially adaptive genetic variation into conservation decision-making while accounting for the importance of which *types* of adaptive variation are under consideration (not just the

overall amount of variation). When combined with a multivariate technique for detecting loci under selection (Forester *et al.* In review, 2016), the adaptive dissimilarity metric provides an integrated assessment of how covarying adaptive markers differ (or are similar) across populations. This is particularly important given that many locally adaptive traits are expected to be influenced by sets of genetic loci that may be under weak selection (Le Corre & Kremer 2012; Savolainen *et al.* 2013).

4.4.1 Scenario 1: Site prioritization for conservation

In this scenario we contrasted how rankings of “important” populations can change based on the type of genetic data under consideration, and how those data are evaluated and weighted. For Weller’s salamander, the most striking difference is in prioritization based on maximizing within and between population neutral genetic variation versus prioritization to maximize the evolutionary potential of the species (i.e. conserve as much breadth in adaptive markers as possible). Whereas the lower elevation, warmer-adapted IM population is ranked low in terms of neutral variation, it is the population that holds the largest amount of unique adaptive genetic variation sampled across the species range. The population that has potentially adaptive genetic variation that best complements the variation present in the Iron Mts. is the other low elevation (warm) site, Unaka Low, which also shows a signal of local adaptation to drier conditions. Finally, the population that best complements this set of warm/dry adapted

genotypes is Grandfather Mt., which represents the coldest and wettest site of all locations sampled (Table 1). By contrast, an assessment of the top three sites based on neutral variation would fail to include Iron and Grandfather Mts., potentially compromising the overall evolutionary potential of the species. Consideration of both neutral and adaptive diversity would strike the best balance in real-world applications (e.g. see frameworks provided in Guia & Saitoh 2007; Funk *et al.* 2012). However, conservation assessments that include an assessment of adaptive dissimilarity can help ensure protection of the full range of environmentally-mediated local adaptation across populations. By prioritizing populations that show large dissimilarities in adaptive markers, we can maximize both intraspecific adaptive genetic diversity and the evolutionary resiliency of the species.

Of course, genetic variation is just part of site prioritization, which includes many other considerations such as budget, land availability and ownership status, site history, and coexisting species of conservation concern. In this case, all but two Weller's populations are on land that is protected in some form (e.g. state or federal public lands, private easements). In one of these cases, Weller's salamanders have not been relocated at that location since the original record in 1984, and the site has seen residential development and significant changes to forest structure over that time period. In the second case, Sugar Mt., a portion of the site is under partial private conservation, while the remainder is slated for residential development. For Weller's salamander then, as for

most species of conservation concern, site prioritization to ensure species persistence is a complex decision-making process toward which genomic information can make an important contribution.

4.4.2 Scenario 2: Genetic rescue

Genetic rescue has been used successfully in a number of high profile conservation genetic efforts (e.g. Florida panthers, Johnson *et al.* 2010; wolves, Vilà *et al.* 2003, Adams *et al.* 2011; and bighorn sheep, Miller *et al.* 2012). Genetic rescue can be beneficial for populations that are at risk of or are currently experiencing deleterious effects from inbreeding depression. Concerns about outbreeding depression have limited the use of genetic rescue (Edmands 2007), however recent reviews have highlighted the potentially large benefits and limited risks when genetic rescue is carefully implemented (Hedrick & Fredrickson 2010; Weeks *et al.* 2011; Whiteley *et al.* 2015; Frankham 2015). Assessments of potentially adaptive genetic variation can help alleviate risks from outbreeding depression by identifying source populations that minimize adaptive divergence and therefore reduce the risk of adaptive incompatibilities. The adaptive dissimilarity index is well suited to this task since it represents (dis)similarity based on multilocus adaptive genotypes.

In the case of Weller's salamander, the Blackstack Cliffs population, at the southwestern range boundary for the species, is a population that should continue to be

monitored for changes in population size and genetic diversity. Its high F_{ST} relative to the closest populations, comparatively low genetic diversity, and small population size are indicators of negative isolation effects. Based on adaptive dissimilarity, Flattop Mt. would be the best source population for genetic rescue to minimize the risk of outbreeding depression while maximizing the potential for improved fitness and population restoration.

Information that can help reduce the risk of outbreeding depression, such as adaptive dissimilarity, should encourage a more proactive use of genetic rescue in small, isolated populations. Even before the negative effects of inbreeding depression are manifested in these populations, they can lose adaptive genetic variation to drift, lowering their tolerance for and ability to adapt to changing environmental conditions (Armbruster & Reed 2005; Keyghobadi 2007; Bijlsma & Loeschcke 2012). With habitat loss, fragmentation, and degradation interacting with climate change, pollutants, and invasive species, populations are placed under increasing stress from these changing and deteriorating environmental conditions. Increasing population size and fitness in these populations through carefully planned genetic rescue should, ideally, be combined with efforts to increase habitat availability and/or habitat connectivity. Additional efforts to supplement adaptive genetic variation (such as assisted gene flow, scenario 3) can be implemented to restore adaptive capacity once healthy population sizes have been reestablished.

4.4.3 Scenario 3: Assisted gene flow

This proactive approach, which involves the directional movement of individuals within a species range to facilitate adaptation to changing conditions, has been advocated for long-lived, sessile species such as trees (e.g. Steane *et al.* 2014), and populations/species that have a limited ability to track climate conditions that they are currently adapted to (Sgro *et al.* 2011; Aitken & Whitlock 2013). Weller's salamander is an exemplar of the latter situation: a range-restricted, dispersal limited species, with a small number of populations isolated on the highest available mountain peaks, and no possibility of movement through warm low-elevation valleys. Climate change forecasts for the Southern Appalachians indicate dramatic changes in the coming decades (Figure 15). Although terrestrial salamanders can potentially alter their behavior or phenology to adjust to these changing conditions, physiological stresses due to increasing temperatures and seasonal changes in water balance are likely to impose significant selective pressures on populations (Bernardo & Spotila 2006). Geographic variation in important traits such as resistance to cutaneous water loss (Winters & Gifford 2013; Riddell & Sears 2015) indicates that there is environmentally-mediated variation among terrestrial salamander populations that could be advantageous in rapidly changing climates. Given some genetic basis for this variation, movement of individuals that are adapted to warmer and drier conditions could help mitigate maladaptation of isolated,

high elevation populations by increasing the genetic variation available for future evolutionary responses.

The concerns about assisted gene flow are similar to those for genetic rescue: disruption of local adaptation, the loss of distinct, locally adapted lineages, and outbreeding depression. For example, other biologically relevant environmental conditions that are important for salamanders, such as pH, vary with elevation. Movement of individuals across elevation may result in migrants that are poorly adapted to the local pH, reducing survival and fitness in spite of beneficial adaptation to changing climatic conditions. However, for many populations and species that either lack the capacity for long-distance movement or have no available suitable habitats to disperse into, adaptation in place will be the only alternative to maladaptation, extirpation, and extinction. In these cases, consideration of the potentially far-reaching benefits and careful evaluation to minimize the risks of assisted gene flow can provide an important option for the management of vulnerable populations (Aitken & Whitlock 2013).

In the case of Weller's salamander, there are one (and possibly two) long elevation gradients that would be an excellent case study for the potential use of assisted gene flow across populations. The Unaka Mt. populations are almost certainly continuously distributed along a > 800 m elevation gradient, while the Iron Mts. likely has a similarly continuous distribution (though surveys at higher elevations have not yet

been completed). Periodic genomic monitoring of populations along these transects could determine if shifts in potentially adaptive allele distributions are occurring in response to changing conditions. Assessment of gene flow along these gradients could help establish the potential benefits of moving individuals not just within, but also across mountain peaks. The identified options of assisted gene flow across populations include the large, cool-adapted populations at Grandfather and Flattop Mts., which have no low-elevation counterparts. Although there has been reasonable skepticism of the value (versus the risks) of assisted gene flow to improve species adaptive responses to climate change, it remains a potentially highly effective means of improving the evolutionary potential of species that are critically tied to climate and must adapt to changing conditions in place. Careful planning, implementation, and monitoring of assisted gene flow in wild populations will help improve our understanding of how and in which cases this approach will provide the most benefit to species.

4.4.4 Conclusions

While the use of genomics in conservation is relatively recent, applications are increasing, though many of these may not be well represented in the peer-reviewed literature (Garner *et al.* 2016). It will be important to document both the successful uses of genomics for conservation, as well as the failures. There is much that is still unknown about best practices for management applications (e.g. sample sizes for assisted gene

flow, Aitken & Whitlock 2013), so field experiments and simulation studies will be vital to the practical advancement of landscape genomics in conservation (Chapter 5). As anthropogenic change continues to have negative environmental impacts globally, landscape genomics can assist conservation efforts by providing unprecedented insight into the genetic variability and evolutionary potential of wild populations. Data at this intraspecific scale are essential to ensuring that conservation actions are protecting the genetic diversity and evolutionary processes that are the foundation of all levels of biodiversity (Moritz 2002; Sgro *et al.* 2011; Harrisson *et al.* 2014; Hoffmann *et al.* 2015).

5. Concluding remarks

The three components of adaptive capacity in response to environmental change are dispersal, phenotypic plasticity, and evolutionary potential. Evolutionary potential has been identified as an essential but underutilized approach for managing species responses to anthropogenic change (Dawson *et al.* 2011; Nicotra *et al.* 2015). The overarching goal of this research has been to improve the utility of landscape genomics for the proactive management of evolutionary potential in populations and species in the absence of prior genomic information. The adaptive capacity framework for understanding species vulnerability is most commonly applied in the climate change literature (IPCC 2014), but is useful in planning conservation measures across anthropogenic threats, such as habitat fragmentation and disease dynamics.

A species' vulnerability to climate change (or other threats) is determined by the magnitude of its exposure and sensitivity to the threat, and its adaptive capacity in response (Dawson *et al.* 2011). By definition, most species of conservation concern, such as Weller's salamander, are both highly exposed and sensitive to the interacting suite of anthropogenic stressors they face. Their adaptive capacity in response is a product of their ability to move to more suitable conditions and to show a plastic and/or evolutionary response. For endemic, dispersal-limited species like Weller's salamander, plasticity and evolutionary adaptation are the only alternatives to extirpation and extinction in the face of dramatic changes in environmental conditions. While plasticity

can play a pivotal role in short and medium-term responses to changing conditions, it is complex and can be costly and even maladaptive (Ghalambor *et al.* 2007; Chevin *et al.* 2010; Bijlsma & Loeschcke 2012; Chevin & Lande 2015).

Fortunately, technological advances have dramatically increased our ability to evaluate the evolutionary potential of wild species in response to changing conditions. A landscape genomic approach to assessing evolutionary potential holds a key advantage over other methods, such as common garden experiments and reciprocal transplants, in that it is applicable to any species, regardless of conservation status or life history traits (e.g. generation time, tractability of experimental approaches). With an understanding of adaptive genetic variation and the drivers of natural selection across populations, we can better target management toward maximizing evolutionary resiliency in the face of complex and interacting environmental changes (Sgro *et al.* 2011; Funk *et al.* 2012; Harrisson *et al.* 2014).

5.1 Synopsis

Many challenges remain, however, in the technical and practical applications of landscape genomics. In this research, I focused on a fundamental component of effective landscape genomic analyses: the partitioning of genomic data into neutral and adaptive sets of markers. I tested the ability of genotype-environment association (GEA) methods to correctly partition simulated genomic data across a broad range of landscape

heterogeneities, selection strengths, dispersal abilities, demographic histories, sample sizes, sampling designs, and genetic architectures. I found that multivariate GEA methods showed a superior combination of low false positive and high true positive rates across simulation scenarios, providing a powerful tool for investigating the genetic basis of local adaptation and better informing management actions.

I then applied this GEA approach to a reduced representation genomic data set for Weller's salamander. This endemic Southern Appalachian salamander, like other species that share its relictual, high-elevation habitat, faces a variety of anthropogenically-mediated threats including climate change and habitat degradation and fragmentation. Genomic-scale assessments of genetic variability indicated that, despite isolation on “sky island” habitats, the majority of sampled Weller’s populations had larger than expected effective population sizes and reasonable levels of genetic diversity. I used adaptive dissimilarity to characterize the scope of adaptive variation across the Weller’s range, and addressed a series of conservation scenarios that were improved by the inclusion of explicit consideration of differences in adaptive variation across populations. Given overall healthy population sizes and levels of genetic diversity, in addition to a breadth of adaptive variation across populations, the prospects for continued persistence of Weller’s salamander appear positive. Continued surveys will be needed to identify additional populations across the range, and site prioritization efforts that focus on vulnerable populations (due to development or

timber harvest, for example) and the conservation of adaptive variation are important to maximize the long-term health and resiliency of known populations. Genetic monitoring of smaller, isolated populations (e.g. Blackstack Cliffs) will be essential to determining if and when genetic rescue is needed to ensure population fitness and persistence. Finally, assisted gene flow for large, cold-adapted, high elevation populations should remain a management option in the coming decades to improve the breadth of adaptive variation available for natural selection in these populations and to maximize evolutionary resiliency to changing environmental conditions.

5.2 Prospectus for future research

We are making excellent progress with statistical methods in landscape genomics. However, it will be important to continue testing new methods in rigorous, simulation frameworks that include more realistic genetic architectures and ecological parameters. This includes locus interaction effects, the simulation of complex polygenic traits, and their interaction with heterogeneous environmental surfaces. Empirical systems are complex and rarely meet statistical or theoretical population genetic assumptions. Only by understanding where methods succeed and where they fail can we confidently apply them to empirical data, especially when important management decisions are dependent on the results. This is especially the case when studying species

of conservation concern, where few additional resources (e.g. fitness data, common garden studies) may be available to corroborate results from genomic studies.

Genomic-focused studies of wild populations, in the absence of supporting data, mean that we must use caution in our interpretation and use of the downstream information. There are a number of technical issues in the genomics data-development pipeline that can result in apparent biological signals that are actually technical artifacts. The careful use of genotyping methods, data development and screening pipelines, and data analysis techniques is essential. On-going research into these technical concerns (e.g. the effect of non-random missing data on downstream results) is vital to improving the utility of landscape genomic data for management (e.g, Xuereb *et al.* In review; Gautier *et al.* 2013; Gosselin & Bernatchez 2016).

It is also important to recognize that reduced-representation genomic methods can (by design) only sample a portion of the adaptive genetic variation across individuals (Pearse 2016; McKinney *et al.* 2016). Even when we use GEA methods that are sensitive to multilocus selection, we cannot detect adaptive variation that has not been sampled. Therefore, proactive management of evolutionary potential through approaches such as assisted gene flow should be implemented cautiously, and the effects well documented so that we build an improved, more empirically grounded understanding of risks and benefits. These management actions are well-suited to a risk-assessment approach, based in an adaptive management framework (plan, act, monitor,

react), a practice that is robust in the face of uncertainty about future change (Polasky *et al.* 2011).

Finally, adaptive management includes not just assessment but also monitoring (Schwartz *et al.* 2007) that is integrated into a plan for action and response (Grantham *et al.* 2009; Martin *et al.* 2012; Lindenmayer *et al.* 2013). Temporal monitoring is essential to assess genetic erosion, changes in connectivity (e.g. due to habitat fragmentation or barriers), the effectiveness of genetic rescue, and the outcomes of assisted migration. Simulation studies have been used to identify the best strategies for genetic monitoring (e.g. temporal and spatial sampling designs, the most effective metrics and markers; Landguth *et al.* 2010; Hoban *et al.* 2013, 2014), however additional simulation work is needed to inform monitoring requirements that are specific to different management actions. Importantly, monitoring is not useful unless specific “trigger points” for management action have been identified in advance; otherwise we risk monitoring species to extinction (Lindenmayer *et al.* 2013).

Landscape genomics must be part of a broader effort to stem the biodiversity crisis. A focus on genetic diversity may seem reductionist in the face of species extinctions and ecosystem degradation. However, one of the most valuable parts of a landscape genomic perspective on conservation is a clear understanding of the importance of conserving not just genetic diversity, but also the ecological and evolutionary processes that sustain all levels of biodiversity (Moritz 2002).

Appendix A: Supporting information for Chapter 2 - Detecting spatial genetic signatures of local adaptation in heterogeneous landscapes

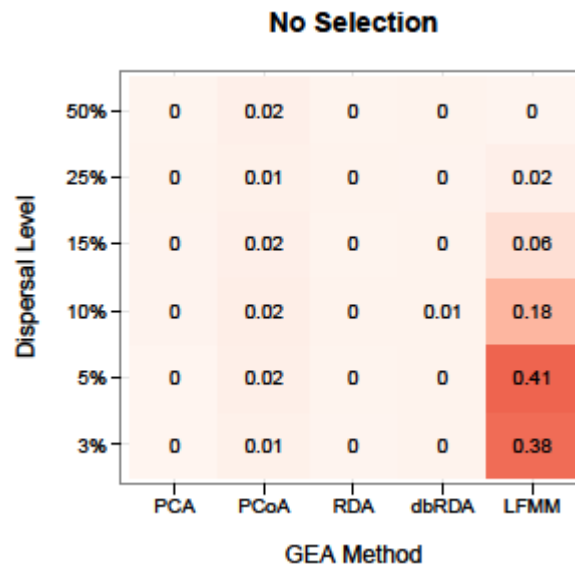


Figure A1: Average false positive rate (FPR) across ten replicates of “no selection” simulations. False positive rate scales from 0 (best performance, 0% FPR, in light red) to 1 (worst performance, 100% FPR, in red). Results for principal components analysis (PCA), principal coordinates analysis (PCoA), redundancy analysis (RDA), distance-based redundancy analysis (dbRDA), and latent factor mixed models (LFMM, Patterson K).

Table A1. Average TPR, FPR, and genotype-environment association indices across ten replicates of each simulation scenario for no mutation (NM) and mutation (M) runs, as well as the difference between them (M-NM). The lower table provides averaged results for isolation by distance and local adaptation. Bold and starred differences are significant at $\alpha=0.05$ using a paired t-test.

Simulation	Method	True Positive Rate (TPR)			False Positive Rate (FPR)			Genotype-Environment Association		
		NM	M	M-NM	NM	M	M-NM	NM	M	M-NM
H5-S10-D03	PCA	0.1	0.2	0.1	0.00	0.00	0.00	0.3	0.5	0.2
	RDA	1.0	1.0	0.0	0.00	0.00	0.00	2.8	2.7	-0.1
	PCoA	0.2	0.4	0.2	0.02	0.01	-0.01*	0.5	1.0	0.5
	dbRDA	1.0	1.0	0.0	0.00	0.00	0.00	2.8	2.7	-0.1
	LFMM-mK	1.0	1.0	0.0	0.63	0.55	-0.08*	2.8	2.8	0.0
	LFMM-pK	1.0	1.0	0.0	0.50	0.37	-0.12*	2.7	2.8	0.1
H5-S10-D10	PCA	0.7	0.9	0.2	0.00	0.00	0.00	1.5	1.9	0.4
	RDA	1.0	1.0	0.0	0.01	0.00	-0.01	2.3	2.2	-0.1
	PCoA	0.7	0.9	0.2	0.03	0.01	-0.01	1.6	1.9	0.3
	dbRDA	1.0	1.0	0.0	0.01	0.00	0.00	2.3	2.2	-0.1
	LFMM-mK	1.0	1.0	0.0	0.22	0.19	-0.03	2.3	2.2	-0.1
	LFMM-pK	1.0	1.0	0.0	0.22	0.19	-0.03	2.3	2.2	-0.1
H5-S10-D25	PCA	0.1	0.0	-0.1	0.00	0.00	0.00	0.2	0.0	-0.2
	RDA	0.8	0.7	-0.1	0.00	0.01	0.00	1.6	1.4	-0.2
	PCoA	0.3	0.2	-0.1	0.02	0.02	0.00	0.6	0.4	-0.2
	dbRDA	0.8	0.7	-0.1	0.01	0.01	0.00	1.6	1.3	-0.3
	LFMM-mK	0.8	0.8	0.0	0.01	0.00	-0.01*	1.4	1.4	0.0
	LFMM-pK	0.8	0.8	0.0	0.01	0.00	-0.01	1.4	1.4	0.0

Simulation	Isolation by Distance (MEM-RDA R^2_{adj})			Local Adaptation (Pearson correlation)		
	NM	M	M-NM	NM	M	M-NM
H5-S10-D03	0.382	0.317	-0.065*	0.638	0.640	0.002
H5-S10-D10	0.071	0.066	-0.005*	0.463	0.457	-0.006
H5-S10-D25	0.019	0.017	-0.002	0.232	0.228	-0.004

Table A2. Comparison of isolation by distance measures: simple Mantel's tests (Mantel r^2) and spatial eigenfunction and redundancy analysis (MEM-RDA R^2_{adj}); both metrics are averaged across ten replicates of each simulation scenario.

Landscape		H1		H5		H9		G	
Selection	Dispersal	Mantel	MEM-RDA	Mantel	MEM-RDA	Mantel	MEM-RDA	Mantel	MEM-RDA
1%	3%	0.227	0.315	0.239	0.320	0.222	0.313	0.228	0.313
	5%	0.112	0.167	0.103	0.162	0.123	0.167	0.122	0.167
	10%	0.019	0.057	0.023	0.059	0.021	0.060	0.018	0.056
	15%	0.008	0.031	0.007	0.032	0.007	0.028	0.007	0.031
	25%	0.002	0.018	0.001	0.017	0.001	0.015	0.002	0.016
	50%	0.001	0.011	0.001	0.008	0.000	0.009	0.001	0.010
5%	3%	0.242	0.319	0.231	0.317	0.240	0.323	0.236	0.319
	5%	0.119	0.168	0.121	0.167	0.129	0.172	0.123	0.169
	10%	0.026	0.059	0.023	0.062	0.029	0.064	0.025	0.060
	15%	0.008	0.031	0.008	0.033	0.008	0.031	0.009	0.032
	25%	0.001	0.015	0.001	0.016	0.002	0.016	0.001	0.016
	50%	0.000	0.008	0.001	0.009	0.000	0.009	0.001	0.009
10%	3%	0.233	0.320	0.246	0.317	0.253	0.332	0.266	0.326
	5%	0.124	0.173	0.132	0.177	0.136	0.175	0.137	0.175
	10%	0.027	0.061	0.031	0.066	0.032	0.067	0.035	0.066
	15%	0.008	0.033	0.009	0.034	0.010	0.034	0.011	0.037
	25%	0.002	0.016	0.002	0.017	0.002	0.017	0.002	0.016
	50%	0.000	0.010	0.000	0.008	0.000	0.010	0.000	0.009
50%	3%	0.263	0.344	0.275	0.356	0.248	0.344	0.288	0.347
	5%	0.155	0.200	0.168	0.202	0.170	0.208	0.208	0.206
	10%	0.043	0.077	0.047	0.082	0.055	0.085	0.086	0.097
	15%	0.018	0.043	0.019	0.047	0.023	0.050	0.033	0.055
	25%	0.004	0.020	0.004	0.023	0.007	0.027	0.009	0.028
	50%	0.001	0.012	0.001	0.014	0.001	0.018	0.002	0.017

Table A3. The average value of K (the number of latent factors) across ten simulation replicates determined using the Minimum Average Partial Test (MAP) and Patterson approaches.

Landscape		H1		H5		H9		G		None		
Selection	Dispersal	MAP	Patterson	MAP	Patterson	MAP	Patterson	MAP	Patterson	Selection	MAP	Patterson
1%	3%	7.8	14.6	8.6	14.8	8.1	14.6	8.5	14.3	None	8.5	14.8
	5%	4.7	9.1	4.3	8.7	4.2	8.3	4.3	8.2		3.9	9.0
	10%	1.8	3.8	1.7	3.7	1.7	3.5	1.8	3.1		1.7	4.0
	15%	1.0	2.1	1.0	2.1	1.0	2.2	1.0	2.2		1.0	2.3
	25%	1.0	1.1	1.0	1.0	1.0	1.2	1.0	1.0		1.0	1.1
	50%	1.0	1.0	1.0	1.0	1.0	1.0	1.0	1.0		1.0	1.0
5%	3%	8.4	14.5	8.8	15.4	8.6	14.7	8.1	14.8			
	5%	4.0	7.7	4.1	8.6	4.6	8.2	4.3	8.4			
	10%	1.8	3.6	1.9	3.6	2.0	3.7	1.8	3.4			
	15%	1.0	2.1	1.0	2.4	1.0	2.0	1.0	2.0			
	25%	1.0	1.0	1.0	1.1	1.0	1.0	1.0	1.0			
	50%	1.0	1.0	1.0	1.0	1.0	1.0	1.0	1.0			
10%	3%	7.7	15.3	8.2	15.6	8.7	14.8	8.0	14.8			
	5%	4.7	8.3	4.8	8.8	4.5	8.6	4.0	8.5			
	10%	1.9	3.8	2.0	3.8	2.0	3.7	2.0	3.8			
	15%	1.0	2.6	1.0	2.1	1.0	2.2	1.0	2.4			
	25%	1.0	1.0	1.0	1.3	1.0	1.2	1.0	1.0			
	50%	1.0	1.0	1.0	1.0	1.0	1.0	1.0	1.0			
50%	3%	8.4	15.4	9.4	16.1	9.2	15.6	8.6	15.7			
	5%	5.3	9.2	5.3	9.5	5.2	10.5	4.3	8.5			
	10%	2.2	4.4	2.4	4.1	2.4	4.5	3.3	4.1			
	15%	1.4	2.6	1.7	2.6	1.4	2.8	1.6	3.0			
	25%	1.0	1.5	1.0	1.3	1.0	1.8	1.0	1.7			
	50%	1.0	1.0	1.0	1.3	1.0	1.2	1.0	1.3			

Table A4. Average true positive rate (TPR), false positive rate (FPR), and genotype-environment associations (GEA) across ten replicates of each simulation scenario for latent factor mixed models (LFMM) using the Minimum Average Partial Test (MAP) and Patterson K approaches.

Landscape	Selection	Dispersal	LFMM - MAP K			LFMM - Patterson K		
			TPR	FPR	GEA	TPR	FPR	GEA
H1	1%	3%	0.9	0.56	1.1	0.8	0.42	1.1
		5%	0.6	0.45	0.7	0.5	0.39	0.7
		10%	0.1	0.17	0.1	0.1	0.17	0.1
		15%	0.1	0.06	0.1	0.1	0.05	0.1
		25%	0.0	0.01	0.0	0.0	0.01	0.0
		50%	0.0	0.00	0.0	0.0	0.00	0.0
	5%	3%	1.0	0.56	2.1	0.8	0.38	1.9
		5%	0.9	0.45	1.6	0.9	0.43	1.6
		10%	0.8	0.18	1.1	0.7	0.18	1.0
		15%	0.8	0.06	1.0	0.7	0.06	0.9
		25%	0.0	0.01	0.0	0.0	0.01	0.0
		50%	0.0	0.00	0.0	0.0	0.00	0.0
	10%	3%	1.0	0.53	2.4	1.0	0.37	2.3
		5%	1.0	0.45	2.1	1.0	0.43	2.1
		10%	0.9	0.20	1.9	0.9	0.20	1.9
		15%	0.9	0.06	1.5	0.9	0.06	1.5
		25%	0.5	0.00	0.5	0.4	0.00	0.4
		50%	0.0	0.00	0.0	0.0	0.00	0.0
	50%	3%	1.0	0.58	2.9	1.0	0.43	3.0
		5%	1.0	0.49	2.8	1.0	0.42	2.8
		10%	1.0	0.27	2.6	1.0	0.26	2.7
		15%	1.0	0.11	2.5	1.0	0.11	2.4
		25%	1.0	0.01	2.6	1.0	0.01	2.6
		50%	1.0	0.00	2.9	1.0	0.00	2.9

Landscape	Selection	Dispersal	LFMM - MAP K			LFMM - Patterson K		
			TPR	FPR	GEA	TPR	FPR	GEA
H5	1%	3%	1.0	0.57	1.8	1.0	0.41	1.7
		5%	0.8	0.43	1.4	0.8	0.38	1.6
		10%	0.6	0.17	0.7	0.6	0.17	0.7
		15%	0.1	0.06	0.1	0.0	0.06	0.0
		25%	0.0	0.01	0.0	0.0	0.02	0.0
		50%	0.0	0.00	0.0	0.0	0.00	0.0
	5%	3%	1.0	0.51	2.5	1.0	0.41	2.4
		5%	1.0	0.45	2.3	1.0	0.40	2.3
		10%	1.0	0.17	2.0	1.0	0.17	2.0
		15%	0.8	0.06	1.2	0.8	0.06	1.2
		25%	0.1	0.01	0.2	0.1	0.01	0.2
		50%	0.0	0.00	0.0	0.0	0.00	0.0
	10%	3%	1.0	0.55	2.8	1.0	0.37	2.8
		5%	1.0	0.45	2.5	1.0	0.39	2.6
		10%	1.0	0.19	2.2	1.0	0.19	2.2
		15%	1.0	0.07	2.3	1.0	0.06	2.2
		25%	0.8	0.00	1.4	0.8	0.00	1.4
		50%	0.1	0.00	0.2	0.1	0.00	0.2
	50%	3%	1.0	0.59	3.0	1.0	0.41	3.0
		5%	1.0	0.55	3.0	1.0	0.49	3.0
		10%	1.0	0.29	2.8	1.0	0.29	2.8
		15%	1.0	0.14	2.7	1.0	0.13	2.7
		25%	1.0	0.02	2.5	1.0	0.02	2.5
		50%	1.0	0.00	2.9	1.0	0.00	2.9

Landscape	Selection	Dispersal	LFMM - MAP K			LFMM - Patterson K		
			TPR	FPR	GEA	TPR	FPR	GEA
H9	1%	3%	0.8	0.56	1.8	0.8	0.41	1.8
		5%	0.8	0.47	1.7	0.8	0.44	1.7
		10%	0.3	0.19	0.7	0.3	0.19	0.6
		15%	0.0	0.06	0.0	0.0	0.05	0.0
		25%	0.0	0.01	0.0	0.0	0.01	0.0
		50%	0.0	0.00	0.0	0.0	0.00	0.0
	5%	3%	1.0	0.56	2.7	1.0	0.47	2.8
		5%	1.0	0.47	2.5	1.0	0.44	2.4
		10%	1.0	0.22	2.1	1.0	0.21	2.0
		15%	0.9	0.07	2.0	0.9	0.06	2.0
		25%	0.5	0.01	0.6	0.5	0.01	0.7
		50%	0.0	0.00	0.0	0.0	0.00	0.0
	10%	3%	1.0	0.56	2.9	1.0	0.43	2.8
		5%	1.0	0.47	2.7	1.0	0.43	2.6
		10%	1.0	0.20	2.6	1.0	0.19	2.6
		15%	1.0	0.06	2.3	1.0	0.06	2.3
		25%	0.8	0.01	2.1	0.8	0.01	2.0
		50%	0.2	0.00	0.4	0.2	0.00	0.4
	50%	3%	1.0	0.56	3.0	1.0	0.44	2.9
		5%	1.0	0.55	3.0	1.0	0.46	3.0
		10%	1.0	0.31	2.9	1.0	0.31	2.9
		15%	1.0	0.16	2.8	1.0	0.16	2.8
		25%	1.0	0.02	2.8	1.0	0.02	2.7
		50%	1.0	0.00	3.0	1.0	0.00	3.0

Landscape	Selection	Dispersal	LFMM - MAP K			LFMM - Patterson K		
			TPR	FPR	GEA	TPR	FPR	GEA
G	1%	3%	0.9	0.53	2.4	0.8	0.37	2.3
		5%	0.8	0.44	2.4	0.8	0.42	2.4
		10%	0.4	0.17	1.0	0.4	0.16	1.1
		15%	0.3	0.06	0.7	0.3	0.06	0.7
		25%	0.0	0.01	0.0	0.0	0.01	0.0
		50%	0.0	0.00	0.0	0.0	0.00	0.0
	5%	3%	1.0	0.51	3.0	1.0	0.38	3.0
		5%	1.0	0.47	3.0	1.0	0.41	3.0
		10%	1.0	0.19	3.0	1.0	0.18	3.0
		15%	1.0	0.06	3.0	1.0	0.07	3.0
		25%	0.6	0.01	1.8	0.6	0.01	1.8
		50%	0.0	0.00	0.0	0.0	0.00	0.0
	10%	3%	1.0	0.57	3.0	1.0	0.35	3.0
		5%	1.0	0.50	3.0	1.0	0.46	3.0
		10%	1.0	0.21	3.0	1.0	0.20	3.0
		15%	1.0	0.06	3.0	1.0	0.06	3.0
		25%	0.9	0.01	2.7	0.9	0.01	2.7
		50%	0.3	0.00	0.9	0.3	0.00	0.9
	50%	3%	1.0	0.59	3.0	1.0	0.44	3.0
		5%	1.0	0.60	3.0	1.0	0.55	3.0
		10%	1.0	0.42	3.0	1.0	0.41	3.0
		15%	1.0	0.22	3.0	1.0	0.22	3.0
		25%	1.0	0.03	3.0	1.0	0.03	3.0
		50%	1.0	0.00	3.0	1.0	0.00	3.0

Appendix B: Supporting information for Chapter 3 - Using genotype-environment associations to identify multilocus local adaptation

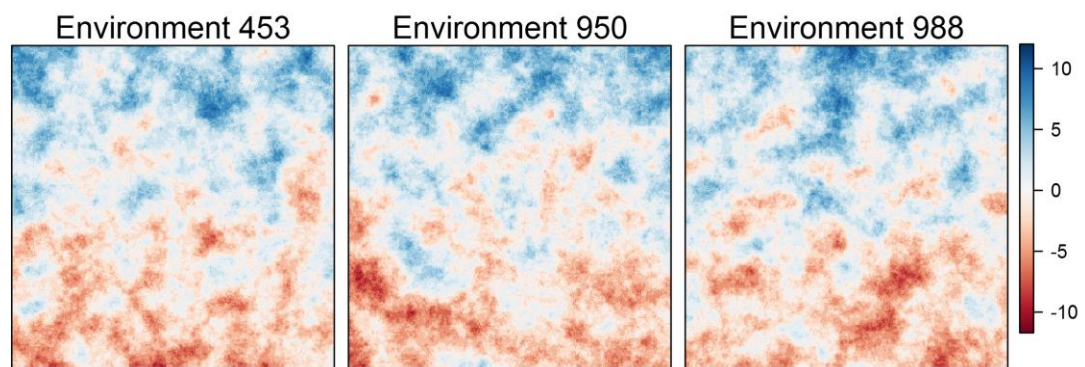


Figure B1. The three environmental surfaces used as replicates from Lotterhos & Whitlock (2015). Colors represent values of the environment.

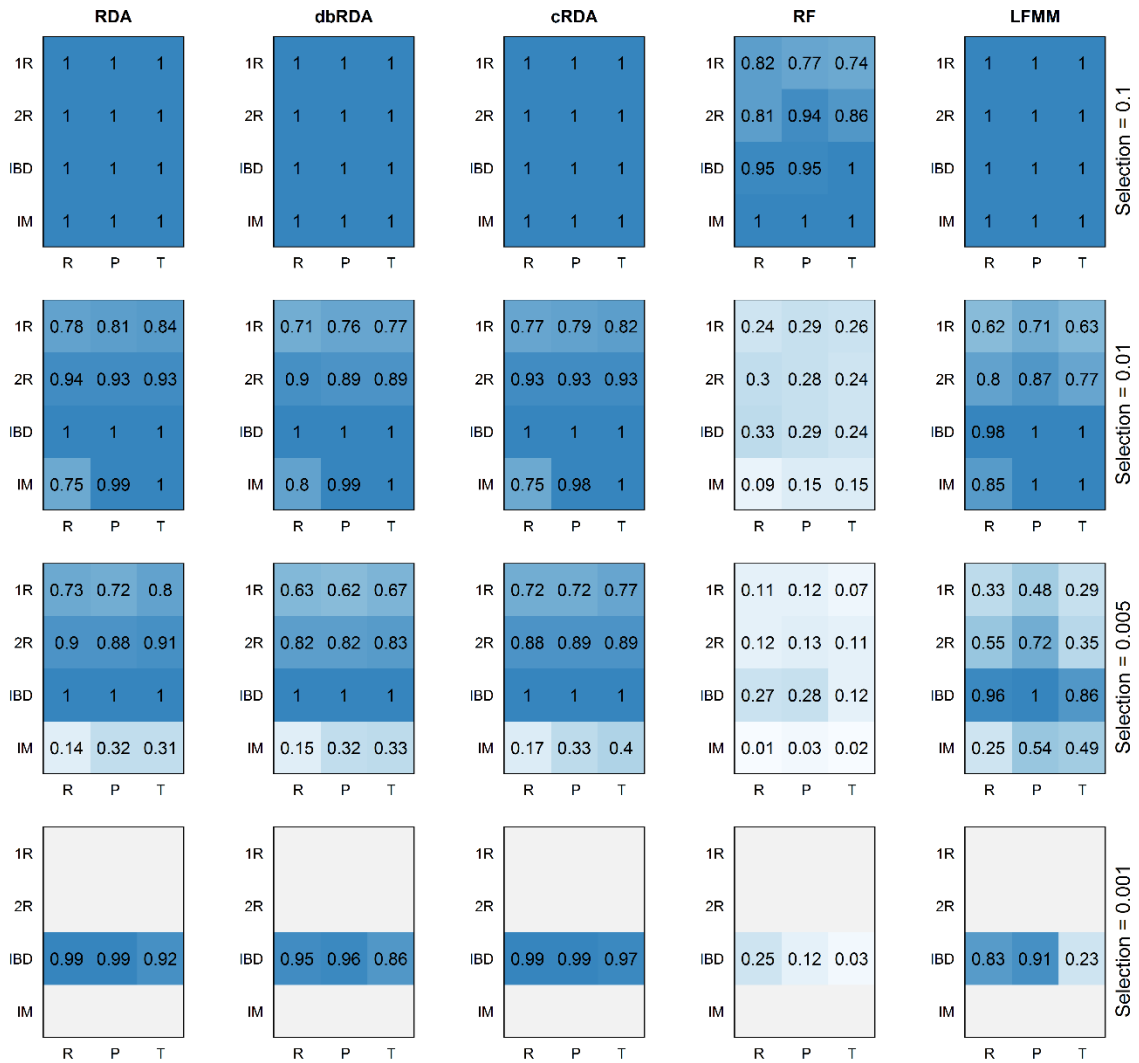


Figure B2. Average true positive rates for different levels of selection (rows) from five methods (columns) using locus rankings and a sample size of 6 individuals per deme. Each method shows results for different sampling strategies (R = random, P = pairs, T = transects) and demographies (1R and 2R = refugial expansion, IBD = equilibrium isolation by distance, IM = equilibrium island model). Only the IBD demography included very weak selection (s=0.001).

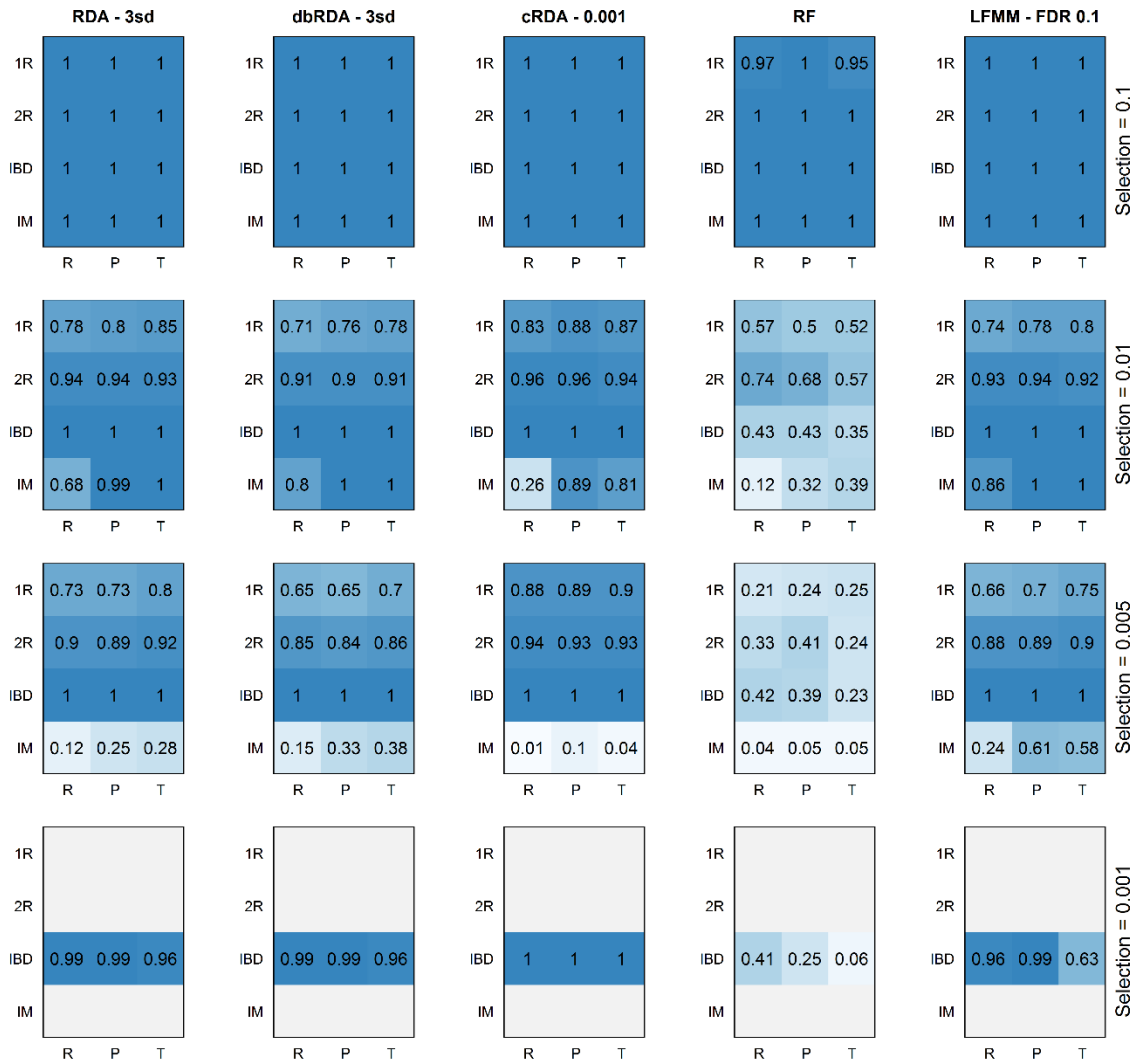


Figure B3. Average true positive rates for different levels of selection (rows) from five methods (columns) using the best cutoff for each method and a sample size of 6 individuals per deme. Each method shows results for different sampling strategies (R = random, P = pairs, T = transects) and demographies (1R and 2R = refugial expansion, IBD = equilibrium isolation by distance, IM = equilibrium island model). Only the IBD demography included very weak selection (s=0.001).

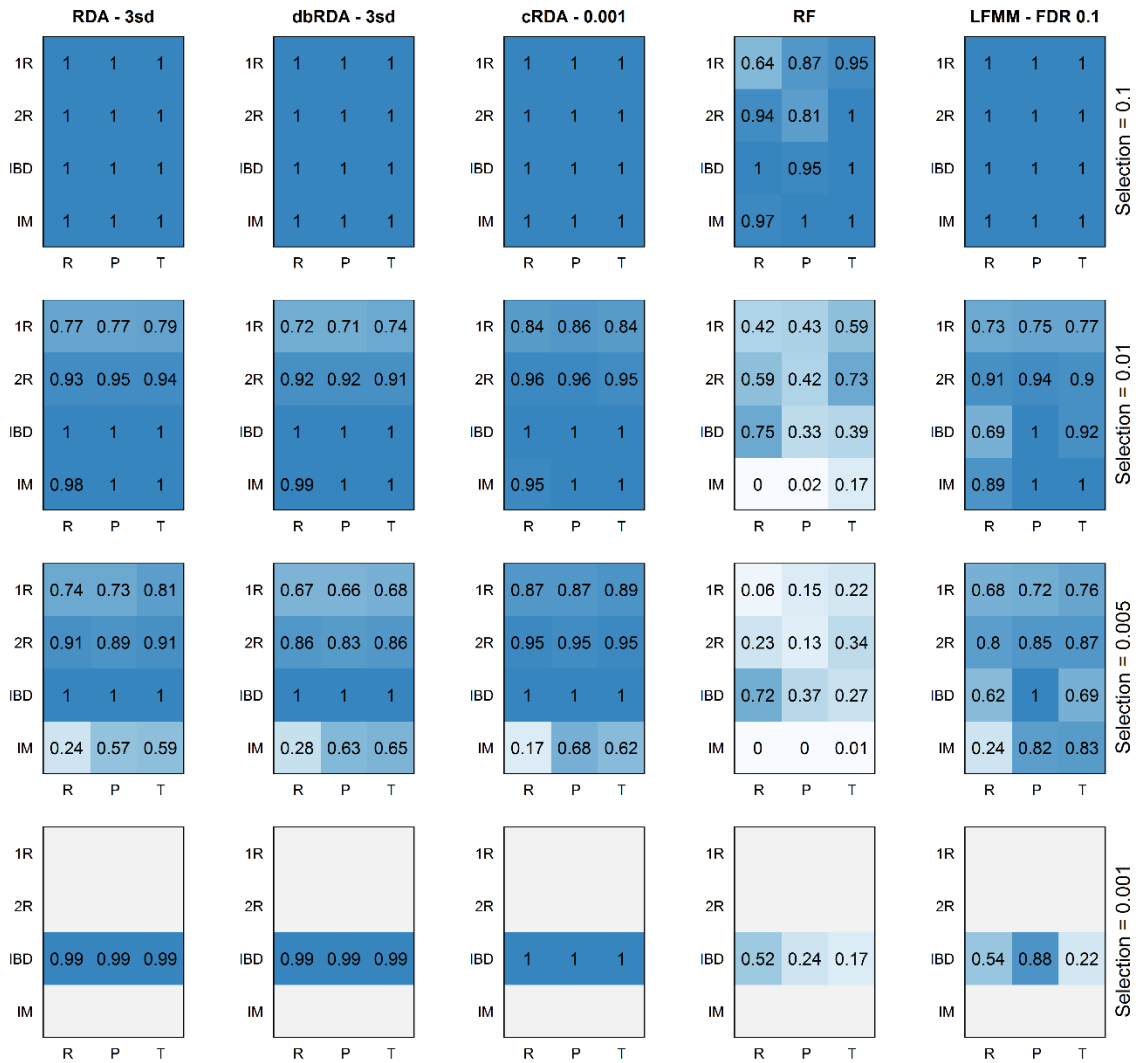


Figure B4. Average true positive rates for different levels of selection (rows) from five methods (columns) using the best cutoff for each method and a sample size of 20 individuals per deme. Each method shows results for different sampling strategies (R = random, P = pairs, T = transects) and demographies (1R and 2R = refugial expansion, IBD = equilibrium isolation by distance, IM = equilibrium island model). Only the IBD demography included very weak selection (s=0.001).

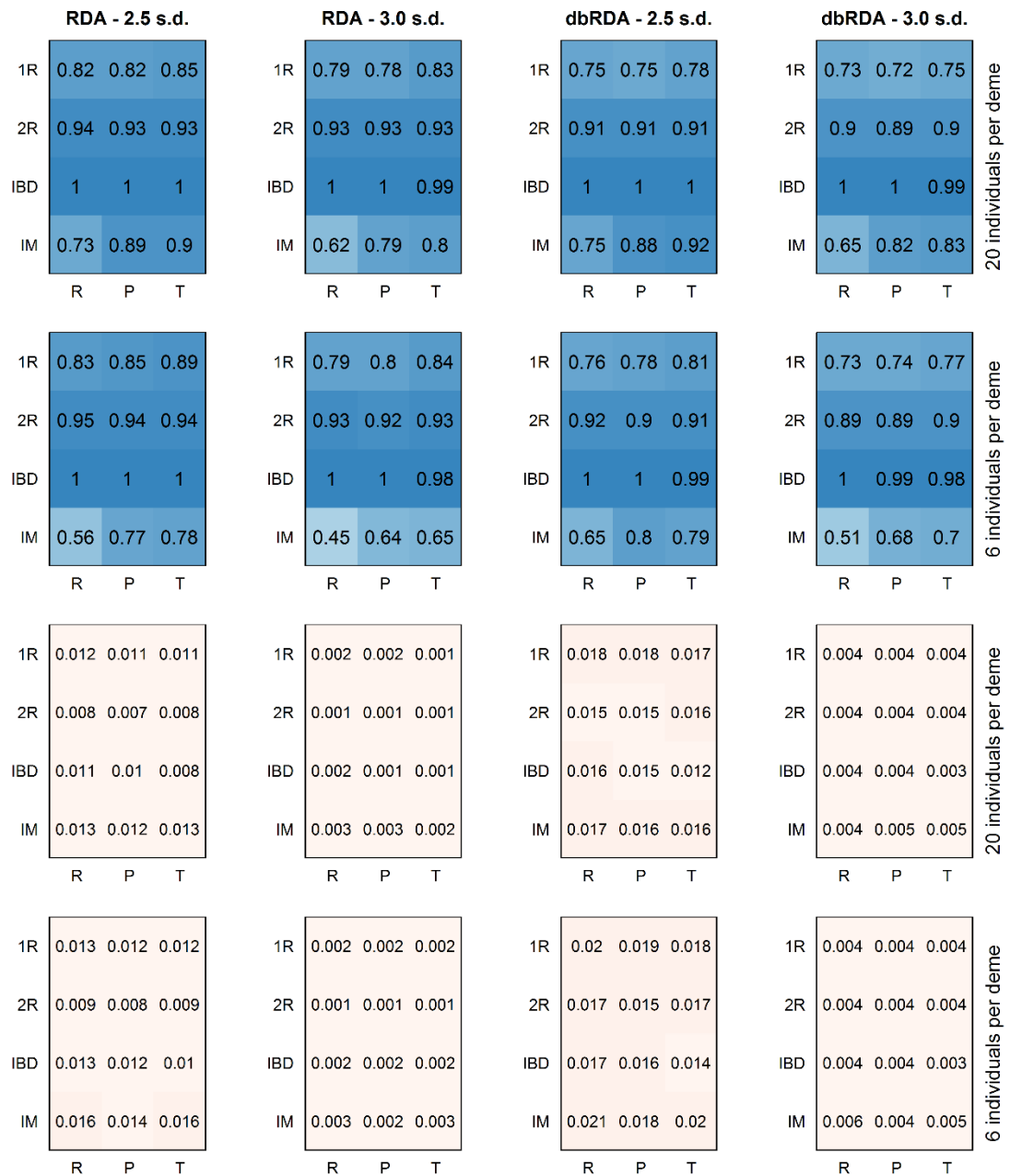


Figure B5. Average true positive (blue) and false positive (red) rates for constrained ordinations using +/- 2.5 and 3.0 SD cutoffs. Each method and cutoff shows results for different sampling strategies (R = random, P = pairs, T = transects), demographies (1R and 2R = refugial expansion, IBD = equilibrium isolation by distance, IM = equilibrium island model), and sample sizes (rows).

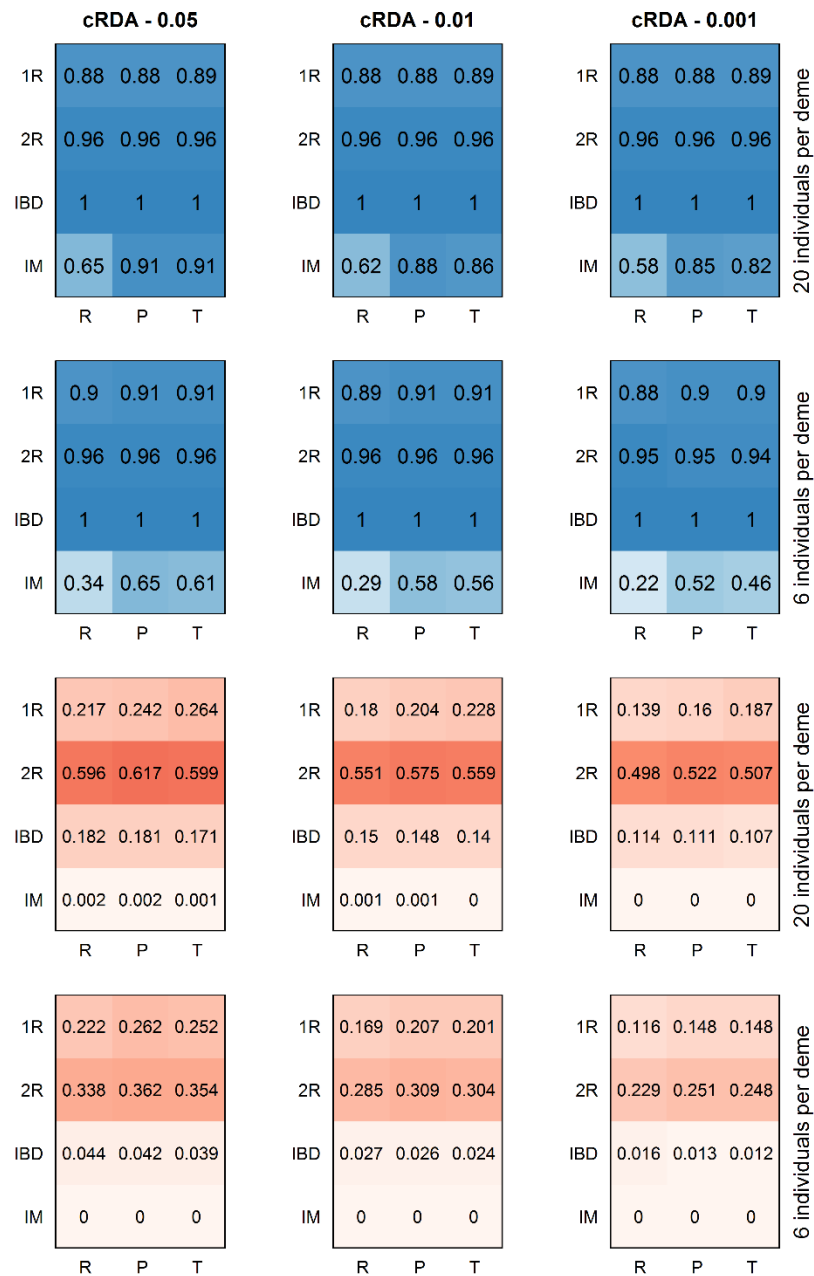


Figure B6. Average true positive (blue) and false positive (red) rates for cRDA using SNP-component correlation cutoffs of $\alpha = 0.05, 0.01, \text{ and } 0.001$. Each cutoff shows results for different sampling strategies (R = random, P = pairs, T = transects), demographies (1R and 2R = refugial expansion, IBD = equilibrium isolation by distance, IM = equilibrium island model), and sample sizes (rows).

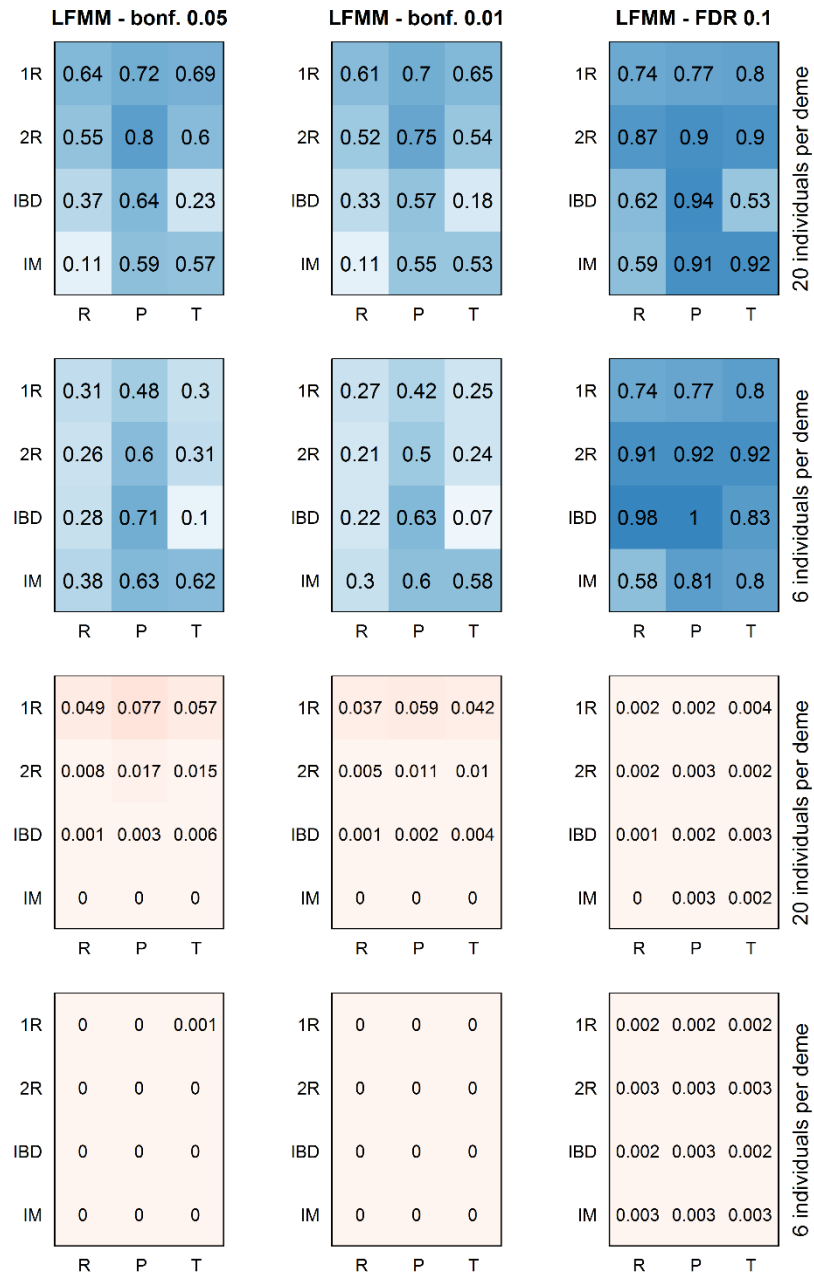


Figure B7. Average true positive (blue) and false positive (red) rates for LFMM using Bonferroni-corrected cutoffs of 0.05 and 0.01, and a false discovery rate cutoff of 0.1. Each cutoff shows results for different sampling strategies (R = random, P = pairs, T = transects), demographics (1R and 2R = refugial expansion, IBD = equilibrium isolation by distance, IM = equilibrium island model), and sample sizes (rows).

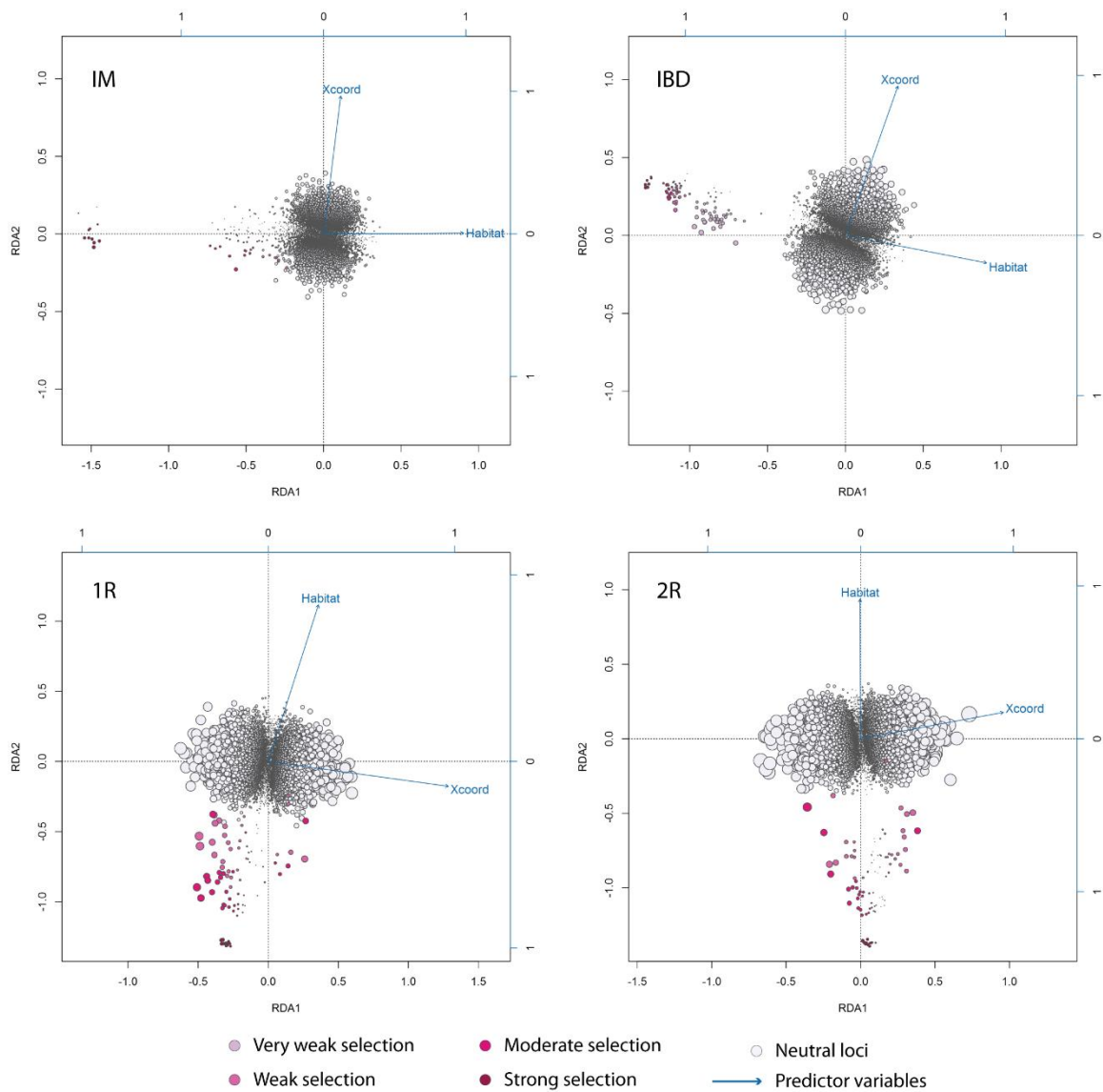


Figure B8. Redundancy analysis plots showing loci with point size scaled by their correlation with the spurious X-coordinate variable (“Xcoord”), and correlation of predictor variables with the constrained RDA axes (arrows). Plots are shown for an equilibrium island model (IM), equilibrium isolation by distance model (IBD), and non-equilibrium one- and two- refugial expansion models (1R and 2R) for paired sampling (6 individuals/deme) on environmental surface “453”.

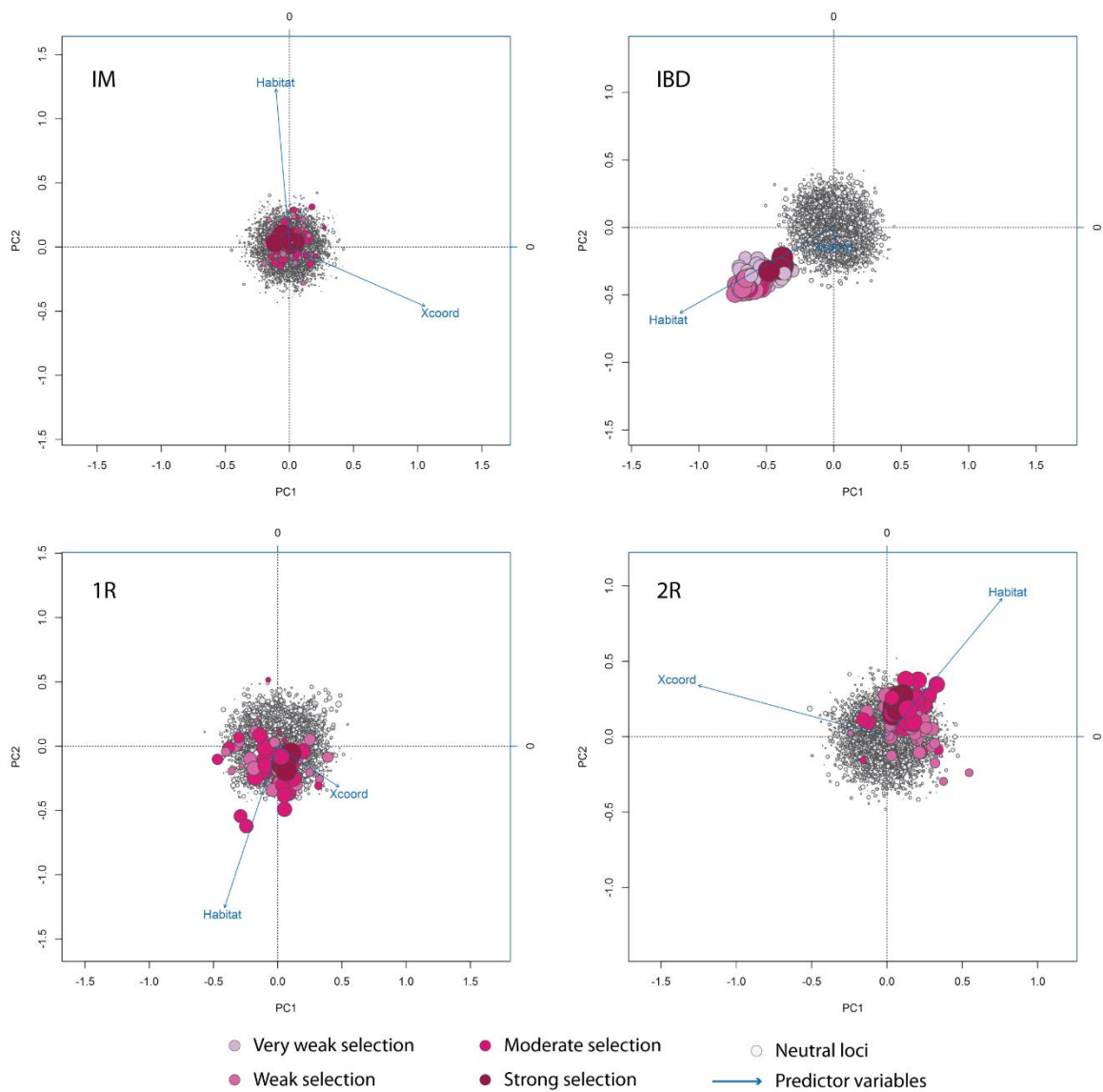


Figure B9. Plots of the first two unconstrained (“PC”) axes from redundancy analysis showing loci with point size scaled by their correlation with the driving environmental variable (“Habitat”), and correlation of predictor variables with the unconstrained PC axes (arrows). Plots are shown for an equilibrium island model (IM), equilibrium isolation by distance model (IBD), and non-equilibrium one- and two- refugial expansion models (1R and 2R) for paired sampling (6 individuals/deme) on environmental surface “453”.

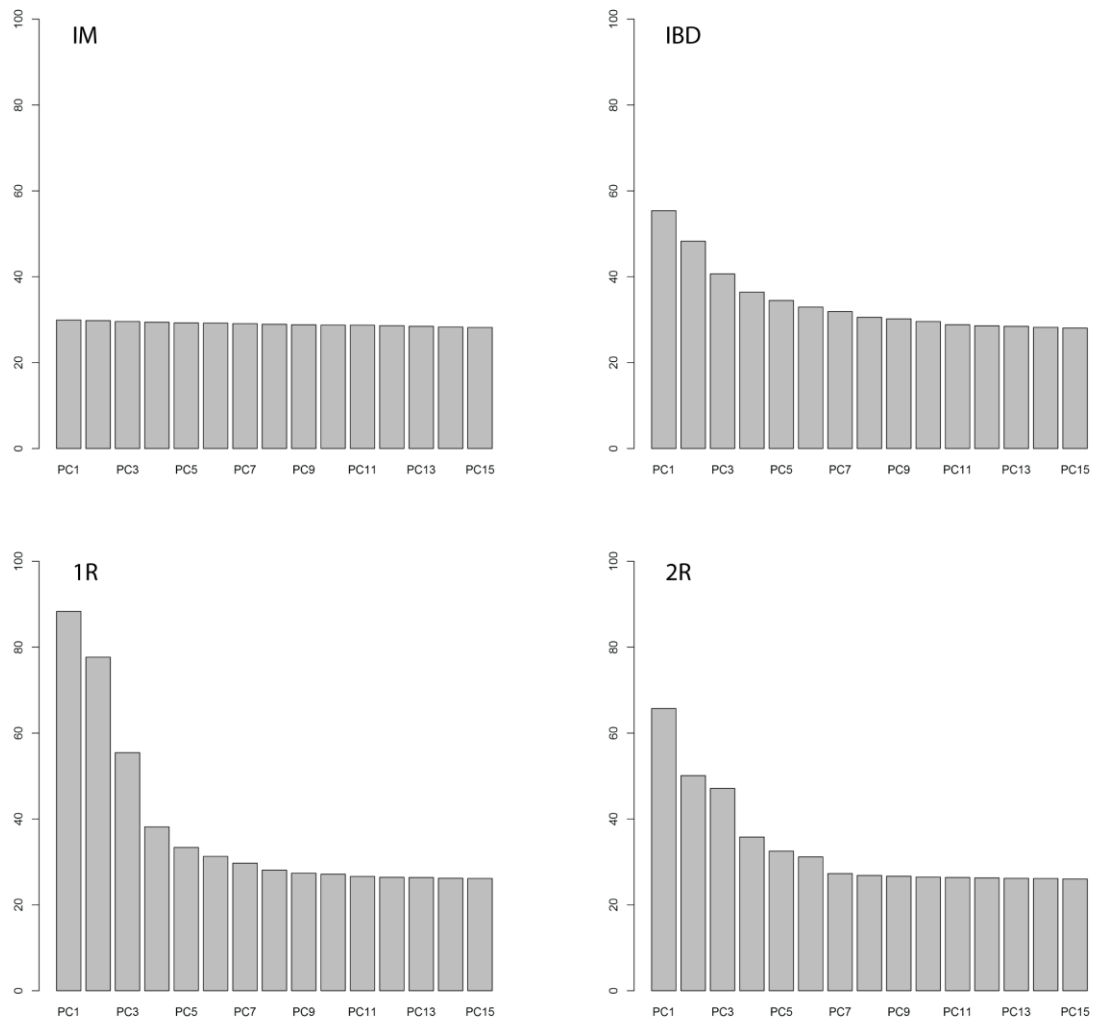


Figure B10. Screeplots of the eigenvalues for the first 15 (of 537 total) unconstrained (“PC”) axes from redundancy analysis. All screeplots use the same y-axis scale. Plots are shown for an equilibrium island model (IM), equilibrium isolation by distance model (IBD), and non-equilibrium one- and two- refugial expansion models (1R and 2R) for paired sampling (6 individuals/deme) on environmental surface “453”.

Table B1. Parameters from latent factor mixed model runs: values of K and genomic inflation factors (GIF) for habitat and x-coordinate predictors.

Demography	Sampling Design	Envir. Surface	6 individuals per deme			20 individuals per deme		
			K	GIFh	GIFx	K	GIFh	GIFx
1R	P	453	5	0.45	1.26	5	0.86	6.70
1R	P	950	5	0.67	1.47	5	1.26	8.32
1R	P	988	5	0.48	1.30	5	1.00	6.97
1R	R	453	5	0.52	1.45	5	1.12	5.42
1R	R	950	5	0.43	1.42	5	0.98	5.19
1R	R	988	5	0.40	1.35	5	1.07	5.37
1R	T	453	5	0.38	1.72	5	0.89	7.45
1R	T	950	5	0.40	1.53	5	0.88	5.61
1R	T	988	5	0.33	1.31	5	0.64	5.83
2R	P	453	5	0.30	1.39	5	0.62	2.98
2R	P	950	5	0.38	1.24	5	0.59	4.27
2R	P	988	5	0.29	1.11	5	0.71	4.01
2R	R	453	5	0.31	1.02	5	0.81	2.46
2R	R	950	5	0.23	1.10	5	0.57	2.93
2R	R	988	5	0.27	1.00	5	0.64	2.96
2R	T	453	5	0.27	1.60	5	0.54	4.46
2R	T	950	5	0.28	1.48	5	0.71	3.06
2R	T	988	5	0.18	1.36	5	0.42	2.85
IBD	P	453	4	0.40	0.62	4	0.97	1.97
IBD	P	950	4	0.44	0.78	4	1.10	2.67
IBD	P	988	4	0.39	0.65	4	1.01	2.23
IBD	R	453	4	0.37	0.61	4	1.13	2.05
IBD	R	950	4	0.37	0.60	4	1.27	2.02
IBD	R	988	4	0.39	0.59	4	1.07	1.94
IBD	T	453	4	0.46	0.88	4	1.26	2.85
IBD	T	950	4	0.34	0.66	4	0.75	2.68
IBD	T	988	4	0.38	0.68	4	0.97	2.50
IM	P	453	1	1.16	1.05	2	0.58	0.85
IM	P	950	1	1.12	1.07	2	0.61	0.72
IM	P	988	1	1.13	1.08	2	0.65	0.91
IM	R	453	1	1.14	1.14	4	0.27	0.30
IM	R	950	1	1.13	1.15	4	0.22	0.29
IM	R	988	1	1.13	1.12	4	0.25	0.30
IM	T	453	1	1.09	1.06	2	0.65	0.85
IM	T	950	1	1.11	1.06	2	0.73	0.87
IM	T	988	1	1.09	1.11	2	0.60	0.88

Table B2: Correlations between habitat and x- and y-coordinates of demes for each simulation; average and maximum trend in neutral markers; average and maximum levels of local adaptation.

Demograph	De-sign	Env	Correlations:		Neutral trend: 6 indiv./deme		Neutral trend: 20 indiv./deme		Local adaptation: 6 indiv./deme		Local adaptation: 20 indiv./deme	
			Habitat and X	Habitat and Y	Avg.	Max.	Avg.	Max.	Avg.	Max.	Avg.	Max.
1R	R	453	0.00	0.65	0.11	0.61	0.20	0.79	0.49	0.76	0.55	0.80
1R	R	950	0.05	0.63	0.11	0.63	0.20	0.80	0.37	0.68	0.42	0.70
1R	R	988	0.03	0.55	0.11	0.64	0.20	0.80	0.36	0.65	0.42	0.67
1R	P	453	0.00	0.84	0.12	0.64	0.21	0.80	0.52	0.80	0.57	0.80
1R	P	950	0.00	0.69	0.13	0.68	0.22	0.83	0.52	0.83	0.56	0.83
1R	P	988	-0.11	0.70	0.12	0.62	0.21	0.82	0.44	0.83	0.50	0.84
1R	T	453	0.13	0.82	0.13	0.67	0.23	0.84	0.42	0.70	0.46	0.71
1R	T	950	0.12	0.83	0.12	0.68	0.22	0.84	0.38	0.73	0.42	0.76
1R	T	988	-0.14	0.78	0.12	0.60	0.21	0.80	0.36	0.70	0.41	0.73
2R	R	453	0.00	0.65	0.14	0.71	0.25	0.83	0.55	0.74	0.62	0.75
2R	R	950	0.05	0.63	0.13	0.70	0.24	0.83	0.45	0.67	0.51	0.68
2R	R	988	0.03	0.55	0.14	0.69	0.25	0.83	0.42	0.68	0.49	0.70
2R	P	453	0.00	0.84	0.14	0.70	0.25	0.85	0.58	0.80	0.64	0.81
2R	P	950	0.00	0.69	0.14	0.76	0.26	0.85	0.61	0.83	0.66	0.84
2R	P	988	-0.11	0.70	0.15	0.73	0.26	0.84	0.54	0.83	0.61	0.84
2R	T	453	0.13	0.82	0.15	0.80	0.27	0.91	0.49	0.71	0.55	0.73
2R	T	950	0.12	0.83	0.14	0.70	0.26	0.87	0.45	0.74	0.51	0.76
2R	T	988	-0.14	0.78	0.14	0.70	0.26	0.82	0.41	0.71	0.48	0.71
IBD	R	453	0.00	0.65	0.06	0.42	0.11	0.58	0.61	0.72	0.65	0.74
IBD	R	950	0.05	0.63	0.06	0.43	0.10	0.59	0.48	0.68	0.52	0.69
IBD	R	988	0.03	0.55	0.06	0.41	0.10	0.56	0.44	0.68	0.48	0.69
IBD	P	453	0.00	0.84	0.06	0.43	0.11	0.56	0.63	0.81	0.68	0.82
IBD	P	950	0.00	0.69	0.07	0.44	0.11	0.63	0.68	0.83	0.72	0.83
IBD	P	988	-0.11	0.70	0.06	0.41	0.10	0.57	0.60	0.83	0.64	0.84
IBD	T	453	0.13	0.82	0.07	0.47	0.12	0.63	0.43	0.71	0.46	0.71
IBD	T	950	0.12	0.83	0.06	0.56	0.10	0.69	0.42	0.71	0.46	0.72
IBD	T	988	-0.14	0.78	0.07	0.41	0.11	0.58	0.35	0.69	0.37	0.69
IM	R	453	0.00	0.65	0.02	0.25	0.02	0.22	0.17	0.74	0.26	0.79
IM	R	950	0.05	0.63	0.02	0.18	0.02	0.20	0.16	0.76	0.24	0.82
IM	R	988	0.03	0.55	0.02	0.25	0.02	0.28	0.18	0.72	0.26	0.77
IM	P	453	0.00	0.84	0.02	0.17	0.02	0.18	0.26	0.82	0.38	0.87
IM	P	950	0.00	0.69	0.02	0.20	0.02	0.22	0.27	0.85	0.40	0.87
IM	P	988	-0.11	0.70	0.02	0.20	0.02	0.20	0.26	0.82	0.39	0.86
IM	T	453	0.13	0.82	0.02	0.21	0.02	0.18	0.25	0.76	0.38	0.81
IM	T	950	0.12	0.83	0.02	0.19	0.02	0.21	0.24	0.82	0.36	0.84
IM	T	988	-0.14	0.78	0.02	0.27	0.02	0.22	0.25	0.80	0.37	0.83

Table B3: Detection rates (using locus rankings) for simulation scenarios (6 individuals sampled per deme) with and without correction for population structure.

Demography	Design	Env	True Positive Rates							
			RDA	RDA corr	dbRDA	dbRDA corr	cRDA	cRDA corr	RF	RF corr
1R	P	453	0.83	0.84	0.76	0.75	0.85	0.85	0.26	0.17
1R	P	950	0.79	0.79	0.74	0.75	0.76	0.76	0.30	0.10
1R	P	988	0.76	0.76	0.67	0.67	0.74	0.74	0.24	0.10
1R	R	453	0.82	0.81	0.73	0.72	0.78	0.78	0.29	0.09
1R	R	950	0.75	0.74	0.70	0.71	0.75	0.75	0.24	0.09
1R	R	988	0.80	0.80	0.71	0.69	0.80	0.80	0.26	0.11
1R	T	453	0.90	0.91	0.80	0.78	0.87	0.87	0.26	0.13
1R	T	950	0.76	0.79	0.71	0.71	0.76	0.76	0.23	0.12
1R	T	988	0.86	0.88	0.75	0.74	0.83	0.83	0.22	0.12
2R	P	453	0.92	0.93	0.86	0.87	0.92	0.92	0.28	0.18
2R	P	950	0.93	0.93	0.89	0.89	0.93	0.93	0.32	0.12
2R	P	988	0.90	0.91	0.86	0.86	0.91	0.91	0.26	0.12
2R	R	453	0.94	0.94	0.90	0.89	0.94	0.94	0.30	0.10
2R	R	950	0.93	0.93	0.88	0.88	0.90	0.90	0.31	0.14
2R	R	988	0.91	0.88	0.85	0.81	0.91	0.91	0.22	0.09
2R	T	453	0.95	0.95	0.89	0.89	0.94	0.94	0.33	0.15
2R	T	950	0.91	0.91	0.87	0.86	0.90	0.90	0.21	0.10
2R	T	988	0.93	0.92	0.87	0.86	0.92	0.92	0.21	0.10
IBD	P	453	0.99	0.99	0.98	0.98	1.00	1.00	0.27	0.10
IBD	P	950	0.99	0.99	0.98	0.98	0.99	0.99	0.28	0.08
IBD	P	988	1.00	1.00	0.99	0.99	1.00	1.00	0.21	0.09
IBD	R	453	1.00	1.00	0.98	0.98	1.00	1.00	0.27	0.07
IBD	R	950	0.98	0.98	0.97	0.96	0.99	0.99	0.31	0.06
IBD	R	988	1.00	1.00	0.98	0.98	1.00	1.00	0.37	0.08
IBD	T	453	0.94	0.94	0.94	0.94	1.00	1.00	0.14	0.07
IBD	T	950	0.97	0.96	0.90	0.93	0.98	0.98	0.24	0.11
IBD	T	988	0.98	0.96	0.97	0.97	0.98	0.98	0.10	0.07
IM	P	453	0.66	NA	0.66	NA	0.73	NA	0.20	0.30
IM	P	950	0.67	NA	0.67	NA	0.68	NA	0.18	0.22
IM	P	988	0.68	NA	0.68	NA	0.61	NA	0.19	0.18
IM	R	453	0.50	NA	0.51	NA	0.49	NA	0.19	0.21
IM	R	950	0.44	NA	0.47	NA	0.46	NA	0.10	0.14
IM	R	988	0.51	NA	0.54	NA	0.54	NA	0.15	0.15
IM	T	453	0.70	NA	0.70	NA	0.69	NA	0.19	0.26
IM	T	950	0.63	NA	0.65	NA	0.72	NA	0.16	0.16
IM	T	988	0.67	NA	0.69	NA	0.73	NA	0.20	0.30

			False Positive Rates							
Demography	Design	Env	RDA	RDA corr	dbRDA	dbRDA corr	cRDA	cRDA corr	RF	RF corr
1R	P	453	0.17	0.16	0.24	0.25	0.15	0.15	0.74	0.83
1R	P	950	0.21	0.21	0.26	0.25	0.24	0.24	0.70	0.90
1R	P	988	0.24	0.24	0.33	0.33	0.26	0.26	0.76	0.90
1R	R	453	0.18	0.19	0.27	0.28	0.22	0.22	0.71	0.91
1R	R	950	0.25	0.26	0.30	0.29	0.25	0.25	0.76	0.91
1R	R	988	0.20	0.20	0.29	0.31	0.20	0.20	0.74	0.38
1R	T	453	0.10	0.09	0.20	0.22	0.13	0.13	0.74	0.87
1R	T	950	0.24	0.21	0.29	0.29	0.24	0.24	0.77	0.88
1R	T	988	0.14	0.12	0.25	0.26	0.17	0.17	0.78	0.88
2R	P	453	0.08	0.07	0.14	0.13	0.08	0.08	0.72	0.82
2R	P	950	0.07	0.07	0.11	0.11	0.07	0.07	0.68	0.88
2R	P	988	0.10	0.09	0.14	0.14	0.09	0.09	0.74	0.88
2R	R	453	0.06	0.06	0.10	0.11	0.06	0.06	0.70	0.90
2R	R	950	0.07	0.07	0.12	0.12	0.10	0.10	0.69	0.86
2R	R	988	0.09	0.12	0.15	0.19	0.09	0.09	0.78	0.91
2R	T	453	0.05	0.05	0.11	0.11	0.06	0.06	0.67	0.85
2R	T	950	0.09	0.09	0.13	0.14	0.10	0.10	0.79	0.90
2R	T	988	0.07	0.08	0.13	0.14	0.08	0.08	0.79	0.90
IBD	P	453	0.01	0.01	0.02	0.02	0.00	0.00	0.73	0.90
IBD	P	950	0.01	0.01	0.02	0.02	0.01	0.01	0.72	0.92
IBD	P	988	0.00	0.00	0.01	0.01	0.00	0.00	0.79	0.91
IBD	R	453	0.00	0.00	0.02	0.02	0.00	0.00	0.73	0.93
IBD	R	950	0.02	0.02	0.03	0.04	0.01	0.01	0.69	0.94
IBD	R	988	0.00	0.00	0.02	0.02	0.00	0.00	0.63	0.92
IBD	T	453	0.06	0.06	0.06	0.06	0.00	0.00	0.86	0.93
IBD	T	950	0.03	0.04	0.10	0.07	0.02	0.02	0.76	0.89
IBD	T	988	0.02	0.04	0.03	0.03	0.02	0.02	0.90	0.93
IM	P	453	0.34	NA	0.34	NA	0.27	NA	0.80	0.69
IM	P	950	0.33	NA	0.33	NA	0.32	NA	0.82	0.78
IM	P	988	0.32	NA	0.32	NA	0.39	NA	0.81	0.82
IM	R	453	0.50	NA	0.49	NA	0.51	NA	0.81	0.79
IM	R	950	0.56	NA	0.53	NA	0.54	NA	0.90	0.86
IM	R	988	0.49	NA	0.46	NA	0.46	NA	0.85	0.85
IM	T	453	0.30	NA	0.30	NA	0.31	NA	0.81	0.74
IM	T	950	0.37	NA	0.35	NA	0.28	NA	0.84	0.84
IM	T	988	0.33	NA	0.31	NA	0.27	NA	0.80	0.70

Table B4: Detection rates (using locus rankings) for simulation scenarios (20 individuals sampled per deme) with and without correction for population structure.

Demography	Design	Env	True Positive Rates							
			RDA	RDA corr	dbRDA	dbRDA corr	cRDA	cRDA corr	RF	RF corr
1R	P	453	0.83	0.84	0.76	0.76	0.86	0.86	0.30	0.07
1R	P	950	0.74	0.75	0.70	0.70	0.77	0.77	0.19	0.10
1R	P	988	0.78	0.78	0.68	0.68	0.79	0.79	0.23	0.18
1R	R	453	0.80	0.80	0.74	0.74	0.85	0.85	0.17	0.13
1R	R	950	0.74	0.74	0.68	0.68	0.76	0.76	0.21	0.11
1R	R	988	0.81	0.80	0.73	0.72	0.82	0.82	0.24	0.13
1R	T	453	0.88	0.88	0.78	0.78	0.85	0.85	0.33	0.06
1R	T	950	0.78	0.78	0.69	0.69	0.79	0.79	0.37	0.18
1R	T	988	0.85	0.85	0.73	0.73	0.84	0.84	0.32	0.14
2R	P	453	0.93	0.93	0.88	0.87	0.91	0.91	0.33	0.23
2R	P	950	0.91	0.91	0.87	0.87	0.91	0.91	0.25	0.13
2R	P	988	0.93	0.93	0.87	0.87	0.91	0.91	0.07	0.16
2R	R	453	0.93	0.94	0.90	0.89	0.93	0.93	0.43	0.14
2R	R	950	0.91	0.91	0.88	0.88	0.88	0.88	0.28	0.11
2R	R	988	0.93	0.93	0.86	0.86	0.91	0.91	0.16	0.12
2R	T	453	0.95	0.95	0.89	0.89	0.92	0.92	0.39	0.19
2R	T	950	0.89	0.89	0.86	0.86	0.89	0.89	0.28	0.12
2R	T	988	0.95	0.95	0.89	0.89	0.93	0.93	0.23	0.08
IBD	P	453	1.00	1.00	0.98	0.98	1.00	1.00	0.16	0.08
IBD	P	950	0.99	0.99	0.98	0.98	0.99	0.99	0.39	0.07
IBD	P	988	1.00	1.00	0.99	0.99	1.00	1.00	0.30	0.16
IBD	R	453	1.00	1.00	0.98	0.98	1.00	1.00	0.29	0.08
IBD	R	950	0.99	0.99	0.98	0.98	0.99	0.99	0.22	0.07
IBD	R	988	1.00	1.00	0.99	0.99	1.00	1.00	0.24	0.08
IBD	T	453	0.98	0.98	0.96	0.96	1.00	1.00	0.28	0.07
IBD	T	950	0.98	0.98	0.96	0.96	0.99	0.99	0.29	0.12
IBD	T	988	0.99	0.99	0.98	0.97	1.00	1.00	0.09	0.07
IM	P	453	0.77	NA	0.75	NA	0.92	NA	0.10	0.08
IM	P	950	0.80	NA	0.79	NA	0.86	NA	0.12	0.09
IM	P	988	0.77	NA	0.79	NA	0.85	NA	0.09	0.02
IM	R	453	0.64	NA	0.64	NA	0.72	NA	0.09	0.08
IM	R	950	0.61	NA	0.62	NA	0.66	NA	0.08	0.07
IM	R	988	0.68	NA	0.68	NA	0.66	NA	0.09	0.07
IM	T	453	0.80	NA	0.79	NA	0.93	NA	0.10	0.07
IM	T	950	0.77	NA	0.73	NA	0.84	NA	0.10	0.08
IM	T	988	0.80	NA	0.77	NA	0.71	NA	0.16	0.10

Demography	De-sign	Env	False Positive Rates							
			RDA	RDA corr	dbRDA	dbRDA corr	cRDA	cRDA corr	RF	RF corr
1R	P	453	0.17	0.16	0.24	0.24	0.14	0.14	0.70	0.93
1R	P	950	0.26	0.25	0.30	0.30	0.23	0.23	0.81	0.90
1R	P	988	0.22	0.22	0.32	0.32	0.21	0.21	0.77	0.82
1R	R	453	0.20	0.20	0.26	0.26	0.15	0.15	0.83	0.88
1R	R	950	0.26	0.26	0.32	0.32	0.24	0.24	0.79	0.89
1R	R	988	0.19	0.20	0.27	0.28	0.18	0.18	0.76	0.88
1R	T	453	0.12	0.12	0.22	0.22	0.15	0.15	0.67	0.94
1R	T	950	0.22	0.22	0.31	0.31	0.21	0.21	0.63	0.82
1R	T	988	0.15	0.15	0.27	0.27	0.16	0.16	0.68	0.86
2R	P	453	0.07	0.07	0.12	0.13	0.09	0.09	0.67	0.77
2R	P	950	0.09	0.09	0.13	0.13	0.09	0.09	0.75	0.87
2R	P	988	0.07	0.07	0.13	0.13	0.09	0.09	0.93	0.84
2R	R	453	0.07	0.06	0.10	0.11	0.07	0.07	0.57	0.86
2R	R	950	0.09	0.09	0.12	0.12	0.12	0.12	0.72	0.89
2R	R	988	0.07	0.07	0.14	0.14	0.09	0.09	0.84	0.88
2R	T	453	0.05	0.05	0.11	0.11	0.08	0.08	0.61	0.81
2R	T	950	0.11	0.11	0.14	0.14	0.11	0.11	0.72	0.88
2R	T	988	0.05	0.05	0.11	0.11	0.07	0.07	0.77	0.92
IBD	P	453	0.00	0.00	0.02	0.02	0.00	0.00	0.84	0.92
IBD	P	950	0.01	0.01	0.02	0.02	0.01	0.01	0.61	0.93
IBD	P	988	0.00	0.00	0.01	0.01	0.00	0.00	0.70	0.84
IBD	R	453	0.00	0.00	0.02	0.02	0.00	0.00	0.71	0.92
IBD	R	950	0.01	0.01	0.02	0.02	0.01	0.01	0.78	0.93
IBD	R	988	0.00	0.00	0.01	0.01	0.00	0.00	0.76	0.92
IBD	T	453	0.02	0.02	0.04	0.04	0.00	0.00	0.72	0.93
IBD	T	950	0.02	0.02	0.04	0.04	0.01	0.01	0.71	0.88
IBD	T	988	0.01	0.01	0.02	0.03	0.00	0.00	0.91	0.93
IM	P	453	0.23	NA	0.25	NA	0.08	NA	0.90	0.92
IM	P	950	0.20	NA	0.21	NA	0.14	NA	0.88	0.91
IM	P	988	0.23	NA	0.21	NA	0.15	NA	0.91	0.98
IM	R	453	0.36	NA	0.36	NA	0.28	NA	0.91	0.92
IM	R	950	0.39	NA	0.38	NA	0.34	NA	0.92	0.93
IM	R	988	0.32	NA	0.32	NA	0.34	NA	0.91	0.93
IM	T	453	0.20	NA	0.21	NA	0.07	NA	0.90	0.93
IM	T	950	0.23	NA	0.27	NA	0.16	NA	0.90	0.92
IM	T	988	0.20	NA	0.23	NA	0.29	NA	0.84	0.90

Table B5: Parameters from cRDA runs: number of axes retained by the parallel analysis criterion, and component axes significantly correlated with constrained ordination axes. Data are shown for all selection strengths (full simulation data set) and simulation data with weak selection only.

Demo- graphy	De- sign	Env	Retained axes		All selection strengths		Weak selection only	
			6 ind.	20 ind.	Significant components: 6 ind.	Significant components: 20 ind.	Significant components: 6 ind.	Significant components: 20 ind.
1R	P	453	540	1800	2,1	2	1,2	NA
1R	P	950	540	1800	2,1	2	2,1	2
1R	P	988	540	1800	1,2	2	1,2	8,11,1300
1R	R	453	540	1800	2,1	2	1,3	NA
1R	R	950	540	1800	1,2	2	2,1	NA
1R	R	988	540	1800	2,1	2	1,2	9
1R	T	453	540	1800	2,1	2,1	1,3	1,7,995,1421
1R	T	950	540	1800	1,2	2	1,3	8
1R	T	988	540	1800	2,1	2	2,1	7,9
2R	P	453	540	1800	1,2	2,1	2,1	1,2
2R	P	950	540	1800	1,2	1,2	1,2	1,2
2R	P	988	540	1800	1,2	2,1	1,2	2,1
2R	R	453	540	1800	1,2	2,1	1,2	2,1
2R	R	950	540	1800	1,2	1,2	1,2	1,2
2R	R	988	540	1800	2,1	2,1	1,2	11,348
2R	T	453	540	1800	1,2	1,2	1,2	2,1
2R	T	950	540	1800	2,1	1,2	1,2	1,2
2R	T	988	540	1800	2,1	2,1	1,2	1,2
IBD	P	453	540	1800	1	1	1	1
IBD	P	950	540	1800	1,2	1	1	1
IBD	P	988	540	1800	1	1	2,1	1
IBD	R	453	540	1800	1	1	2,1	1
IBD	R	950	540	1800	1	1	1	1
IBD	R	988	540	1800	1	1	1	1
IBD	T	453	540	1800	1	1	1	1
IBD	T	950	540	1800	183,1	1	1	1
IBD	T	988	540	1800	263,1	1	1	1
IM	P	453	540	1800	1	1	NA	31,726
IM	P	950	540	1800	1	1	NA	13,704,024,
IM	P	988	540	1800	235,1	1	NA	2,66,207,1295,27
IM	R	453	540	1800	1	1	NA	NA
IM	R	950	540	1800	1	1	NA	1,371,254
IM	R	988	540	1800	1	1	NA	47
IM	T	453	540	1800	1	1	NA	3,891,131,
IM	T	950	540	1800	1	1	NA	NA
IM	T	988	540	1800	1	935,1	NA	184,512,191,681

Table B6: Percent variance explained for uncorrected and corrected Random Forest models.

			6 individuals sampled per deme			
			Uncorrected		Corrected	
Demo- graphy	Design	Env	PVE: Habitat	PVE: Xcoord	PVE: Habitat	PVE: Xcoord
1R	P	453	0.88	0.87	0.88	0.97
1R	P	950	0.90	0.88	0.88	0.98
1R	P	988	0.88	0.87	0.89	0.98
1R	R	453	0.86	0.85	0.87	0.98
1R	R	950	0.81	0.84	0.85	0.98
1R	R	988	0.81	0.86	0.85	0.98
1R	T	453	0.83	0.91	0.86	0.99
1R	T	950	0.87	0.89	0.89	0.99
1R	T	988	0.82	0.88	0.86	0.99
2R	P	453	0.87	0.88	0.87	0.96
2R	P	950	0.90	0.89	0.87	0.97
2R	P	988	0.89	0.88	0.88	0.96
2R	R	453	0.85	0.87	0.88	0.97
2R	R	950	0.80	0.86	0.82	0.98
2R	R	988	0.81	0.86	0.85	0.98
2R	T	453	0.83	0.91	0.87	0.98
2R	T	950	0.86	0.90	0.91	0.98
2R	T	988	0.82	0.88	0.89	0.97
IBD	P	453	0.88	0.66	0.86	0.97
IBD	P	950	0.89	0.71	0.86	0.96
IBD	P	988	0.89	0.66	0.88	0.97
IBD	R	453	0.86	0.67	0.86	0.96
IBD	R	950	0.81	0.65	0.81	0.96
IBD	R	988	0.80	0.64	0.82	0.96
IBD	T	453	0.84	0.73	0.85	0.99
IBD	T	950	0.84	0.66	0.87	0.97
IBD	T	988	0.82	0.66	0.85	0.98
IM	P	453	0.88	0.42	0.88	0.38
IM	P	950	0.91	0.38	0.90	0.36
IM	P	988	0.88	0.39	0.88	0.37
IM	R	453	0.83	0.41	0.83	0.39
IM	R	950	0.85	0.39	0.83	0.39
IM	R	988	0.81	0.40	0.81	0.36
IM	T	453	0.86	0.36	0.85	0.35
IM	T	950	0.88	0.40	0.87	0.36
IM	T	988	0.85	0.38	0.85	0.36

Appendix C: Supporting information for Chapter 4 - Conserving adaptive capacity in a Southern Appalachian salamander threatened by climate change

Temperature and relative humidity models

Data for environmental modeling were collected using Onset HOBO U23 Pro v2 temperature and relative humidity data loggers (model U23-001). Loggers were wired to the north-facing side of trees such that the relative humidity sensor was at ~5cm above the surface of the leaf litter. Data were collected at Grandfather Mt. (10 stations) and Unaka Mt. (6 stations) using a stratified sampling design across elevation and aspect between October 2013 and October 2015. Validation data were collected from three sites (each with a high and low elevation station) between May-October 2015 (Figure C1).

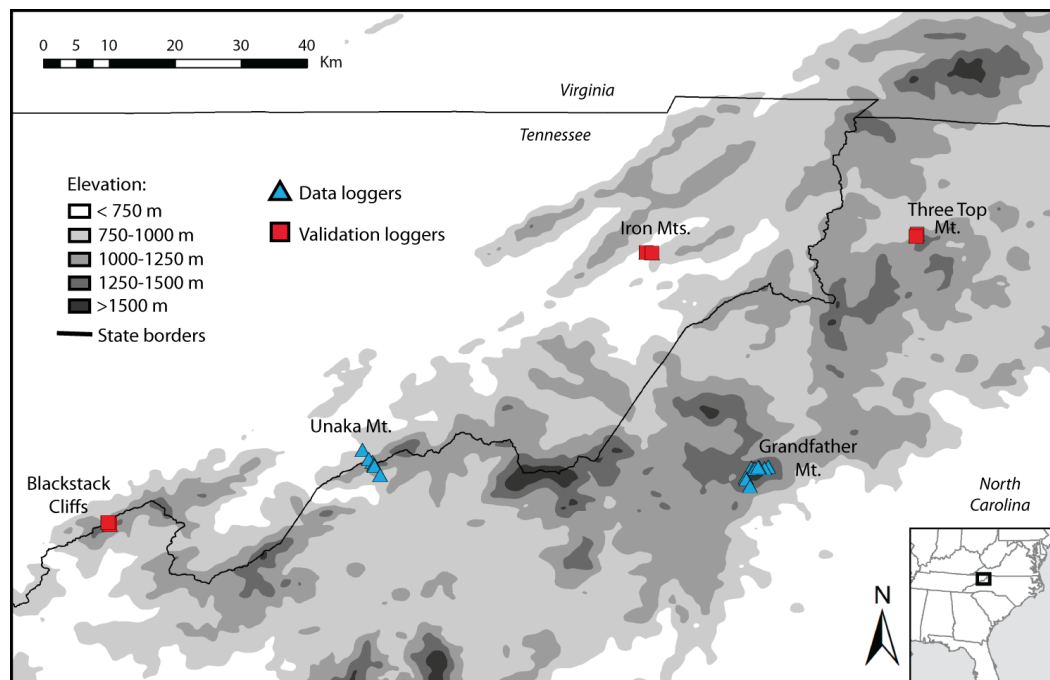


Figure C1. Location of data loggers across the Weller's salamander range.

Raw HOBO data were cleaned to account for missing data (e.g. when part of a day was missing, data were removed for the entire day). For each station, we calculated mean monthly daily maximum and minimum values of temperature and relative humidity to serve as the model response. We developed a set of predictors in ArcGIS 10.2.1: elevation, monthly potential relative radiation (PRR, Pierce *et al.* 2005), log of the distance to streams (LogStmDst), square root of aspect (SqRtAspect), slope, and topographic convergence index (TCI, see Table C1 for details). Variables were checked for collinearity; only one comparison had a correlation greater than $|0.7|$ (Elevation and StmDst, $r = -0.82$); both variable were retained. StmDst and Aspect were transformed using log and square root transformations, respectively, to meet normality assumptions.

Table C1. Predictor variables used to model temperature and relative humidity.

Predictor	Source
Elevation	Digital elevation map (DEM) from USGS NED (2013); 1-arc-second resolution
PRR	Hillshade tool in ArcGIS 10.2.1; azimuth and elevation angle from NOAA Solar Calculator
LogStmDst	National Atlas of the United States (2014) 1:1,000,000 scale
SqRtAspect	Calculated from DEM in ArcGIS 10.2.1
Slope	Calculated from DEM in ArcGIS 10.2.1
TCI	Calculated from DEM using David Tarboton's TauDEM (Terrain Analysis Using Digital Elevation Models), http://hydrology.usu.edu/taudem/taudem5/index.html

Because “year” resulted in a significant effect across the pooled data, we ran separate models for each month-year combination (25 models total) using R v. 3.2.3. We tested each month-year combination for a “site” effect (Unaka-Grandfather); significant effects were found only in a small number of cases, and never in a full model. We chose not to include site for subsequent analyses.

We modeled anomalies from a base station as our response. For temperature we used the NOAA station in Banner Elk, NC, which had no missing data for the study period. For relative humidity, base station data were not available, so we used the Calloway station (summit) at Grandfather Mt. Each month-year combination was modeled separately using a linear regression model with stepwise (both forward and backward) AICc function (<http://wwwuser.gwdg.de/~cscherb1/stepAICc.txt>) to select the most parsimonious model. “Predict” was used to develop month-year predictions for salamander and data logger locations.

Model residuals were checked for correlation with predictors to assess model bias; there were no significant correlations between residuals and predictors for any month-year model.

Temperature models performed better than relative humidity models: average R^2_{adj} for Tmax and Tmin models were 0.89 and 0.94, respectively, while average R^2_{adj} for RHmax and RHmin were 0.43 and 0.59. All models used elevation as a predictor most frequently, with PRR and SqRtAspect also important for Tmax and LogStmDst

important for Tmin. For RH models, PRR, SqRtAspect and LogStmDst were among other important predictors.

Predicted and observed anomalies were evaluated for verification and validation of the models. Model bias was assessed by calculating the absolute difference between predicted and observed anomalies. Model accuracy was assessed using mean absolute error (the difference between predicted and observed anomalies after making all observations positive). Average verification and validation statistics are provided in Table C2.

Table C2. Average verification and validation statistics for temperature and relative humidity models. MAE = mean absolute error.

	Verification		Validation	
	Average Bias	Average MAE	Average Bias	Average MAE
Tmax	0.01	0.56	-1.39	1.78
Tmin	0.03	0.26	0.01	0.50
RHmax	-0.02	1.08	-0.98	2.12
RHmin	0.05	3.41	5.77	8.99

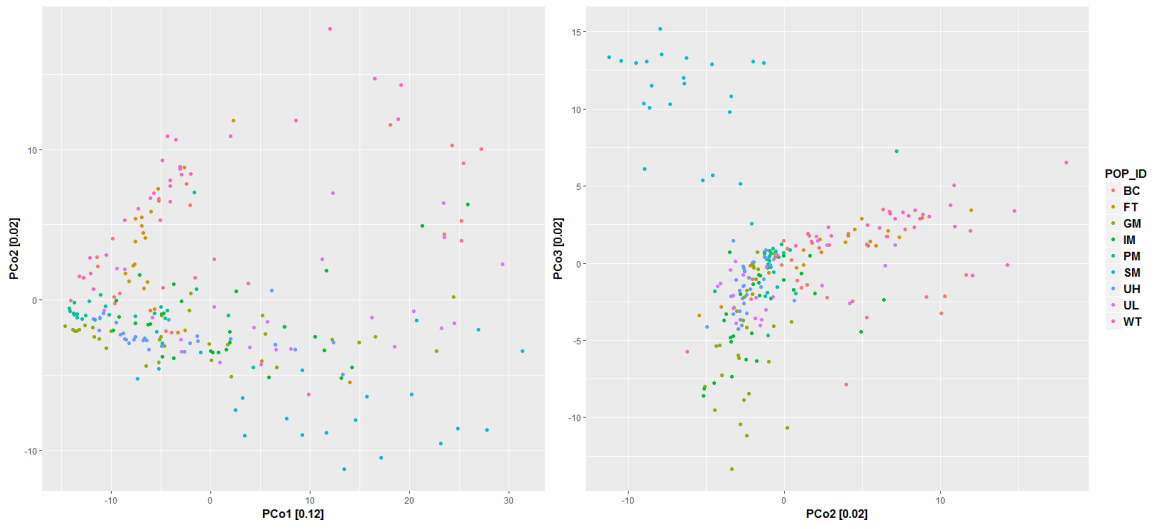


Figure C2. Principal coordinates analysis of Weller’s salamander genomic data (6,070 SNP markers genotyped across 237 individuals). Identity by missing data stratified by population.

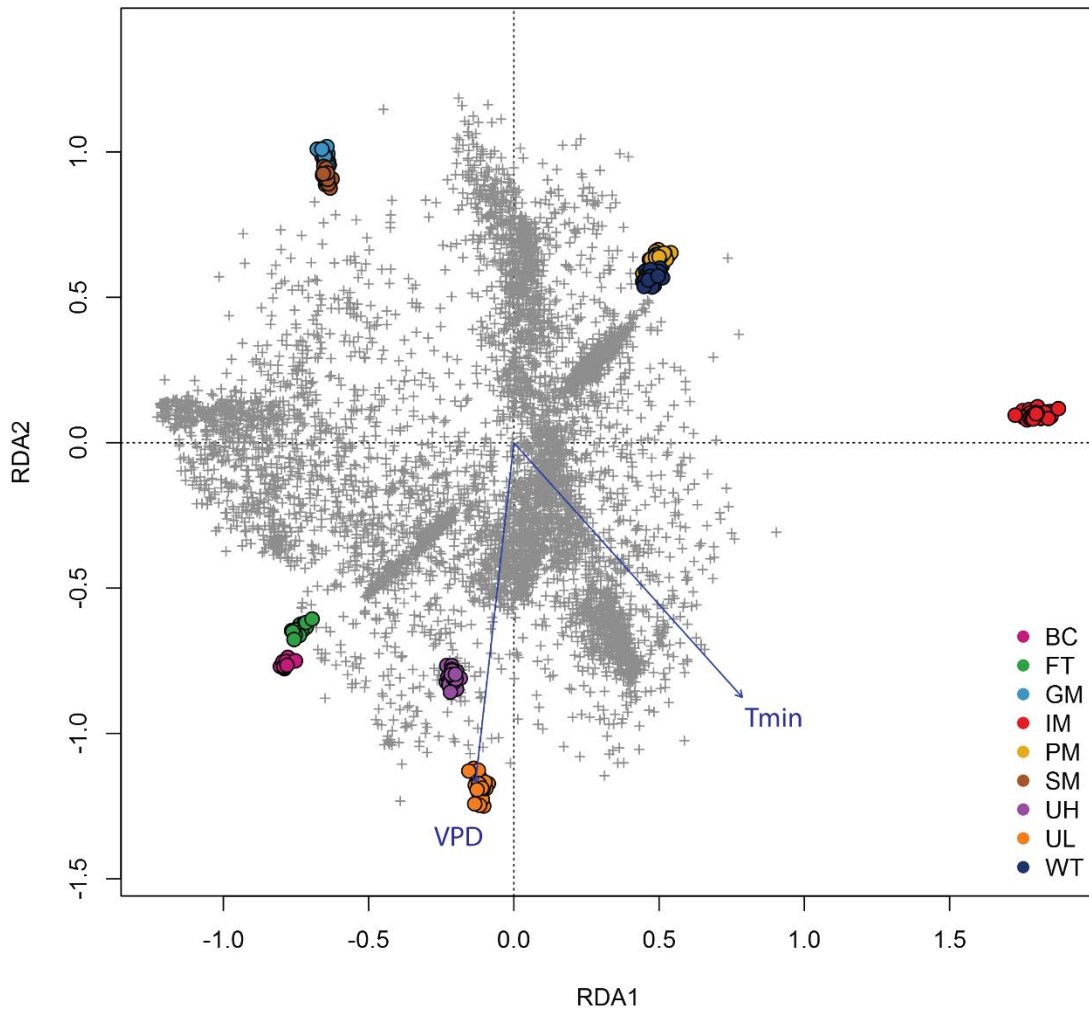


Figure C3. Redundancy analysis of Weller’s salamander genomic data (6,070 SNP markers genotyped across 237 individuals). Color-coded points represent individuals in different populations; gray pluses are SNP loci; blue vectors represent the correlation of the environmental predictors with the RDA axes. VPD = vapor pressure deficit from March-November; Tmin = mean daily minimum temperature from March to November.

References

- Adams JR, Vucetich LM, Hedrick PW, Peterson RO, Vucetich JA (2011) Genomic sweep and potential genetic rescue during limiting environmental conditions in an isolated wolf population. *Proceedings of the Royal Society B: Biological Sciences*, **278**, 3336–3344.
- AdaptWest Project (2015) *Gridded current and projected climate data for North America at 1km resolution, interpolated using the ClimateNA v5.10 software* (T. Wang et al., 2016). Available at adaptwest.databasin.org.
- Aitken SN, Whitlock MC (2013) Assisted gene flow to facilitate local adaptation to climate change. *Annual Review of Ecology, Evolution, and Systematics*, **44**, 367–388.
- Allen WR, Sheppard PM (1971) Copper tolerance in some Californian populations of the monkey flower, *Mimulus guttatus*. *Proceedings of the Royal Society B: Biological Sciences*, **177**, 177–196.
- Andrews KR, Good JM, Miller MR, Luikart G, Hohenlohe PA (2016) Harnessing the power of RADseq for ecological and evolutionary genomics. *Nature Reviews Genetics*, **17**, 81–92.
- Angers B, Magnan P, Plante M, Bernatchez L (1999) Canonical correspondence analysis for estimating spatial and environmental effects on microsatellite gene diversity in brook charr (*Salvelinus fontinalis*). *Molecular Ecology*, **8**, 1043–1053.
- Armbruster P, Reed DH (2005) Inbreeding depression in benign and stressful environments. *Heredity*, **95**, 235–242.
- Austin MP (1987) Models for the analysis of species' response to environmental gradients. *Vegetatio*, **69**, 35–45.
- Balkenhol N, Cushman SA, Storfer AT, Waits LP (Eds.) (2016) *Landscape genetics: concepts, method, applications*. John Wiley & Sons, Ltd., West Sussex, UK.
- Balloux F (2001) EASYPOP (Version 1.7): a computer program for population genetics simulations. *Journal of Heredity*, **92**, 301–302.
- Barton N (1979) Gene flow past a cline. *Heredity*, **43**, 333–339.

- Barton NH (2001) Adaptation at the edge of a species' range. In: *Integrating Ecology and Evolution in a Spatial Context* (eds Silvertown J, Antonovics J), pp. 365–392. Blackwell Science Ltd, Oxford, UK.
- Behrman KD, Kirkpatrick M (2011) Species range expansion by beneficial mutations. *Journal of Evolutionary Biology*, **24**, 665–675.
- Bell G, Gonzalez A (2011) Adaptation and evolutionary rescue in metapopulations experiencing environmental deterioration. *Science*, **332**, 1327–1330.
- Benjamini Y, Hochberg Y (1995) Controlling the false discovery rate - a practical and powerful approach. *Journal of the Royal Statistical Society Series B-Methodological*, **57**, 289–300.
- Bernardo J, Spotila JR (2006) Physiological constraints on organismal response to global warming: mechanistic insights from clinally varying populations and implications for assessing endangerment. *Biology Letters*, **2**, 135–139.
- Bijlsma R, Loeschcke V (2012) Genetic erosion impedes adaptive responses to stressful environments. *Evolutionary Applications*, **5**, 117–129.
- Bivand R, Hauke J, Kossowski T (2013) Computing the Jacobian in Gaussian spatial autoregressive models: an illustrated comparison of available methods. *Geographical Analysis*, **45**, 150–179.
- Blanchet FG, Legendre P, Borcard D (2008) Forward selection of explanatory variables. *Ecology*, **89**, 2623–2632.
- Bonin A, Nicole F, Pompanon F, Miaud C, Taberlet P (2007) Population adaptive index: a new method to help measure intraspecific genetic diversity and prioritize populations for conservation. *Conservation Biology*, **21**, 697–708.
- Bourret V, Dionne M, Bernatchez L (2014) Detecting genotypic changes associated with selective mortality at sea in Atlantic salmon: polygenic multilocus analysis surpasses genome scan. *Molecular Ecology*, **23**, 4444–4457.
- ter Braak CJF (1987) The analysis of vegetation-environment relationships by canonical correspondence analysis. In: *Theory and models in vegetation science* Advances in vegetation science. (eds Prentice IC, Maarel E van der), pp. 69–77. Springer Netherlands.

- Brauer CJ, Hammer MP, Beheregaray LB (2016) Riverscape genomics of a threatened fish across a hydroclimatically heterogeneous river basin. *Molecular Ecology*, **25**, 5093–5113.
- Bray JR, Curtis JT (1957) An ordination of the upland forest communities of southern Wisconsin. *Ecological Monographs*, **27**, 325–349.
- Breiman L (2001) Random Forests. *Machine Learning*, **45**, 5–32.
- Bridle JR, Polechová J, Kawata M, Butlin RK (2010) Why is adaptation prevented at ecological margins? New insights from individual-based simulations. *Ecology Letters*, **13**, 485–494.
- Brieuc MSO, Ono K, Drinan DP, Naish KA (2015) Integration of Random Forest with population-based outlier analyses provides insight on the genomic basis and evolution of run timing in Chinook salmon (*Oncorhynchus tshawytscha*). *Molecular Ecology*, **24**, 2729–2746.
- Butchart SHM, Walpole M, Collen B *et al.* (2010) Global biodiversity: indicators of recent declines. *Science*, **328**, 1164–1168.
- Canty A, Ripley B (2012) *boot: Bootstrap R (S-Plus) Functions*. R package version 1.3-4.
- Caruso NM, Lips KR (2013) Truly enigmatic declines in terrestrial salamander populations in Great Smoky Mountains National Park. *Diversity and Distributions*, **19**, 38–48.
- Catchen J, Amores A, Hohenlohe P, Cresko W, Postlethwait J (2011) Stacks: building and genotyping loci *de novo* from short-read sequences. *G3 Genes Genomes Genetics*, **1**, 171–182.
- Catchen J, Hohenlohe PA, Bassham S, Amores A, Cresko WA (2013) Stacks: an analysis tool set for population genomics. *Molecular Ecology*, **22**, 3124–3140.
- Cavalli-Sforza LL (1966) Population structure and human evolution. *Proceedings of the Royal Society B: Biological Sciences*, **164**, 362–379.
- Chevin L-M, Lande R (2015) Evolution of environmental cues for phenotypic plasticity. *Evolution*, **69**, 2767–2775.

- Chevin L-M, Lande R, Mace GM (2010) Adaptation, plasticity, and extinction in a changing environment: towards a predictive theory. *PLoS Biol*, **8**, e1000357.
- Coop G, Witonsky D, Rienzo AD, Pritchard JK (2010) Using environmental correlations to identify loci underlying local adaptation. *Genetics*, **185**, 1411–1423.
- Crandall KA, Bininda-Emonds ORP, Mace GM, Wayne RK (2000) Considering evolutionary processes in conservation biology. *Trends in Ecology & Evolution*, **15**, 290–295.
- Davey JW, Hohenlohe PA, Etter PD *et al.* (2011) Genome-wide genetic marker discovery and genotyping using next-generation sequencing. *Nature Reviews Genetics*, **12**, 499–510.
- Dawson TP, Jackson ST, House JI, Prentice IC, Mace GM (2011) Beyond predictions: biodiversity conservation in a changing climate. *Science*, **332**, 53–58.
- De Mita S, Thuillet A-C, Gay L *et al.* (2013) Detecting selection along environmental gradients: analysis of eight methods and their effectiveness for outbreeding and selfing populations. *Molecular Ecology*, **22**, 1383–1399.
- De'ath G, Fabricius KE (2000) Classification and regression trees: a powerful yet simple technique for ecological data analysis. *Ecology*, **81**, 3178–3192.
- Diniz-Filho JAF, Soares TN, Lima JS *et al.* (2013) Mantel test in population genetics. *Genetics and Molecular Biology*, **36**, 475–485.
- Dirzo R, Young HS, Galetti M *et al.* (2014) Defaunation in the Anthropocene. *Science*, **345**, 401–406.
- Do C, Waples RS, Peel D *et al.* (2014) NeEstimator v2: re-implementation of software for the estimation of contemporary effective population size (Ne) from genetic data. *Molecular Ecology Resources*, **14**, 209–214.
- Dray S, Blanchet G, Borcard D *et al.* (2016) *adespatial: Multivariate multiscale spatial analysis*. R package version 0.0-7.
- Dray S, Legendre P, Blanchet G (2011) *packfor: Forward selection with permutation (Canoco p.46)*. R package version 0.0-8/r100.

- Dray S, Legendre P, Peres-Neto PR (2006) Spatial modelling: a comprehensive framework for principal coordinate analysis of neighbour matrices (PCNM). *Ecological Modelling*, **196**, 483–493.
- Dray S, Pélissier R, Couteron P *et al.* (2012) Community ecology in the age of multivariate multiscale spatial analysis. *Ecological Monographs*, **82**, 257–275.
- Duforet-Frebourg N, Luu K, Laval G, Bazin E, Blum MGB (2016) Detecting genomic signatures of natural selection with principal component analysis: Application to the 1000 Genomes data. *Molecular Biology and Evolution*, **33**, 1082–1093.
- Edmands S (2007) Between a rock and a hard place: evaluating the relative risks of inbreeding and outbreeding for conservation and management. *Molecular Ecology*, **16**, 463–475.
- Endler JA (1973) Gene flow and population differentiation studies of clines suggest that differentiation along environmental gradients may be independent of gene flow. *Science*, **179**, 243–250.
- Etter PD, Bassham S, Hohenlohe PA, Johnson EA, Cresko WA (2011) SNP discovery and genotyping for evolutionary genetics using RAD sequencing. In: *Methods in Molecular Biology* Molecular Methods for Evolutionary Genetics. (eds Orgogozo V, Rockman MV), pp. 157–178. Humana Press.
- Feder ME (1983) Integrating the ecology and physiology of plethodontid salamanders. *Herpetologica*, **39**, 291–310.
- Felsenstein J (1976) The theoretical population genetics of variable selection and migration. *Annual Review of Genetics*, **10**, 253–280.
- Felsenstein J (1977) Multivariate normal genetic models with a finite number of loci. In: *Proceedings of the International Conference on Quantitative Genetics* (eds Pollak E, Kempthorne O, Bailey TJ), pp. 227–245. Iowa State University Press, Iowa, USA.
- Fitzpatrick MC, Keller SR (2015) Ecological genomics meets community-level modelling of biodiversity: mapping the genomic landscape of current and future environmental adaptation. *Ecology Letters*, **18**, 1–16.
- Forester BR, Jones MR, Joost S, Landguth EL, Lasky JR (2016) Detecting spatial genetic signatures of local adaptation in heterogeneous landscapes. *Molecular Ecology*, **25**, 104–120.

- Forester BR, Lasky JR, Wagner HH, Urban DL (In review) Using genotype-environment associations to identify multilocus local adaptation. *Molecular Ecology*.
- François O, Martins H, Caye K, Schoville SD (2016) Controlling false discoveries in genome scans for selection. *Molecular Ecology*, **25**, 454–469.
- Frankham R (2005) Genetics and extinction. *Biological Conservation*, **126**, 131–140.
- Frankham R (2015) Genetic rescue of small inbred populations: meta-analysis reveals large and consistent benefits of gene flow. *Molecular Ecology*, **24**, 2610–2618.
- Frankham R, Ballou JD, Eldridge MDB *et al.* (2011) Predicting the probability of outbreeding depression. *Conservation Biology*, **25**, 465–475.
- Fraser DJ, Bernatchez L (2001) Adaptive evolutionary conservation: towards a unified concept for defining conservation units. *Molecular Ecology*, **10**, 2741–2752.
- Frean M, Rainey PB, Traulsen A (2013) The effect of population structure on the rate of evolution. *Proceedings of the Royal Society B: Biological Sciences*, **280**, 1–7.
- Frichot E, François O (2015) LEA: An R package for landscape and ecological association studies. *Methods in Ecology and Evolution*, **6**, 925–929.
- Frichot E, Mathieu F, Trouillon T, Bouchard G, François O (2014) Fast and efficient estimation of individual ancestry coefficients. *Genetics*, **196**, 973–983.
- Frichot E, Schoville SD, Bouchard G, François O (2013) Testing for associations between loci and environmental gradients using latent factor mixed models. *Molecular Biology and Evolution*, **30**, 1687–1699.
- Fridley JD (2009) Downscaling climate over complex terrain: high finescale (<1000 m) spatial variation of near-ground temperatures in a montane forested landscape (Great Smoky Mountains). *Journal of Applied Meteorology and Climatology*, **48**, 1033–1049.
- Funk WC, McKay JK, Hohenlohe PA, Allendorf FW (2012) Harnessing genomics for delineating conservation units. *Trends in Ecology & Evolution*, **27**, 489–496.
- Galinsky KJ, Bhatia G, Loh P-R *et al.* (2016) Fast principal-component analysis reveals convergent evolution of ADH1B in Europe and East Asia. *The American Journal of Human Genetics*, **98**, 456–472.

- Garant D, Forde SE, Hendry AP (2007) The multifarious effects of dispersal and gene flow on contemporary adaptation. *Functional Ecology*, **21**, 434–443.
- García-Ramos G, Kirkpatrick M (1997) Genetic models of adaptation and gene flow in peripheral populations. *Evolution*, **51**, 21–28.
- Gardner RH (1999) RULE: map generation and a spatial analysis program. In: *Landscape Ecological Analysis* (eds Klopatek JM, Gardner RH), pp. 280–303. Springer New York.
- Garner BA, Hand BK, Amish SJ *et al.* (2016) Genomics in conservation: Case studies and bridging the gap between data and application. *Trends in Ecology & Evolution*, **31**, 81–83.
- Gautier M, Gharbi K, Cezard T *et al.* (2013) The effect of RAD allele dropout on the estimation of genetic variation within and between populations. *Molecular Ecology*, **22**, 3165–3178.
- Ghalambor CK, McKAY JK, Carroll SP, Reznick DN (2007) Adaptive versus non-adaptive phenotypic plasticity and the potential for contemporary adaptation in new environments. *Functional Ecology*, **21**, 394–407.
- Gifford ME (2016) Physiology of Plethodontid salamanders: a call for increased efforts. *Copeia*, 42–51.
- Goldstein BA, Hubbard AE, Cutler A, Barcellos LF (2010) An application of Random Forests to a genome-wide association dataset: methodological considerations & new findings. *BMC Genetics*, **11**, 1–13.
- Goslee S, Urban D (2007) The ecodist package for dissimilarity-based analysis of ecological data. *Journal of Statistical Software*, **22**, 1–19.
- Gosselin T, Bernatchez L (2016) *stackr: GBS/RAD data exploration, manipulation and visualization using R*. R package version 0.4.6.
<https://github.com/thierrygosselin/stackr>.
- Grantham HS, Wilson KA, Moilanen A, Rebelo T, Possingham HP (2009) Delaying conservation actions for improved knowledge: how long should we wait? *Ecology Letters*, **12**, 293–301.

- Gratwicke B (Ed.) (2008) *Proceedings of the Appalachian Salamander Conservation Workshop*. IUCN/SSC Conservation Breeding Specialist Group, Apple Valley, MN.
- Grivet D, Sork VL, Westfall RD, Davis FW (2008) Conserving the evolutionary potential of California valley oak (*Quercus lobata* Née): a multivariate genetic approach to conservation planning. *Molecular Ecology*, **17**, 139–156.
- Guia APO de, Saitoh T (2007) The gap between the concept and definitions in the Evolutionarily Significant Unit: the need to integrate neutral genetic variation and adaptive variation. *Ecological Research*, **22**, 604–612.
- Günther T, Coop G (2013) Robust identification of local adaptation from allele frequencies. *Genetics*, **195**, 205–220.
- Hahn MW (2008) Toward a selection theory of molecular evolution. *Evolution*, **62**, 255–265.
- Haldane JBS (1930) A mathematical theory of natural and artificial selection (Part VI, Isolation). *Mathematical Proceedings of the Cambridge Philosophical Society*, **26**, 220–230.
- Hancock AM, Brachi B, Faure N *et al.* (2011) Adaptation to climate across the *Arabidopsis thaliana* genome. *Science*, **334**, 83–86.
- Harrisson KA, Pavlova A, Telonis-Scott M, Sunnucks P (2014) Using genomics to characterize evolutionary potential for conservation of wild populations. *Evolutionary Applications*, **7**, 1008–1025.
- Hecht BC, Matala AP, Hess JE, Narum SR (2015) Environmental adaptation in Chinook salmon (*Oncorhynchus tshawytscha*) throughout their North American range. *Molecular Ecology*, **24**, 5573–5595.
- Hedrick PW (1986) Genetic polymorphism in heterogeneous environments: a decade later. *Annual Review of Ecology and Systematics*, **17**, 535–566.
- Hedrick PW (2006) Genetic polymorphism in heterogeneous environments: the age of genomics. *Annual Review of Ecology, Evolution, and Systematics*, **37**, 67–93.
- Hedrick PW, Fredrickson R (2010) Genetic rescue guidelines with examples from Mexican wolves and Florida panthers. *Conservation Genetics*, **11**, 615–626.

- Hedrick PW, Ginevan ME, Ewing EP (1976) Genetic polymorphism in heterogeneous environments. *Annual Review of Ecology and Systematics*, **7**, 1–32.
- Highton R (2005) Declines of Eastern North American Woodland Salamanders (Plethodon). In: *Amphibian Declines: Conservation Status of United States Species*, pp. 34–46. University of California Press, Berkeley.
- Hijmans RJ (2015) *raster: geographic data analysis and modeling*. R package version 2.5-2.
- Hoban S, Arntzen JA, Bruford MW *et al.* (2014) Comparative evaluation of potential indicators and temporal sampling protocols for monitoring genetic erosion. *Evolutionary Applications*, **7**, 984–998.
- Hoban SM, Gaggiotti OE, Bertorelle G (2013) The number of markers and samples needed for detecting bottlenecks under realistic scenarios, with and without recovery: a simulation-based study. *Molecular Ecology*, **22**, 3444–3450.
- Hoban S, Kelley JL, Lotterhos KE *et al.* (2016) Finding the genomic basis of local adaptation: pitfalls, practical solutions, and future directions. *The American Naturalist*, **188**, 379–397.
- Hoffmann A, Griffin P, Dillon S *et al.* (2015) A framework for incorporating evolutionary genomics into biodiversity conservation and management. *Climate Change Responses*, **2**, 1–23.
- Holliday JA, Wang T, Aitken S (2012) Predicting adaptive phenotypes from multilocus genotypes in Sitka Spruce (*Picea sitchensis*) using Random Forest. *G3: Genes | Genomes | Genetics*, **2**, 1085–1093.
- Holt RD, Barfield M (2011) Theoretical perspectives on the statics and dynamics of species' borders in patchy environments. *The American Naturalist*, **178**, S6–S25.
- Holt RD, Gaines MS (1992) Analysis of adaptation in heterogeneous landscapes: Implications for the evolution of fundamental niches. *Evolutionary Ecology*, **6**, 433–447.
- Horn JL (1965) A rationale and test for the number of factors in factor analysis. *Psychometrika*, **30**, 179–185.
- Huang F (2015) *hornpa: Horn's (1965) Test to Determine the Number of Components/Factors*. R package version 1.0.

- Hughes JB, Daily GC, Ehrlich PR (1997) Population diversity: Its extent and extinction. *Science*, **278**, 689–692.
- Imhof M, Schlötterer C (2001) Fitness effects of advantageous mutations in evolving *Escherichia coli* populations. *Proceedings of the National Academy of Sciences*, **98**, 1113–1117.
- IPCC (2014) Part A: Global and Sectoral Aspects. Contribution of Working Group II to the Fifth Assessment Report of the Intergovernmental Panel on Climate Change. In: *Climate Change 2014: Impacts, Adaptation, and Vulnerability* (eds Field C, Barros V, Dokken D, et al.), p. 1132. Cambridge University Press, UK, New York.
- Jensen JD, Kim Y, DuMont VB, Aquadro CF, Bustamante CD (2005) Distinguishing between selective sweeps and demography using DNA polymorphism data. *Genetics*, **170**, 1401–1410.
- Johnson WE, Onorato DP, Roelke ME et al. (2010) Genetic restoration of the Florida panther. *Science*, **329**, 1641–1645.
- Johnstone IM, Perry PO, Ma Z, Shahram M (2009) *RMT: Distributions, Statistics and Tests derived from Random Matrix Theory*. R package version 0.2.
- Jombart T (2008) adegenet: a R package for the multivariate analysis of genetic markers. *Bioinformatics*, **24**, 1403–1405.
- Jombart T, Ahmed I (2011) adegenet 1.3-1: new tools for the analysis of genome-wide SNP data. *Bioinformatics (Oxford, England)*, **27**, 3070–3071.
- Jombart T, Devillard S, Balloux F (2010) Discriminant analysis of principal components: a new method for the analysis of genetically structured populations. *BMC Genetics*, **11**, 94.
- Jombart T, Pontier D, Dufour A-B (2009) Genetic markers in the playground of multivariate analysis. *Heredity*, **102**, 330–341.
- Jones MR, Forester BR, Teufel AI et al. (2013) Integrating landscape genomics and spatially explicit approaches to detect loci under selection in clinal populations. *Evolution*, **67**, 3455–3468.

- Joost S, Bonin A, Bruford MW *et al.* (2007) A spatial analysis method (SAM) to detect candidate loci for selection: towards a landscape genomics approach to adaptation. *Molecular Ecology*, **16**, 3955–3969.
- Joost S, Vuilleumier S, Jensen JD *et al.* (2013) Uncovering the genetic basis of adaptive change: on the intersection of landscape genomics and theoretical population genetics. *Molecular Ecology*, **22**, 3659–3665.
- Kassen R, Bataillon T (2006) Distribution of fitness effects among beneficial mutations before selection in experimental populations of bacteria. *Nature Genetics*, **38**, 484–488.
- Kawecki TJ, Ebert D (2004) Conceptual issues in local adaptation. *Ecology Letters*, **7**, 1225–1241.
- Keyghobadi N (2007) The genetic implications of habitat fragmentation for animals. *Canadian Journal of Zoology*, **85**, 1049–1064.
- Kirkpatrick M, Barton NH (1997) Evolution of a species' range. *The American Naturalist*, **150**, 1–23.
- Landguth EL, Cushman SA (2010) cdpop: a spatially explicit cost distance population genetics program. *Molecular Ecology Resources*, **10**, 156–161.
- Landguth EL, Cushman SA, Schwartz MK *et al.* (2010) Quantifying the lag time to detect barriers in landscape genetics. *Molecular Ecology*, **19**, 4179–4191.
- Laporte M, Pavey SA, Rougeux C *et al.* (2016) RAD sequencing reveals within-generation polygenic selection in response to anthropogenic organic and metal contamination in North Atlantic Eels. *Molecular Ecology*, **25**, 219–237.
- Laporte M, Rogers SM, Dion-Côté A-M *et al.* (2015) RAD-QTL mapping reveals both genome-level parallelism and different genetic architecture underlying the evolution of body shape in Lake Whitefish (*Coregonus clupeaformis*) species pairs. *G3: Genes | Genomes | Genetics*, **5**, 1481–1491.
- Lasky JR, Des Marais DL, McKay JK *et al.* (2012) Characterizing genomic variation of *Arabidopsis thaliana*: the roles of geography and climate. *Molecular Ecology*, **21**, 5512–5529.

- Lasky JR, Keitt TH (2013) Reserve size and fragmentation alter community assembly, diversity, and dynamics. *The American Naturalist*, **182**, E142-160.
- Lasky JR, Marais D, L D *et al.* (2014) Natural variation in abiotic stress responsive gene expression and local adaptation to climate in *Arabidopsis thaliana*. *Molecular Biology and Evolution*, **31**, 2283–2296.
- Le Corre V, Kremer A (2012) The genetic differentiation at quantitative trait loci under local adaptation. *Molecular Ecology*, **21**, 1548–1566.
- Legendre P, Borcard D, Blanchet FG, Dray S (2012) PCNM: MEM spatial eigenfunction and principal coordinate analyses. R package version 2.1-2/r106.
- Legendre P, Fortin M-J, Borcard D (2015) Should the Mantel test be used in spatial analysis? *Methods in Ecology and Evolution*, **6**, 1239–1247.
- Legendre P, Legendre L (2012) *Numerical Ecology*. Elsevier, Amsterdam, The Netherlands.
- Lenormand T (2002) Gene flow and the limits to natural selection. *Trends in Ecology & Evolution*, **17**, 183–189.
- Li J, Malley JD, Andrew AS, Karagas MR, Moore JH (2016) Detecting gene-gene interactions using a permutation-based random forest method. *BioData Mining*, **9**, 14.
- Lindenmayer DB, Piggott MP, Wintle BA (2013) Counting the books while the library burns: why conservation monitoring programs need a plan for action. *Frontiers in Ecology and the Environment*, **11**, 549–555.
- Lotterhos KE, Whitlock MC (2014) Evaluation of demographic history and neutral parameterization on the performance of FST outlier tests. *Molecular Ecology*, **23**, 2178–2192.
- Lotterhos KE, Whitlock MC (2015) The relative power of genome scans to detect local adaptation depends on sampling design and statistical method. *Molecular Ecology*, **24**, 1031–1046.
- Manel S, Holderegger R (2013) Ten years of landscape genetics. *Trends in Ecology & Evolution*, **28**, 614–621.

- Manichaikul A, Mychaleckyj JC, Rich SS *et al.* (2010) Robust relationship inference in genome-wide association studies. *Bioinformatics*, **26**, 2867–2873.
- Margules CR, Pressey RL (2000) Systematic conservation planning. *Nature*, **405**, 243–253.
- Martel A, Blooi M, Adriaensen C *et al.* (2014) Recent introduction of a chytrid fungus endangers Western Palearctic salamanders. *Science*, **346**, 630–631.
- Martin TG, Nally S, Burbidge AA *et al.* (2012) Acting fast helps avoid extinction. *Conservation Letters*, **5**, 274–280.
- Mayr E (1963) *Animal Species and Evolution*. Harvard University Press, Cambridge, MA, USA.
- McKinney GJ, Larson WA, Seeb LW, Seeb JE (2016) RADseq provides unprecedented insights into molecular ecology and evolutionary genetics: comment on Breaking RAD by Lowry *et al.* (2016). *Molecular Ecology Resources*, doi: 10.1111/1755-0998.12649.
- McMahon BJ, Teeling EC, Höglund J (2014) How and why should we implement genomics into conservation? *Evolutionary Applications*, **7**, 999–1007.
- Meirmans PG (2012) The trouble with isolation by distance. *Molecular Ecology*, **21**, 2839–2846.
- Milanovich JR, Peterman WE, Nibbelink NP, Maerz JC (2010) Projected loss of a salamander diversity hotspot as a consequence of projected global climate change. *PLoS ONE*, **5**, e12189.
- Miller JM, Poissant J, Hogg JT, Coltman DW (2012) Genomic consequences of genetic rescue in an insular population of bighorn sheep (*Ovis canadensis*). *Molecular Ecology*, **21**, 1583–1596.
- Miraldo A, Li S, Borregaard MK *et al.* (2016) An Anthropocene map of genetic diversity. *Science*, **353**, 1532–1535.
- Mitton JB, Linhart YB, Hamrick JL, Beckman JS (1977) Observations on the genetic structure and mating system of Ponderosa Pine in the Colorado front range. *Theoretical and Applied Genetics*, **51**, 5–13.

- Moritz C (1994) Defining “Evolutionarily Significant Units” for conservation. *Trends in Ecology & Evolution*, **9**, 373–375.
- Moritz C (2002) Strategies to protect biological diversity and the evolutionary processes that sustain it. *Systematic Biology*, **51**, 238–254.
- Mouquet N, Loreau M (2003) Community patterns in source-sink metacommunities. *The American Naturalist*, **162**, 544–557.
- Mulley JC, James JW, Barker JSF (1979) Allozyme genotype-environment relationships in natural populations of *Drosophila buzzatii*. *Biochemical Genetics*, **17**, 105–126.
- Nagylaki T (1975) Conditions for the existence of clines. *Genetics*, **80**, 595–615.
- Nicotra AB, Beever EA, Robertson AL, Hofmann GE, O’Leary J (2015) Assessing the components of adaptive capacity to improve conservation and management efforts under global change. *Conservation Biology*, **29**, 1268–1278.
- Oksanen J, Blanchet FG, Kindt R *et al.* (2013) *vegan: Community Ecology Package*. R package version 2.0-10.
- Orsini L, Spanier KI, De Meester L (2012) Genomic signature of natural and anthropogenic stress in wild populations of the waterflea *Daphnia magna*: validation in space, time and experimental evolution. *Molecular Ecology*, **21**, 2160–2175.
- Ottewell KM, Bickerton DC, Byrne M, Lowe AJ (2016) Bridging the gap: a genetic assessment framework for population-level threatened plant conservation prioritization and decision-making. *Diversity and Distributions*, **22**, 174–188.
- Paccard A, Vance M, Willi Y (2013) Weak impact of fine-scale landscape heterogeneity on evolutionary potential in *Arabidopsis lyrata*. *Journal of Evolutionary Biology*, **26**, 2331–2340.
- Palmer MW (1992) The coexistence of species in fractal landscapes. *The American Naturalist*, **139**, 375–397.
- Patterson N, Price AL, Reich D (2006) Population structure and eigenanalysis. *PLoS Genetics*, **2**, e190.

- Pauls SU, Nowak C, Bálint M, Pfenninger M (2013) The impact of global climate change on genetic diversity within populations and species. *Molecular Ecology*, **22**, 925–946.
- Pavey SA, Gaudin J, Normandeau E *et al.* (2015) RAD sequencing highlights polygenic discrimination of habitat ecotypes in the panmictic American Eel. *Current Biology*, **25**, 1666–1671.
- Pearse DE (2016) Saving the spandrels? Adaptive genomic variation in conservation and fisheries management. *Journal of Fish Biology*, **89**, 2697–2716.
- Peterson BK, Weber JN, Kay EH, Fisher HS, Hoekstra HE (2012) Double digest RADseq: an inexpensive method for *de novo* SNP discovery and genotyping in model and non-model species. *PLoS ONE*, **7**, e37135.
- Pierce KB, Lookingbill T, Urban D (2005) A simple method for estimating potential relative radiation (PRR) for landscape-scale vegetation analysis. *Landscape Ecology*, **20**, 137–147.
- Pierson JC, Coates DJ, Oostermeijer JGB *et al.* (2016) Genetic factors in threatened species recovery plans on three continents. *Frontiers in Ecology and the Environment*, **14**, 433–440.
- Polasky S, Carpenter SR, Folke C, Keeler B (2011) Decision-making under great uncertainty: environmental management in an era of global change. *Trends in Ecology & Evolution*, **26**, 398–404.
- Price AL, Patterson NJ, Plenge RM *et al.* (2006) Principal components analysis corrects for stratification in genome-wide association studies. *Nature Genetics*, **38**, 904–909.
- Purcell S, Neale B, Todd-Brown K *et al.* (2007) PLINK: A Tool Set for Whole-Genome Association and Population-Based Linkage Analyses. *The American Journal of Human Genetics*, **81**, 559–575.
- R Development Core Team (2015) *R: a language and environment for statistical computing*. R Foundation for Statistical Computing, Vienna, Austria.
- Reed DH, Frankham R (2003) Correlation between fitness and genetic diversity. *Conservation Biology*, **17**, 230–237.

- Rellstab C, Gugerli F, Eckert AJ, Hancock AM, Holderegger R (2015) A practical guide to environmental association analysis in landscape genomics. *Molecular Ecology*, **24**, 4348–4370.
- Richardson JL, Brady SP, Wang IJ, Spear SF (2016) Navigating the pitfalls and promise of landscape genetics. *Molecular Ecology*, **25**, 849–863.
- Richardson JL, Urban MC, Bolnick DI, Skelly DK (2014) Microgeographic adaptation and the spatial scale of evolution. *Trends in Ecology & Evolution*, **29**, 165–176.
- Riddell EA, Sears MW (2015) Geographic variation of resistance to water loss within two species of lungless salamanders: implications for activity. *Ecosphere*, **6**, 1–16.
- Robinson JD, Moyer GR (2013) Linkage disequilibrium and effective population size when generations overlap. *Evolutionary Applications*, **6**, 290–302.
- Savolainen O, Lascoux M, Merilä J (2013) Ecological genomics of local adaptation. *Nature Reviews Genetics*, **14**, 807–820.
- Schiffers K, Schurr FM, Travis JMJ *et al.* (2014) Landscape structure and genetic architecture jointly impact rates of niche evolution. *Ecography*, **37**, 1218–1229.
- Schoville SD, Bonin A, François O *et al.* (2012) Adaptive genetic variation on the landscape: methods and cases. *Annual Review of Ecology, Evolution, and Systematics*, **43**, 23–43.
- Schwabl P, Llewellyn MS, Landguth EL *et al.* (2016) Prediction and prevention of parasitic diseases using a landscape genomics framework. *Trends in Parasitology*, doi: 10.1016/j.pt.2016.10.008.
- Schwartz MK, Luikart G, Waples RS (2007) Genetic monitoring as a promising tool for conservation and management. *Trends in Ecology & Evolution*, **22**, 25–33.
- Segelbacher G, Cushman SA, Epperson BK *et al.* (2010) Applications of landscape genetics in conservation biology: Concepts and challenges. *Conservation Genetics*, **11**, 375–385.
- Sgro C, Lowe A, Hoffmann A (2011) Building evolutionary resilience for conserving biodiversity under climate change. *Evolutionary Applications*, **4**, 326–337.

- Shriner D (2012) Improved eigenanalysis of discrete subpopulations and admixture using the minimum average partial test. *Human Heredity*, **73**, 73–83.
- Slatkin M (1973) Gene flow and selection in a cline. *Genetics*, **75**, 733–756.
- Slatkin M (1975) Gene flow and selection in a two-locus system. *Genetics*, **81**, 787–802.
- Sork VL, Aitken SN, Dyer RJ *et al.* (2013) Putting the landscape into the genomics of trees: approaches for understanding local adaptation and population responses to changing climate. *Tree Genetics & Genomes*, **9**, 901–911.
- Spielman D, Brook BW, Frankham R (2004) Most species are not driven to extinction before genetic factors impact them. *Proceedings of the National Academy of Sciences*, **101**, 15261–15264.
- Steane DA, Potts BM, McLean E *et al.* (2014) Genome-wide scans detect adaptation to aridity in a widespread forest tree species. *Molecular Ecology*, **23**, 2500–2513.
- Stein BA, Kutner LS, Adams JS (Eds.) (2000) *Precious Heritage: The Status of Biodiversity in the United States*. Oxford University Press, Oxford.
- Storey JD, Bass AJ, Dabney A, Robinson D (2015) *qvalue: Q-value estimation for false discovery rate control*. R package version 2.2.2.
- Storey JD, Tibshirani R (2003) Statistical significance for genomewide studies. *Proceedings of the National Academy of Sciences*, **100**, 9440–9445.
- Storfer A, Murphy MA, Spear SF, Holderegger R, Waits LP (2010) Landscape genetics: Where are we now? *Molecular Ecology*, **19**, 3496–3514.
- Stucki S, Orozco-terWengel P, Forester BR *et al.* (2016) High performance computation of landscape genomic models including local indicators of spatial association. *Molecular Ecology Resources*, doi: 10.1111/1755-0998.12629.
- Swaegers J, Mergeay J, Van Geystelen A *et al.* (2015) Neutral and adaptive genomic signatures of rapid poleward range expansion. *Molecular Ecology*, **24**, 6163–6176.
- Tack AJM, Roslin T (2010) Overrun by the neighbors: landscape context affects strength and sign of local adaptation. *Ecology*, **91**, 2253–2260.
- Tiffin P, Ross-Ibarra J (2014) Advances and limits of using population genetics to understand local adaptation. *Trends in Ecology & Evolution*, **29**, 673–680.

- Urban DL (2002) Prioritizing reserves for acquisition. In: *Learning landscape ecology: a practical guide to concepts and techniques* (eds Gergel SE, Turner MG), pp. 293–305. Springer Verlag, New York.
- Vilà C, Sundqvist A-K, Flagstad Ø *et al.* (2003) Rescue of a severely bottlenecked wolf (*Canis lupus*) population by a single immigrant. *Proceedings of the Royal Society B: Biological Sciences*, **270**, 91–97.
- de Villemereuil P, Frichot É, Bazin É, François O, Gaggiotti OE (2014) Genome scan methods against more complex models: when and how much should we trust them? *Molecular Ecology*, **23**, 2006–2019.
- Wagner HH, Chávez-Pesqueira M, Forester BR (2017) Spatial detection of outlier loci with Moran eigenvector maps. *Molecular Ecology Resources*, doi: 10.1111/1755-0998.12653.
- Wagner HH, Fortin M-J (2005) Spatial analysis of landscapes: concepts and statistics. *Ecology*, **86**, 1975–1987.
- Wang IJ, Bradburd GS (2014) Isolation by environment. *Molecular Ecology*, **23**, 5649–5662.
- Wang T, Hamann A, Spittlehouse D, Carroll C (2016) Locally downscaled and spatially customizable climate data for historical and future periods for North America. *PLOS ONE*, **11**, e0156720.
- Wang IJ, Johnson JR, Johnson BB, Shaffer HB (2011) Effective population size is strongly correlated with breeding pond size in the endangered California tiger salamander, *Ambystoma californiense*. *Conservation Genetics*, **12**, 911–920.
- Waples RS, Antao T, Luikart G (2014) Effects of overlapping generations on linkage disequilibrium estimates of effective population size. *Genetics*, **197**, 769–780.
- Waples RK, Larson WA, Waples RS (2016) Estimating contemporary effective population size in non-model species using linkage disequilibrium across thousands of loci. *Heredity*, **117**, 233–240.
- Waters CN, Zalasiewicz J, Summerhayes C *et al.* (2016) The Anthropocene is functionally and stratigraphically distinct from the Holocene. *Science*, **351**, aad2622.

- Weeks AR, Sgro CM, Young AG *et al.* (2011) Assessing the benefits and risks of translocations in changing environments: a genetic perspective. *Evolutionary Applications*, **4**, 709–725.
- Weir BS, Cockerham CC (1984) Estimating F-statistics for the analysis of population structure. *Evolution*, **38**, 1358–1370.
- Whiteley AR, Fitzpatrick SW, Funk WC, Tallmon DA (2015) Genetic rescue to the rescue. *Trends in Ecology & Evolution*, **30**, 42–49.
- Whittaker RH (1967) Gradient analysis of vegetation. *Biological Reviews*, **42**, 207–264.
- Winham SJ, Colby CL, Freimuth RR *et al.* (2012) SNP interaction detection with Random Forests in high-dimensional genetic data. *BMC Bioinformatics*, **13**, 164.
- Winters A, Gifford ME (2013) Geographic variation in the water economy of a lungless salamander. *Herpetological Conservation and Biology*, **8**, 741–747.
- van den Wollenberg AL (1977) Redundancy analysis an alternative for canonical correlation analysis. *Psychometrika*, **42**, 207–219.
- Wright MN, Ziegler A, König IR (2016) Do little interactions get lost in dark random forests? *BMC Bioinformatics*, **17**, 145.
- Xuereb A, Stahlke A, Bermingham M *et al.* (In review) Missing data have limited effects on the performance of genotype-environment association methods. *Molecular Ecology*.
- Yeaman S (2015) Local adaptation by alleles of small effect. *The American Naturalist*, **186**, **Supplement**, 1–16.
- Yeaman S, Whitlock MC (2011) The genetic architecture of adaptation under migration–selection balance. *Evolution*, **65**, 1897–1911.
- Yoder JB, Stanton-Geddes J, Zhou P *et al.* (2014) Genomic signature of adaptation to climate in *Medicago truncatula*. *Genetics*, **196**, 1263–1275.
- Zhao Y, Chen F, Zhai R *et al.* (2012) Correction for population stratification in random forest analysis. *International Journal of Epidemiology*, **41**, 1798–1806.

Biography

Brenna Renee Forester was born on July 7, 1975 in Columbus, Ohio. She received a B.A. in Biology from Hiram College in 1996, and a second B.A. in Political Economy from The Evergreen State College in 2003. She was a biologist for the City of Bellingham, WA from 2007-2011, where she worked on urban stream habitat restoration following the 1999 Olympic pipeline spill and explosion. She earned a M.Sc. in Environmental Science from Western Washington University's Huxley College in 2012. She is fortunate to collaborate with a number of excellent scientists, with whom she has published many peer-reviewed articles during her tenure at Duke University. She has received funding for her graduate research from Western Washington University, Sigma Xi, the Duke University Graduate School, the Society for the Study of Amphibians and Reptiles, the Foundation for the Conservation of Salamanders, PEO International, the American Museum of Natural History, the American Society of Naturalists, and the National Science Foundation.